AD_____

Award Number: DAMD17-01-1-0446

TITLE: PET Radiotracers for Imaging the Proliferation Status of Breast Tumors

PRINCIPAL INVESTIGATOR: Robert H. Mach, Ph.D.

CONTRACTING ORGANIZATION: Washington University
St. Louis, Missouri 63110

REPORT DATE: December 2004

TYPE OF REPORT: Final

PREPARED FOR: U.S. Army Medical Research and Materiel Command
Fort Detrick, Maryland 21702-5012

REPORT DOCUMENTATION PAGE

Form Approved
OMB No. 074-0188

1. AGENCY USE ONLY (Leave blank)	2. REPORT DATE	3. REPORT TYPE AND DATES COVERED
	December 2004	Final (15 May 2001 - 30 Nov 2004)

4. TITLE AND SUBTITLE
PET Radiotracers for Imaging the Proliferation Status of Breast Tumors

5. FUNDING NUMBERS
DAMD17-01-1-0446

6. AUTHOR(S)
Robert H. Mach, Ph.D.

7. PERFORMING ORGANIZATION NAME(S) AND ADDRESS(ES)
Washington University
St. Louis, Missouri 63110

E-Mail: rhmach@mir.wustl.edu

8. PERFORMING ORGANIZATION REPORT NUMBER

9. SPONSORING / MONITORING AGENCY NAME(S) AND ADDRESS(ES)
U.S. Army Medical Research and Materiel Command
Fort Detrick, Maryland 21702-5012

10. SPONSORING / MONITORING AGENCY REPORT NUMBER

11. SUPPLEMENTARY NOTES
Original contains color plates: All DTIC reproductions will be in black and white.

12a. DISTRIBUTION / AVAILABILITY STATEMENT
Approved for Public Release; Distribution Unlimited

12b. DISTRIBUTION CODE

13. ABSTRACT (Maximum 200 Words)

The goal of this research project is to develop radiotracers for imaging the proliferative status of breast tumors using the noninvasive imaging technique, Positron Emission Tomography (PET). The strategy taken involves developing radiotracers having a high affinity and selectivity for the σ_2 receptor, which has been shown to be a useful receptor-based biomarker of of proliferation in breast tumor cells growing both in vitro and in vivo. During the second year of the three-year IDEA project, we identified a new class of ligands displaying an outstanding affinity and selectivity for σ_2 versus σ_1 receptors. Preliminary in vivo biodistribution and microPET imaging studies with Br-76, C-11 and I-125-labeled analogs indicate that these agents may be useful for use in the diagnosis and determination of the proliferative status of breast tumors in breast cancer patients.

14. SUBJECT TERMS	15. NUMBER OF PAGES
Positron emission tomography, nuclear medicine, breast cancer diagnosis, tumor proliferation, therapeutic monitoring	75
	16. PRICE CODE

17. SECURITY CLASSIFICATION OF REPORT	18. SECURITY CLASSIFICATION OF THIS PAGE	19. SECURITY CLASSIFICATION OF ABSTRACT	20. LIMITATION OF ABSTRACT
Unclassified	Unclassified	Unclassified	Unlimited

Table of Contents

Introduction

The goal of this research is to develop radiotracers that can be used to determine the proliferative status of breast tumors using the noninvasive imaging technique, Positron emission Tomography (PET). Our strategy involves using the sigma-2 (s2) receptor as a biomarker of the proliferative status of breast tumors [1-3]. This report describes the progress achieved during the three-year period of this Army Breast Cancer IDEA grant.

Body

Synthesis and in vivo studies of Azabicyclo[3.3.1]nonane analogs. The initial step of this project was to conduct a structure-activity relationship (SAR) study of our lead compound, **1**, in order to identify a suitable radiotracer for imaging the σ_2 receptor status of breast tumors. The results of this SAR study revealed that *N*-(9-(4-fluorobenzyl))-9-azabicyclo[3.3.1]nonan-3α-yl-*N'*-(2-methoxy-4-methylphenyl)carbamate, **2** (Figure 1), has a modest affinity and moderate selectivity for σ_2 versus σ_1 receptors [4]. The higher affinity of **2** for σ_2 versus σ_1 receptors, and the observation that the fluorine-18 labeled analog of **2** could be prepared via alkylation of the des-benzyl precursor with [^{18}F]4-fluorobenzyl iodide [5], led us to explore the use of [^{18}F]**2** as a potential PET radiotracer for imaging the σ_2 receptor status of breast tumors. Therefore, our initial goal was to synthesize [^{18}F]**2** and conduct in vivo studies of this radiotracer in a murine model of breast cancer.

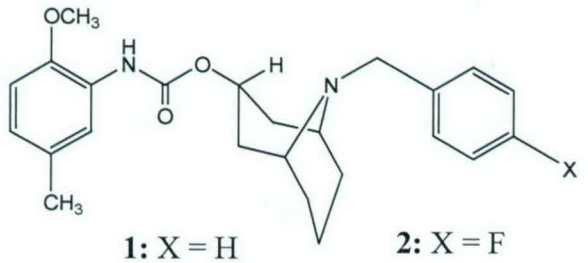

1: X = H
σ_1 = 92.5 nM
σ_2 = 3.1 nM
Ratio = 30

2: X = F
σ_1 = 202 nM
σ_2 = 30 nM
Ratio = 6.7

Figure 1. Structure and in vitro binding properties of compounds **1** and **2**.

The synthesis of [^{18}F]**2** was accomplished via N-alkylation of the des-benzyl precursor, **3**, with [^{18}F]4-fluorobenzyl iodide (Scheme I). The product was purified by reverse-phase semi-preparative HPLC and obtained in an overall yield of ~10% from solublized [^{18}F]CsF. The specific activity of the final product was 2320 ± 1384 mCi/μmol (85.1 ± 51.2 GBq/μmol). The radiotracer was of sufficient radiochemical purity (>95%) for the in vivo tumor uptake studies.

Scheme I

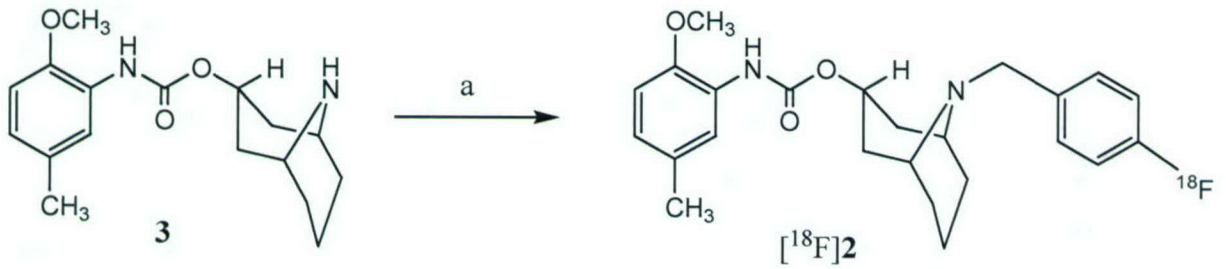

Reagents: (a) [^{18}F]4-fluorobenzyl iodide/triethylamine/DMF/90°C.

Preliminary in vivo biodistribution studies were conducted in nude mice bearing xenografts of the mouse mammary adenocarcinoma tumor cell line, 66. The results of this study are shown in Table I. There was a gradual increase in the uptake of [^{18}F]**2** in the tumor xenografts between 30-min and 60-min post-i.v. injection of the radiotracer. There was a slow rate of washout of radiotracer from the tumor (Table I) and a progressive increase in the tumor:blood and tumor:muscle ratios over time. The tumor:blood and tumor:muscle ratios were 2.5 and 4.0, respectively at 4 hr post-i.v. injection. Blocking studies with haloperidol (50 μg), a known sigma ligand, resulted in a reduction in tumor uptake of the radiotracer at 60 min post-i.v. injection (Figure 2), which represents the time of peak accumulation of the radiotracer in the tumor (Table I). These data are consistent with the labeling of σ_2 receptors in vivo.

Table I. Results of biodistribution studies of [^{18}F]**2** in tumor-bearing mice.

%I.D./c.c. Tissue

Tissue	*30 min*	*60 min*	*120 min*	*240 min*
Brain	1.18 ± 0.19	1.92 ± 0.24	1.18 ± 0.19	0.13 ± 0.01
Blood	1.47 ± 0.10	3.07 ± 0.45	1.90 ± 0.18	0.37 ± 0.06
Lung	6.81 ± 0.85	5.11 ± 1.36	3.77 ± 0.39	0.65 ± 0.11
Heart	2.10 ± 0.18	3.30 ± 0.54	1.80 ± 0.21	0.31 ± 0.05
Liver	7.92 ± 1.18	10.93 ± 1.00	7.36 ± 0.89	1.14 ± 0.18
Kidney	6.40 ± 0.25	14.71 ± 4.57	5.50 ± 0.76	1.08 ± 0.11
Intestine	6.49 ± 0.69	17.92 ± 3.19	9.40 ± 0.87	2.23 ± 0.21
Muscle	1.25 ± 0.23	3.43 ± 0.58	1.84 ± 0.24	0.23 ± 0.02
Spleen	4.55 ± 0.33	5.87 ± 0.71	3.45 ± 0.39	0.55 ± 0.11
Tumor	1.34 ± 0.21	5.02 ± 0.85	3.18 ± 0.12	0.89 ± 0.03
Tumor:Blood[a]	0.80 ± 0.08	1.66 ± 0.23	1.72 ± 0.17	2.48 ± 0.22
Tumor:Muscle[b]	1.13 ± 0.27	1.78 ± 0.48	1.78 ± 0.18	3.98 ± 0.30

[a]%I.D. tumor/%I.D. blood; [b]%I.D. tumor/%I.D. muscle.

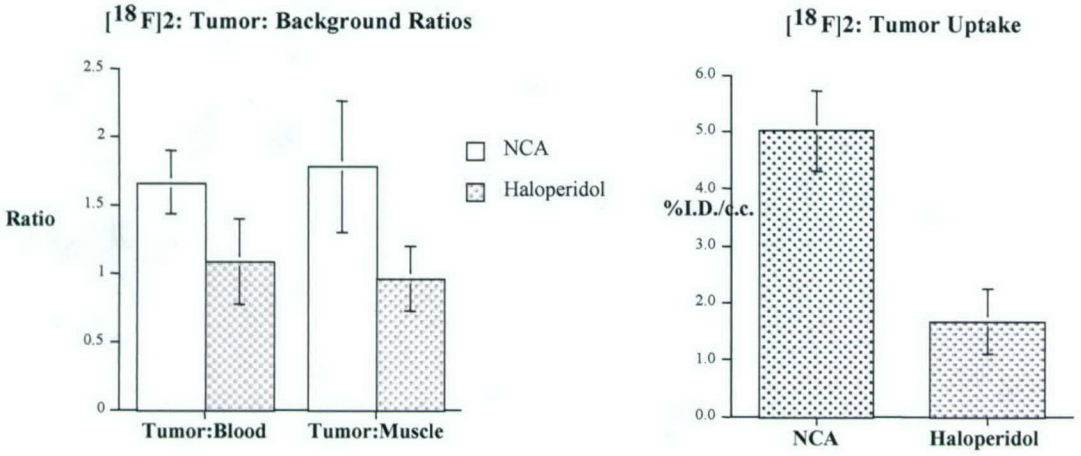

Figure 2. Blocking studies with haloperidol. Co-injection of 50 μg of haloperidol resulted in a reduction in tumor:background ratios and uptake of [^{18}F]**2** at 60 min post-i.v. injection of the radiotracer.

Conclusion. The results of this study indicate that [^{18}F]**1** labels σ_2 receptors in breast tumors. However, the relatively low tumor:background ratios of this radiotracer, which is likely due to the moderate affinity of **2** for σ_2 receptors, prompted us to investigate other ligands having a higher affinity for σ_2 receptors.

2. Synthesis of σ_2 selective conformational-flexible benzamide analogs. During the year 2 of this research project, we turned our attention to the development of a new class of σ_2–selective compounds that were discovered as part of a parallel research program in the laboratory of the P.I.. Over the past 9 years, the P.I. of this Army Breast Cancer grant has had funding from the National Institute on Drug Abuse to develop dopamine receptor antagonists displaying a high affinity and selectivity for dopamine D_3 versus D_2 receptors. Since many D_2 antagonists have been found to have a high affinity for sigma receptors, we typically screen our dopamine antagonists for sigma receptor affinity. An interesting, and somewhat serendipitous, observation was made with the benzamide analogues **5** and **6** (Figure 3). The 2,3-dimethoxy-5-bromo benzamide analogue, **4**, displayed a high affinity for dopamine D_3 receptors and a relatively low affinity for D_2, σ_1 and σ_2 receptors. Introduction of a dimethoxy substitution into the tetrahydroisoquinoline moiety (compound **5**) resulted in a dramatic increase in affinity for σ_2 receptors, no change in D_3 affinity, and a reduction in affinity for D_2 and σ_1 receptors. Since our previous structure-activity relationship studies had demonstrated that removal of the 3-methoxy group from the benzamide moiety results in a dramatic reduction in affinity for D_2 and D_3 receptors [6], compound **6** was prepared as a potential σ_2 receptor. As expected, the results of in vitro binding studies revealed that **6** had a reduced affinity for dopamine D_2 and D_3 receptors, a lower affinity for σ_1 receptors, and an increase in affinity for σ_2 receptors (compare **6** versus **5**). Further structural modifications resulting in the identification of potent σ_2 ligands involved the replacement of the 5-bromo substituent of **6** with a methyl group (compound **7**), and increasing the length of the methylene spacer from 2 carbons in **5** and **7** to four carbons (i.e., compounds **8** and **9**). Compounds **6**, **7**, **8**, and **9** are the most potent and selective σ_2 receptor ligands identified to date.

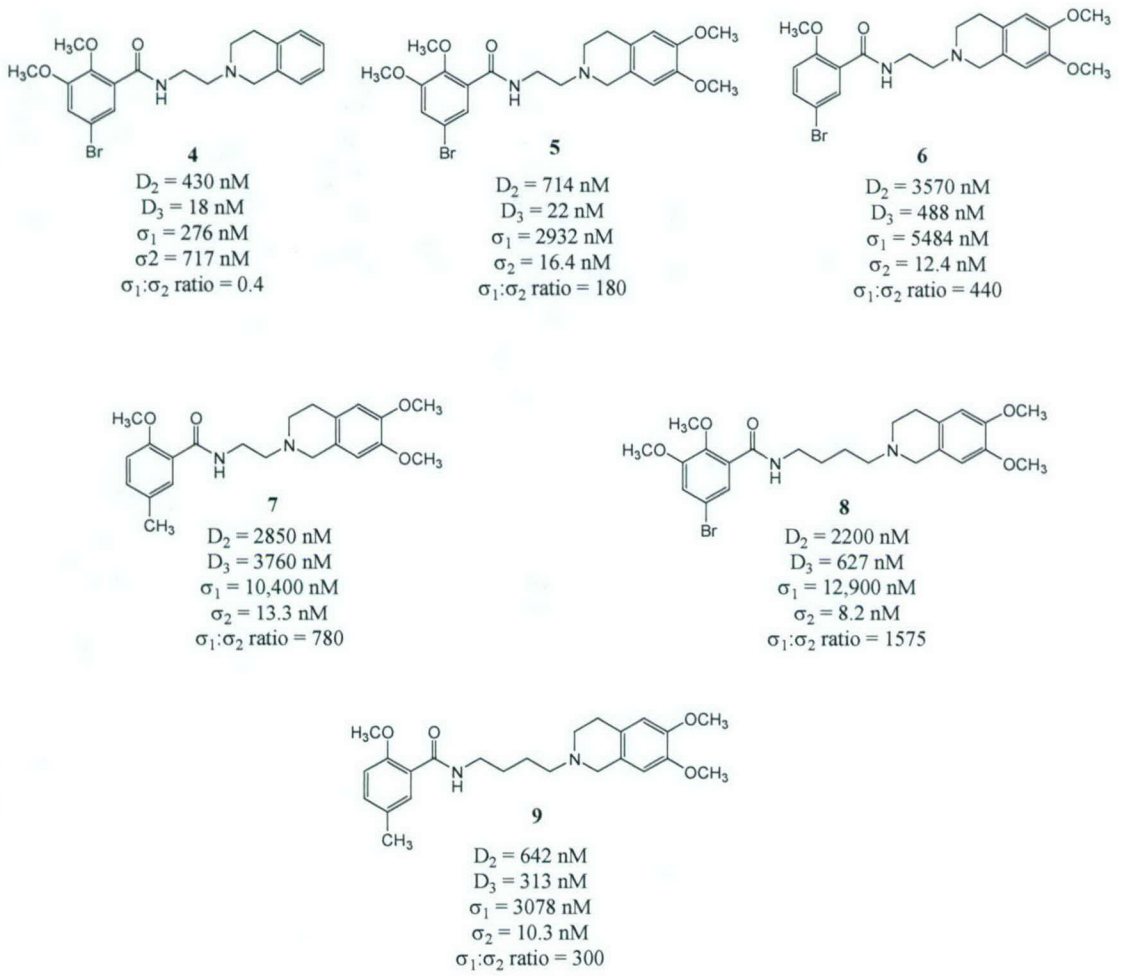

Figure 3. Structures of the σ_2-selective compounds for PET radiotracer development.

2.1. Carbon-11 labeled analogs. The presence of a 2-methoxy group in the lead compounds **6**, **7**, **8**, and **9** indicates that it is possible to prepare a ^{11}C-labeled version of the σ_2 ligands using standard radiochemistry procedures. This was accomplished via O-alkylation of the phenol precursor with [^{11}C]methyliodide. The overall yield (15-75% from [^{11}C]methyl iodide) and specific activity (1000 – 4000 mCi/μmol) of each radiotracer was suitable for in vivo studies.

Table II.

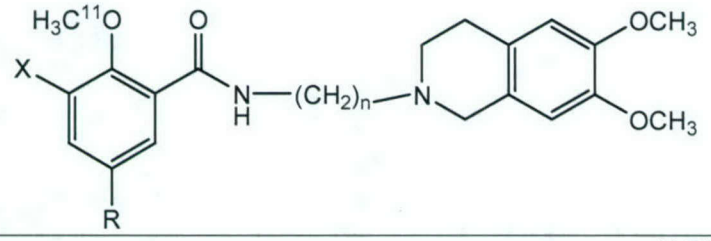

#	X	R	n	σ_1	σ_2	σ_1: σ_2 Ratio	% Yield	Specific Activity (EOB)
7	H	CH_3	2	10,412	13.3	783	60-75	~5,000 mCi/μmol
9	H	CH_3	4	3,078	10.3	300	60-75	~4,000 mCi/μmol
6	H	Br	2	5,484	12.2	442	10-15	~1,000 mCi/μmol
8	OCH_3	Br	4	12,900	8.2	1,573	30-40	~4,000 mCi/μmol

2.2. Biodistribution Studies of the ^{11}C-labeled radiotracers in Tumor-Bearing Mice. Biodistribution studies were conducted in mature Balb/c mice that were implanted with EMT-6 mammary tumors. The mice were implanted in the scapular region 7 days prior to the study. Animals were injected with 100-150 μCi of the ^{11}C-labeled radiotracer and the animals were sacrificed at 5, 30, and 60 min post-i.v. injection of the radiotracer. The results of the biodistribution studies are given in Tables III-VI.

Table III.

[^{11}C]**7** Biodistribution in EMT-6 BALB/C mice

%ID per gram	**5 min**	**30 min**	**1 hour**
blood	5.89 ± 0.29	2.62 ± 0.22	1.98 ± 0.35
lung	5.69 ± 0.70	1.42 ± 0.15	1.39 ± 0.67
liver	18.49 ± 2.87	3.87 ± 0.67	1.70 ± 0.23
kidney	44.07 ± 1.67	2.77 ± 0.42	1.01 ± 0.12
muscle	1.75 ± 0.21	0.56 ± 0.19	0.41 ± 0.22
fat	3.07 ± 0.40	0.38 ± 0.12	0.26 ± 0.09
heart	2.89 ± 0.36	0.76 ± 0.06	0.76 ± 0.46
brain	1.63 ± 0.30	0.11 ± 0.01	0.10 ± 0.04
tumor	3.10 ± 0.25	1.08 ± 0.08	0.85 ± 0.14
ratio			
Tumor:blood	0.53 ± 0.04	0.41 ± 0.02	0.44 ± 0.06
Tumor:lung	0.55 ± 0.07	0.77 ± 0.14	0.68 ± 0.19
Tumor:muscle	1.79 ± 0.20	2.08 ± 0.59	2.40 ± 0.84
Tumor:fat	1.03 ± 0.21	3.10 ± 1.21	3.46 ± 0.91
Tumor:heart	1.08 ± 0.10	1.43 ± 0.14	1.32 ± 0.45

Table IV.

[^{11}C]**9** Biodistribution in EMT-6 BALB/C mice

%ID per gram	5 min	30 min	1 hour
blood	3.09 ± 0.33	1.31 ± 0.11	0.73 ± 0.05
lung	14.02 ± 1.40	2.27 ± 0.42	1.09 ± 0.26
liver	12.32 ± 1.73	9.65 ± 2.00	3.00 ± 0.21
kidney	20.50 ± 1.86	4.12 ± 0.51	2.26 ± 0.36
muscle	4.49 ± 0.45	0.75 ± 0.13	0.49 ± 0.11
fat	1.88 ± 0.50	0.68 ± 0.19	0.33 ± 0.24
heart	5.86 ± 0.47	0.95 ± 0.17	0.50 ± 0.11
brain	2.29 ± 0.28	0.28 ± 0.03	0.15 ± 0.01
tumor	4.22 ± 1.01	2.35 ± 0.27	1.32 ± 0.17
ratio			
Tumor:blood	1.37 ± 0.33	1.80 ± 0.26	1.81 ± 0.11
Tumor:lung	0.31 ± 0.11	1.06 ± 0.24	1.28 ± 0.41
Tumor:muscle	0.93 ± 0.13	3.18 ± 0.51	2.78 ± 0.62
Tumor:fat	2.28 ± 0.32	3.68 ± 1.14	5.36 ± 2.38
Tumor:heart	0.71 ± 0.12	2.53 ± 0.55	2.78 ± 0.79

Table V.

[^{11}C]**6** Biodistribution in EMT-6 BALB/C mice

%ID per gram	5 min	30 min	1 hour
blood	5.25 ± 0.39	2.35 ± 0.16	1.88 ± 0.16
lung	5.72 ± 0.40	1.83 ± 0.13	1.32 ± 0.11
liver	19.88 ± 3.10	5.89 ± 0.82	2.65 ± 0.29
kidney	51.03 ± 7.14	34.19 ± 1.74	19.78 ± 1.99
muscle	1.73 ± 0.11	0.52 ± 0.23	0.36 ± 0.08
fat	2.05 ± 0.49	0.63 ± 0.19	0.37 ± 0.13
heart	3.18 ± 0.26	0.77 ± 0.08	0.56 ± 0.05
brain	2.52 ± 0.15	0.26 ± 0.10	0.14 ± 0.02
tumor	1.82 ± 0.39	1.06 ± 0.09	0.87 ± 0.09
ratio			
Tumor:blood	0.35 ± 0.07	0.45 ± 0.05	0.46 ± 0.02
Tumor:lung	0.32 ± 0.06	0.58 ± 0.07	0.66 ± 0.03
Tumor:muscle	1.05 ± 0.21	2.24 ± 0.63	2.52 ± 0.66
Tumor:fat	0.93 ± 0.27	1.76 ± 0.40	2.64 ± 1.12
Tumor:heart	0.57 ± 0.09	1.39 ± 0.17	1.56 ± 0.16

Table VI.

[^{11}C]**8** Biodistribution in EMT-6 BALB/C mice

%ID per gram	5 min	30 min	1 hour
blood	7.12 ± 1.01	0.99 ± 0.15	0.45 ± 0.04
lung	6.01 ± 0.77	1.34 ± 0.23	0.70 ± 0.26
liver(all)	25.02 ± 3.70	2.48 ± 0.52	1.19 ± 0.17
kidney	19.48 ± 1.46	2.57 ± 0.78	1.34 ± 0.19
muscle	1.94 ± 0.13	1.67 ± 0.14	0.26 ± 0.07
fat	1.66 ± 0.41	0.46 ± 0.19	0.20 ± 0.08
heart	3.54 ± 0.31	0.68 ± 0.12	0.29 ± 0.10
brain	0.33 ± 0.09	0.10 ± 0.00	0.03 ± 0.00
tumor	2.82 ± 0.36	0.92 ± 0.10	0.50 ± 0.09
ratio			
Tumor:blood	0.40 ± 0.01	0.94 ± 0.05	1.10 ± 0.11
Tumor:lung	0.47 ± 0.04	0.69 ± 0.08	0.79 ± 0.30
Tumor:muscle	1.46 ± 0.19	0.59 ± 0.05	1.84 ± 0.25
Tumor:fat	1.82 ± 0.45	2.05 ± 0.57	2.77 ± 0.82
Tumor:heart	0.80 ± 0.07	1.36 ± 0.12	1.86 ± 0.64

2.3. Synthesis of Radiohalogenated σ_2 Receptor Ligands. The presence of a bromine atom in compounds **6** and **8** (Table I) indicates that it is possible to prepare radiohalogenated probes of the σ_2 receptors by isotopic substitution with B-76, or by replacing the bromine atom with I-125. This was accomplished by preparing the corresponding tin precursor and conducting the oxidative radiohalogenation reactions outlined in Schemes II and III. The ^{125}I-labeled analogs, **10** and **11**, were obtained in an overall yield of 50% and a specific activity of 2200 mCi/μmol. Similarly, the ^{76}Br-labeled analogs of **5** and **7** were obtained in a yield of 50-60% and a specific activity >1,000 mCi/μmol. The σ_2 receptor affinity of the radioiodinated probes was 0.5 nM for [^{125}I]**10** and 0.25 nM for [^{125}I]**11** from Scatchard studies using membranes isolated from either rat liver or EMT-6 breast tumor cells.

Scheme II

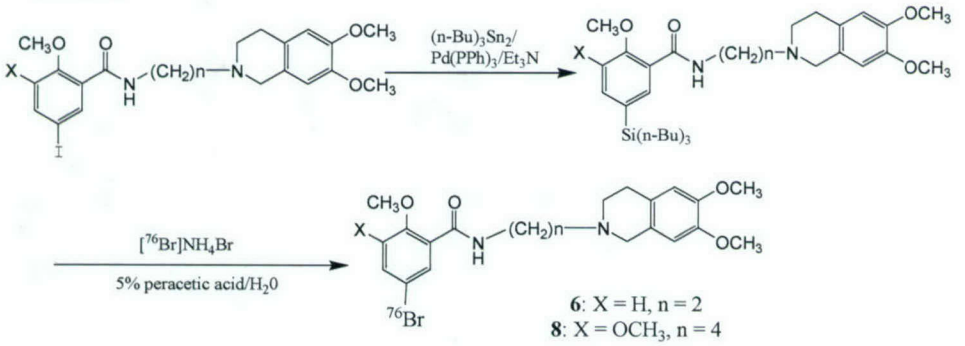

Scheme III

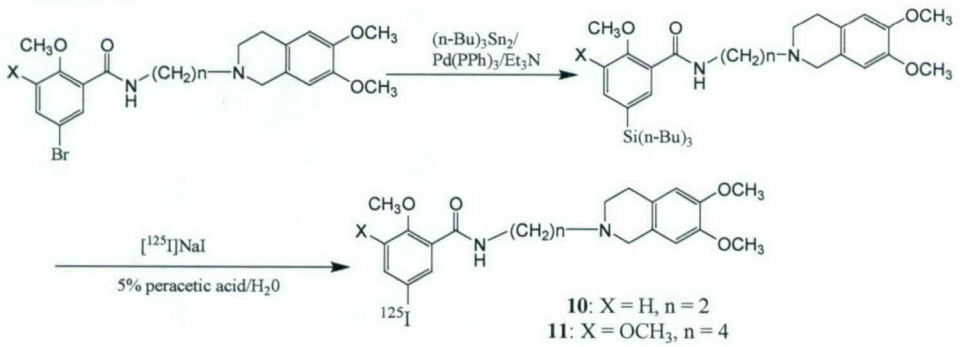

A series of biodistribution studies in tumor-bearing mice were also conducted with [^{76}Br]**6**, [^{76}Br]**8**, [^{125}I]**10**, and [^{125}I]**11**. The results of these studies are presented in Tables VII-X.

Table VII.

[^{76}Br]**6** Biodistribution in EMT-6 BALB/C mice				
%ID per gram	**5 min.**	**30 min.**	**1 hour**	**2 hour**
blood	4.55 ± 0.59	2.55 ± 0.06	2.08 ± 0.69	3.46 ± 0.66
lung	5.52 ± 0.73	1.59 ± 0.10	1.20 ± 0.27	1.75 ± 0.20
liver(all)	17.85 ± 3.17	5.57 ± 1.31	3.09 ± 0.48	3.77 ± 0.80
spleen	3.22 ± 0.75	0.92 ± 0.26	0.59 ± 0.06	0.72 ± 0.05
kidney	50.08 ± 2.09	32.24 ± 4.64	15.60 ± 2.01	3.61 ± 0.52
muscle	1.42 ± 0.05	0.57 ± 0.07	0.56 ± 0.26	0.45 ± 0.02
fat	2.61 ± 0.45	0.80 ± 0.05	0.66 ± 0.11	0.69 ± 0.18
heart	2.44 ± 0.43	0.99 ± 0.13	0.78 ± 0.14	1.23 ± 0.18
brain	1.69 ± 0.18	0.24 ± 0.05	0.15 ± 0.01	0.21 ± 0.01
bone	1.55 ± 0.20	0.52 ± 0.02	0.50 ± 0.17	0.49 ± 0.17
tumor	2.28 ± 0.14	1.30 ± 0.08	1.12 ± 0.20	1.19 ± 0.13
ratio				
Tumor:blood	0.50 ± 0.04	0.51 ± 0.02	0.58 ± 0.22	0.35 ± 0.21
Tumor:lung	0.42 ± 0.05	0.82 ± 0.05	0.98 ± 0.34	0.68 ± 0.10
Tumor:muscle	1.61 ± 0.05	2.31 ± 0.40	2.47 ± 1.53	2.63 ± 2.47
Tumor:fat	0.90 ± 0.20	1.63 ± 0.02	1.71 ± 0.29	1.82 ± 2.22
Tumor:heart	0.95 ± 0.13	1.32 ± 0.19	1.50 ± 0.49	0.98 ± 0.13

Table VIII.

[^{76}Br]**8** Biodistribution in EMT-6 BALB/C mice					
%ID per gram	**5 min.**	**30 min.**	**1 hour**	**2 hour**	**4 hour**
blood	2.12 ± 0.20	2.20 ± 0.24	1.60 ± 0.22	0.46 ± 0.07	0.21 ± 0.03
lung	24.64 ± 2.74	5.81 ± 1.12	2.45 ± 0.17	0.74 ± 0.04	0.29 ± 0.03
liver(all)	10.99 ± 0.29	8.85 ± 0.52	4.58 ± 0.36	1.67 ± 0.10	0.71 ± 0.08
spleen	12.50 ± 1.46	6.91 ± 1.22	2.61 ± 0.62	0.60 ± 0.03	0.20 ± 0.03
kidney	31.20 ± 2.92	18.51 ± 2.66	10.81 ± 1.72	1.85 ± 0.54	0.57 ± 0.12
muscle	3.62 ± 0.27	1.54 ± 0.49	0.61 ± 0.11	0.20 ± 0.03	0.07 ± 0.01
fat	3.78 ± 0.97	2.27 ± 0.16	0.81 ± 0.16	0.22 ± 0.05	0.04 ± 0.02
heart	7.31 ± 0.70	2.15 ± 0.30	1.08 ± 0.07	0.30 ± 0.03	0.11 ± 0.02
brain	1.60 ± 0.15	0.41 ± 0.06	0.17 ± 0.02	0.05 ± 0.00	0.03 ± 0.00
bone	3.10 ± 0.67	2.76 ± 0.58	1.38 ± 0.09	0.56 ± 0.20	0.12 ± 0.03
tumor	4.78 ± 0.78	5.31 ± 0.62	3.98 ± 0.58	1.71 ± 0.17	0.68 ± 0.15
ratio					
Tumor:blood	2.25 ± 0.28	2.41 ± 0.08	2.53 ± 0.54	3.79 ± 0.99	3.17 ± 0.58
Tumor:lung	0.19 ± 0.02	0.93 ± 0.09	1.64 ± 0.30	2.30 ± 0.13	2.36 ± 0.46
Tumor:muscle	1.32 ± 0.16	3.70 ± 1.06	6.76 ± 2.09	8.81 ± 0.91	9.48 ± 2.14
Tumor:fat	1.30 ± 0.24	2.35 ± 0.34	5.09 ± 1.39	7.97 ± 1.95	20.69 ± 10.77
Tumor:heart	0.65 ± 0.07	2.48 ± 0.17	3.72 ± 0.72	5.77 ± 0.60	6.24 ± 1.28

Table IX.

[^{125}I]**10** Biodistribution in EMT-6 BALB/C mice				
%ID per gram	**5 min.**	**30 min.**	**1 hour**	**2 hour**
blood	6.90 ± 1.29	2.44 ± 0.65	1.17 ± 0.29	3.37 ± 1.23
lung	5.95 ± 1.30	1.39 ± 0.29	0.81 ± 0.20	1.27 ± 0.37
liver(all)	41.37 ± 7.23	8.20 ± 1.05	2.87 ± 0.34	3.47 ± 1.05
kidney	54.77 ± 8.42	38.59 ± 2.05	18.07 ± 2.07	8.46 ± 1.26
muscle	1.47 ± 0.20	0.70 ± 0.25	0.37 ± 0.23	0.38 ± 0.06
fat	3.46 ± 0.59	1.03 ± 0.44	0.77 ± 0.66	0.37 ± 0.13
heart	2.79 ± 0.35	0.94 ± 0.19	0.40 ± 0.02	0.86 ± 0.26
brain	1.42 ± 0.33	0.20 ± 0.06	0.06 ± 0.02	0.09 ± 0.03
tumor	2.91 ± 0.40	1.33 ± 0.13	0.71 ± 0.12	0.82 ± 0.09
ratio				
Tumor:blood	0.42 ± 0.03	0.57 ± 0.12	0.62 ± 0.09	0.26 ± 0.08
Tumor:lung	0.50 ± 0.07	0.98 ± 0.16	0.91 ± 0.24	0.67 ± 0.14
Tumor:muscle	2.00 ± 0.37	2.06 ± 0.69	2.14 ± 0.99	2.17 ± 0.23
Tumor:fat	0.84 ± 0.06	1.49 ± 0.65	1.93 ± 1.87	2.44 ± 0.77
Tumor:heart	1.04 ± 0.08	1.44 ± 0.18	1.81 ± 0.32	1.00 ± 0.27

Table X.

[^{125}I]**11** Biodistribution in EMT-6 BALB/C mice					
%ID per gram	**5 min.**	**30 min.**	**1 hour**	**2 hour**	**4 hour**
blood	2.37 ± 0.26	2.19 ± 0.16	1.52 ± 0.49	0.65 ± 0.07	0.29 ± 0.11
lung	27.13 ± 1.61	5.50 ± 0.62	2.12 ± 0.19	1.01 ± 0.18	0.29 ± 0.05
liver(all)	13.20 ± 2.04	8.77 ± 0.88	4.24 ± 0.60	1.91 ± 0.20	0.90 ± 0.21
kidney	29.51 ± 2.23	13.69 ± 0.35	5.94 ± 1.22	2.45 ± 0.25	0.63 ± 0.11
muscle	4.10 ± 0.33	1.21 ± 0.17	0.87 ± 0.22	0.31 ± 0.10	0.10 ± 0.04
fat	4.15 ± 0.91	1.73 ± 0.20	0.74 ± 0.17	0.33 ± 0.08	0.10 ± 0.05
heart	6.55 ± 0.54	1.94 ± 0.09	0.91 ± 0.10	0.40 ± 0.05	0.15 ± 0.04
brain	1.53 ± 0.14	0.39 ± 0.03	0.15 ± 0.03	0.06 ± 0.01	0.02 ± 0.01
tumor	4.02 ± 0.55	4.50 ± 0.43	3.53 ± 0.42	1.88 ± 0.76	0.82 ± 0.09
ratio					
Tumor:blood	1.73 ± 0.46	2.07 ± 0.32	2.44 ± 0.53	2.83 ± 1.62	3.11 ± 0.85
Tumor:lung	0.15 ± 0.02	0.82 ± 0.09	1.66 ± 0.17	1.99 ± 1.04	2.83 ± 0.19
Tumor:muscle	0.98 ± 0.13	3.94 ± 0.55	4.26 ± 0.74	6.99 ± 4.44	8.98 ± 3.01
Tumor:fat	1.00 ± 0.20	2.62 ± 0.27	4.85 ± 0.67	5.86 ± 2.93	9.59 ± 4.55
Tumor:heart	0.61 ± 0.07	2.32 ± 0.18	3.89 ± 0.08	4.85 ± 2.31	5.91 ± 1.65

2.4. Blocking studies. The results of the above biodistribution studies in tumor bearing rodents indicate that [^{11}C]**9**, [^{76}Br]**8**, and [^{125}I]**11** are potential candidates for further evaluation. The next step in the project was to conduct blocking studies in order to confirm that the radiotracer labeled σ_2 receptors in the breast tumors. These studies were conducted using the nonselective sigma ligand, YUN 143 (1 mg/kg, i.v.), which has a high affinity for both σ_1 and σ_2 receptors. We have previously reported that [^{18}F]YUN 143 labels σ_1 and σ_2 receptors in breast tumor xenografts [7]. The results of the blocking study are shown in Figure 4 and are consistent with the labeling of σ_2 receptors in vivo.

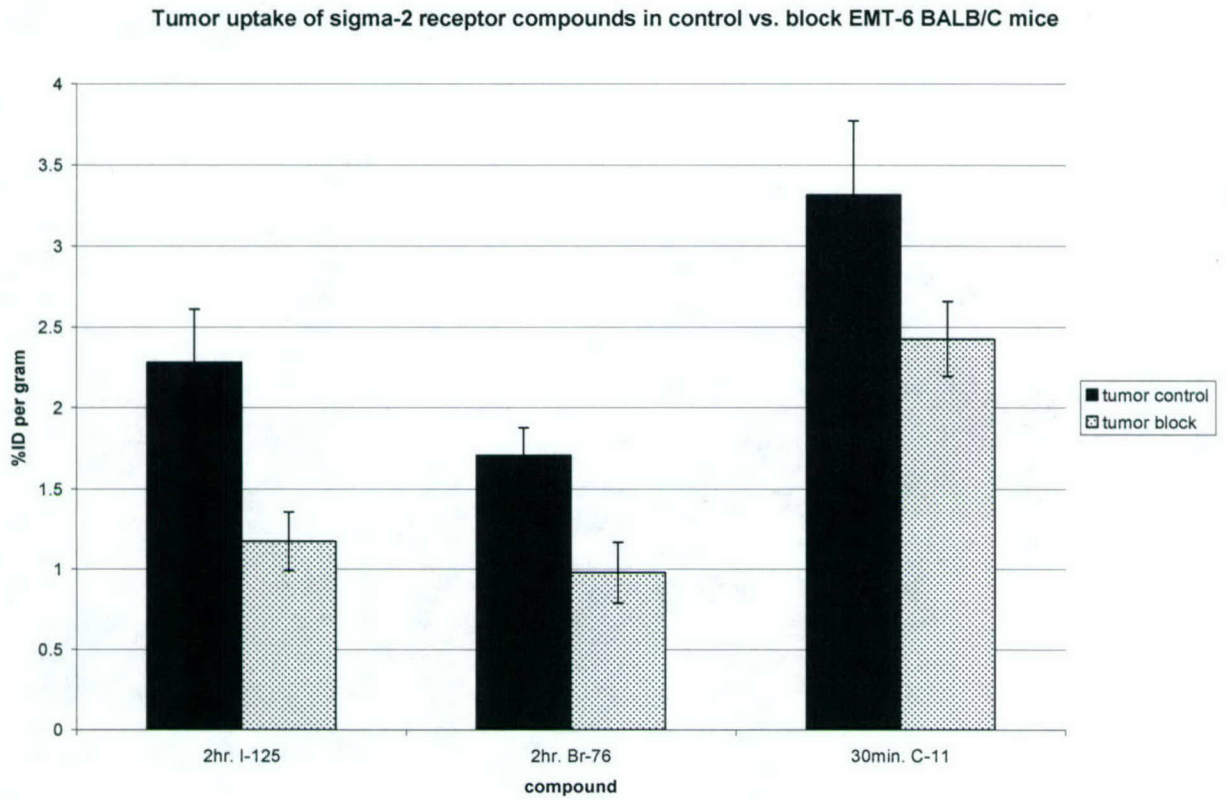

Figure 4. In vivo blocking studies of [^{125}I]**11** (left), [^{76}Br]**8** (center), and [^{11}C]**9** (right) in tumor-bearing mice. The blocking agent was YUN 143, which has a high affinity for σ_1 and σ_2 receptors. Animals were sacrificed at the time point displaying the highest %I.D./gram tumor. The data are consistent with the labeling of σ_2 receptors in vivo by each radiotracer.

2.5. Comparison with [^{18}F]FLT. Although not a part of this IDEA grant award, we have also conducted a series of studies comparing the σ_2 receptor imaging approach with [^{18}F]FLT. [^{18}F]FLT is a the nucleoside-based approach that has been hypothesized to measure the proliferation in solid tumors. These studies were funded in part through the NIH grant CA102869 and the results are summarized in Figures 5-7. In this study, the uptake of [^{18}F]FLT at 1 hr was compared with the 1 hr data for [^{11}C]**9**. For studies comparing [^{18}F]FLT with [^{76}Br]**8** and [^{125}I]**11**, the 2 hr post-i.v. injection time point was used. The results of these studies can be summarized as follows:

1. [^{11}C]**9**, has tumor:lung and tumor:fat ratios equal to [^{18}F]FLT and tumor:blood, tumor:muscle and tumor:heart ratios that are greater than that of [^{18}F]FLT;

2. [^{76}Br]**8**, has higher tumor:background ratios greater than that observed with [^{18}F]FLT;

3. [^{125}I]**11**, has a similar tumor:fat ratio as [^{18}F]FLT and exceeds [^{18}F]FLT in all other tumor:background ratios.

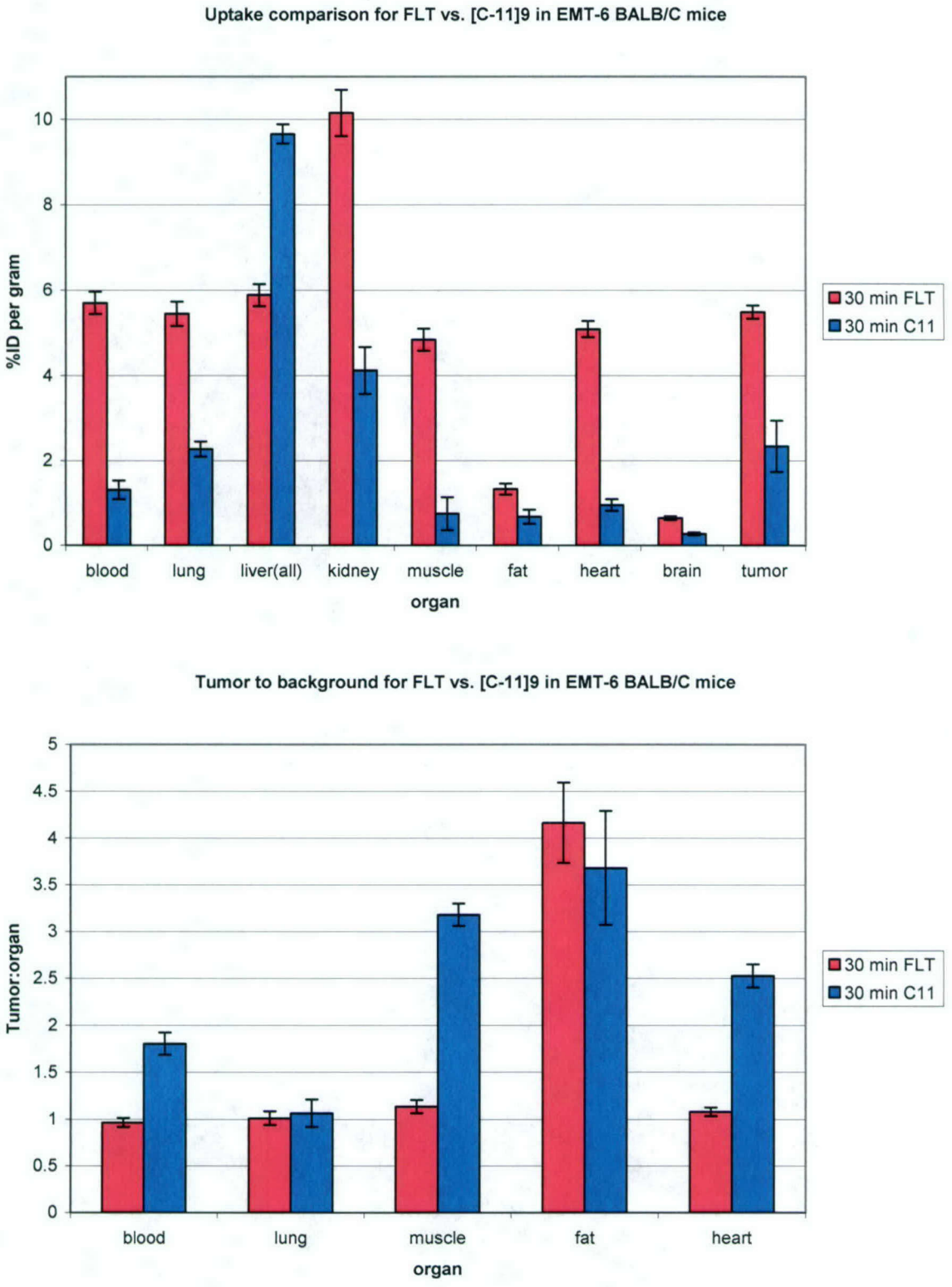

Figure 5. Comparison of [^{18}F]FLT and [^{11}C]**9**. Although [^{18}F]FLT has a high uptake in tumors (top graph), the high uptake of radioactivity in normal tissues results in a lower tumor:background radio of [^{18}F]FLT relative to [^{11}C]**9**, particularly the tumor:muscle, tumor:blood, and tumor:heart ratios (bottom graph).

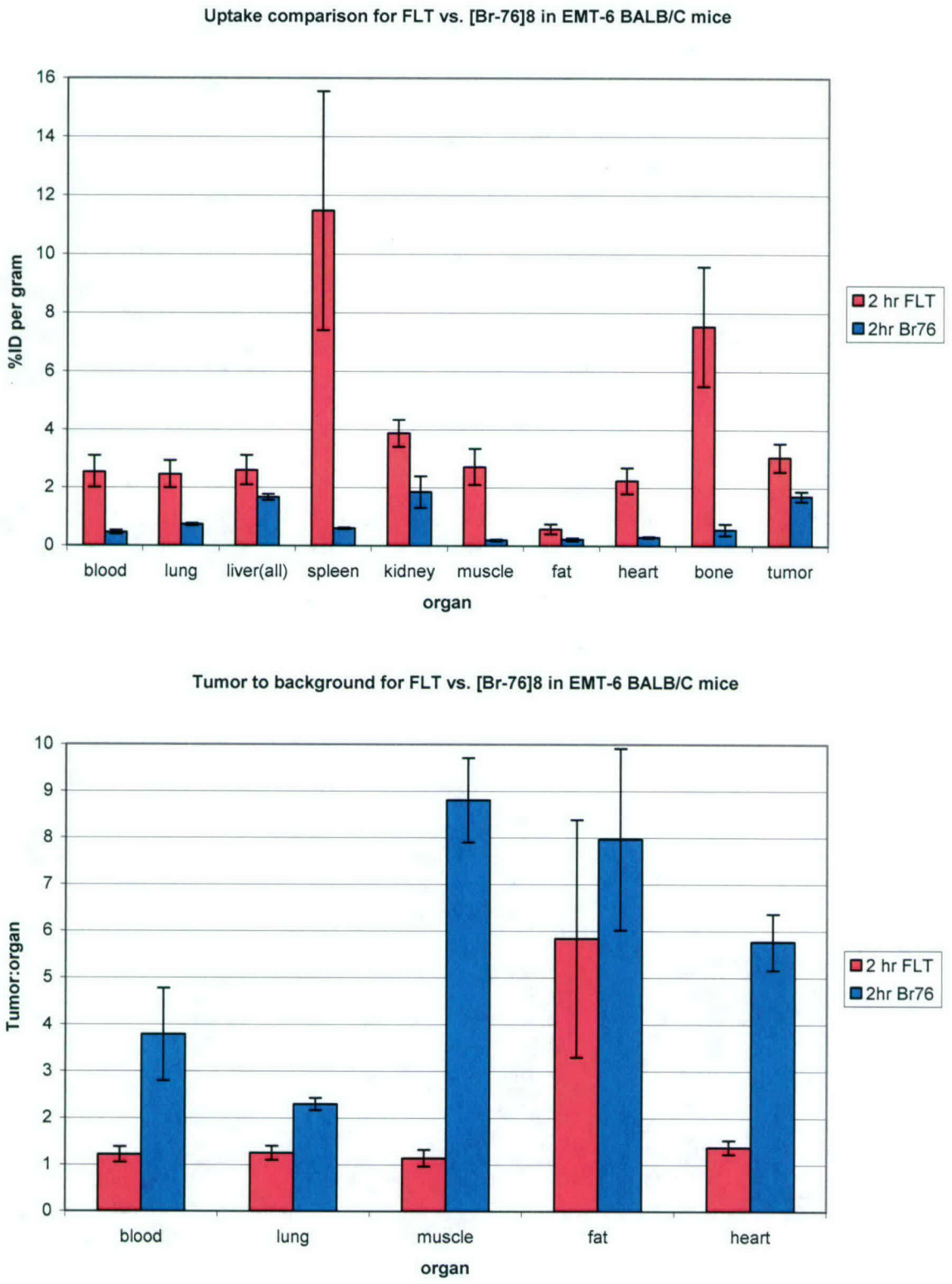

Figure 6. Comparison of [^{18}F]FLT with [^{76}Br]**8** at 2 hrs post-i.v. injection. Notice the higher tumor:background ratios of [^{76}Br]**7** versus that of [^{18}F]FLT.

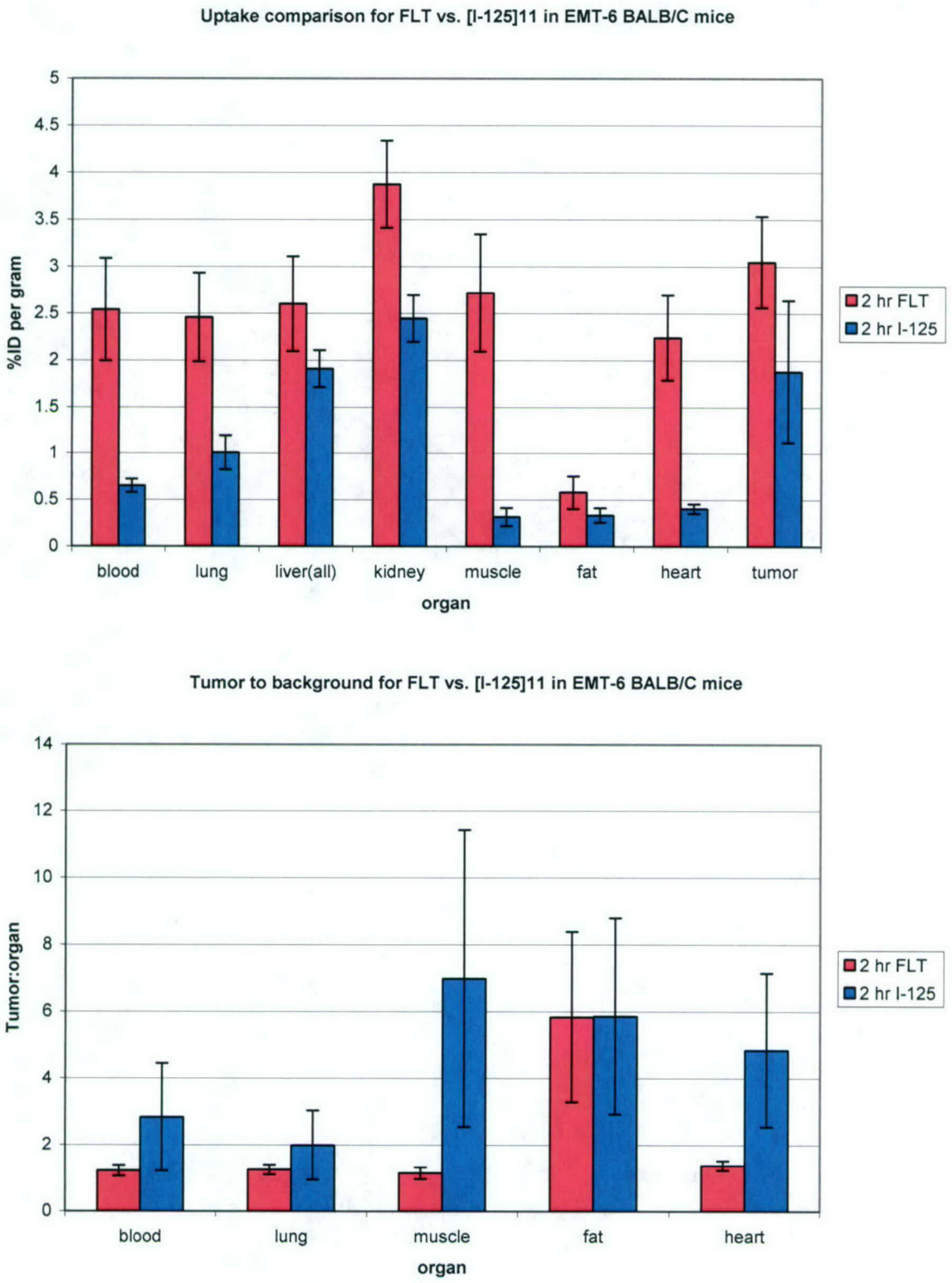

Figure 7. Comparison of [^{18}F]FLT with [^{125}I]**11** at 2 hrs post-i.v. injection. Notice the higher tumor:blood, tumor:muscle, and tumor:heart ratios of [^{125}I]**11** versus that of [^{18}F]FLT.

2.6. MicroPET Imaging Studies. We have also conducted microPET imaging studies with [^{76}Br]**8** in Balb-c mice bearing EMT-6 breast tumor xenografts. The results of the imaging studies are shown in Figure 8. Note the high uptake of the radiotracer in the NCA study (left image), which can be blocked with a known sigma receptor ligand (right image). These data indicate that [^{76}Br]**8** is a potential radiotracer for imaging the σ_2 receptor status of breast tumors.

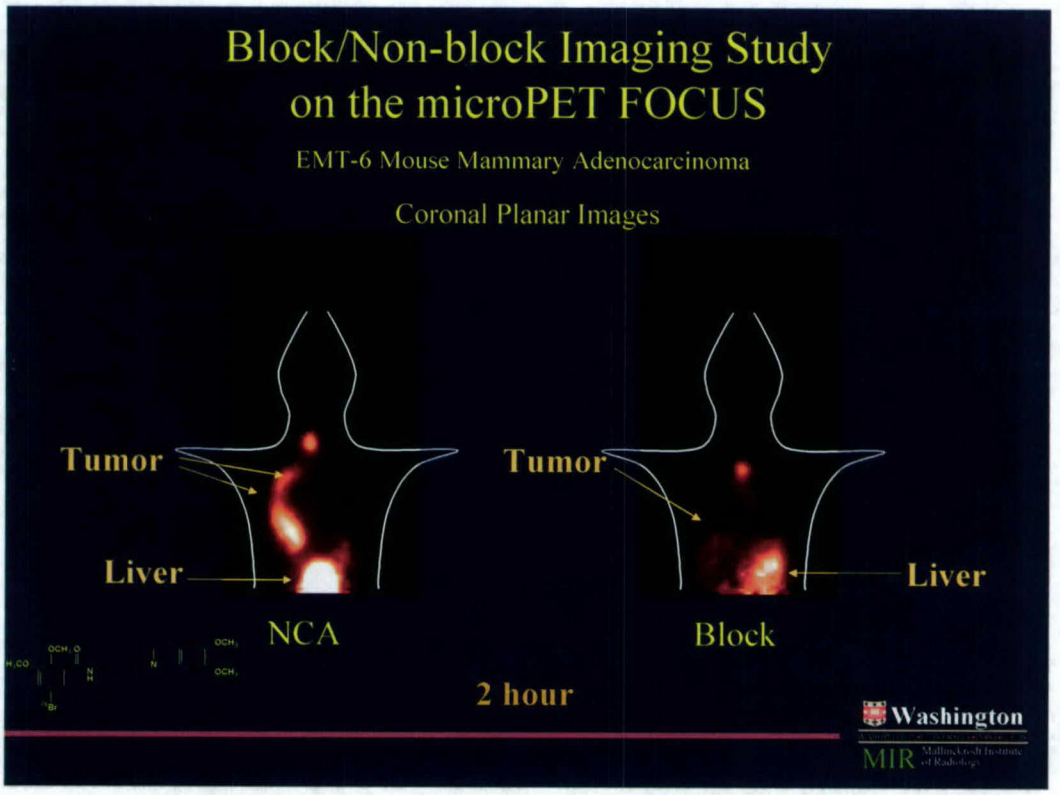

Figure 8. MicroPET imaging studies of [^{76}Br]**8** in Balb-c mice bearing an EMT-6 breast tumor xenograft. The no-carrier-added (NCA) study is on the left and the sigma receptor blocking study (1 mg/kg, i.v. YUN-143) is shown on the right.

Key Research Accomplishments

- Identification of a new lead compound for PET radiotracer development and completion of a structure-activity relationship study aimed at improving the affinity and selectivity of the lead compound for σ_2 versus σ_1, D_2 and D_3 receptors.
- Preparation of a ^{11}C-, ^{125}I, and ^{76}Br-labeled σ_2 receptor ligands and completion of in vivo biodistribution and microPET imaging studies.
- Comparison of the σ_2 receptor imaging approach with that of the nucleoside-based imaging agent, [^{18}F]FLT, and demonstration that the σ_2 receptor approach yields signal:noise ratios equal or greater than that of [^{18}F]FLT.

Reportable Outcomes

Mach R.H., Vangveravong S., Huang Y., Yang B., Blair J.B., Wu L. Synthesis of N-substituted 9-azabicyclo[3.3.1]nonan-3α-yl phenylcarbamate analogs as sigma-2 receptor ligands. *Medicinal Chemistry Research* 2003; 11: 380-398.

Mach R.H., Huang Y., Freeman R.A., Wu L., Vangveravong S., Luedtke R.R. Conformationally-flexible benzamide analogs as dopamine D_3 and σ_2 receptor ligands. *Bioorg Med. Chem. Lett* 2004; 14: 195-202.

Mach R.H., Brown-Proctor C., Vangveravong S., Blair J.B., Buchheimer N., Bottoms J., Wheeler K.T. Receptor-based radiotracers for imaging the proliferative status of breast tumors. *Synthesis and Applications of Isotopically Labelled Compounds, Volume* 8; 2004: 157-160.

Tu Z., Dence C.S., Ponde D.E., Jones L., Wheeler K.T., Welch M.J., Mach R.H. Carbon-11 labeled σ_2 receptor ligands for imaging breast cancer. *Nucl. Med. Biol.*, accepted for publication.

Rowland D.J., Tu Z., Mach R.H., Welch M.J. Investigation of a new sigma-2 receptor ligand for detecting breast cancer. *J. Label. Compd. Radiopharm.* 2003; 46: S6.

Tu Z., Dence C.S., Wheeler K.T., Welch M.J., Mach R.H. Carbon-11 labeled sigma-2 receptor ligands for imaging breast cancer. *J. Nucl. Med.* 2004; 45: 168P.

Mach R.H., Kung M.-P., Tu Z., Vangveravong S., Wheeler K.T., Kung H.F., Welch M.J. Radioiodinated probes for imaging the σ_2 receptor status of breast tumors. *J. Nucl. Med.* 2004; 45: 170P.

Conclusions

We have made outstanding progress over the course of this research project. For example, we have identified a new class of σ_2-selective radiotracers that can be readily radiolabeled with C-11, I-125/I-123, and Br-76. Preliminary biodistribution studies indicate that [^{11}C]**8**, [^{76}Br]**7**, and [^{125}I]**11** display a high tumor uptake and reasonable target:background ratios. Comparison studies with [^{18}F]FLT indicate that the σ_2 receptor imaging approach may give a higher signal:noise background ratio versus the labeled nucleoside approach. The results of this IDEA grant have been used as the preliminary data to obtain funding from the National Cancer Institute (CA102869) to continue this avenue of research. We hope to initiate a clinical trial in breast cancer patients with one of the radiotracers described in this progress report.

References

[1] Mach RH, Smith CR, Al-Nabulsi I, Whirrett BR, Childers SR, Wheeler KT. Sigma-2 receptors as potential biomarkers of profileration in breast cancer. *Cancer Res* 1997; 57:156-161.

[2] Al-Nabulsi I, Mach RH, Wang L-M, Wallen CA, Keng PC, Sten K, Childers SR, Wheeler KT. Effect of ploidy, recruitment, environmental factors, and tamoxifen treatment on the expression of sigma-2 receptors in proliferating and quiescent tumor cells. *Br J Cancer* 1999; 81:925-933.

[3] Wheeler KT, Wang L-M, Wallen CA, Childers SR, Cline JM, Keng PC, Mach RH. Sigma-2 receptors as a biomarker of proliferation in solid tumors. *Br J Cancer* 2000; 86:1223-1232.

[4] Mach RH, Yang B, Wu L, Kuhner RJ, Whirrett BR, West T. Synthesis and sigma receptor binding affinities of 8-azabicyclo[3.2.1]octan-3α-yl and 9 azabicyclo[3.3.1]nonan-3α-yl phenyl carbamates. *Med Chem Res* 2001; 10(6):399-355.

[5] Mach RH, Elder ST, Morton TE, Nowak PA, Evora PH, Scripko JG, Luedtke RR, Unsworth CD, Filtz T, Rao AV, Molinoff PB, Ehrenkaufer RL. The use of [^{18}F]4-fluorobenzyliodide (FBI) in PET radiotracer synthesis: model alkylation studies and its application in the design of dopamine D_1 and D_2 receptor-based imaging agents. *Nucl Med Biol* 1993; 20:777-794.

[6] Mach RH, Hammond PS, Huang Y, Yang B, Xu Y, Cheney JT, Freeman R, Luedtke RR. Structure-activity relationship studies of N-(9-benzyl)-9-azabicyclo-[3.3.1]nonan-3β-yl benzamide analogues for dopamine D_2 and D_3 receptors. *Med Chem Res* 1999; 9:355-373.

[7] Mach RH, Huang Y, Buchheimer N, Kuhner R, Wu L, Morton TE, Wang L-M, Ehrenkaufer RL, Wallen CA, Wheeler KT. [^{18}F]N-4'-fluorobenzyl-4-(3-bromophenyl)acetamide for imaging the sigma receptor status of tumors: comparison with [^{18}F]FDG and [^{125}I]IUDR. *Nucl Med Biol* 2001; 28:451-458.

Appendices

Mach R.H., Vangveravong S., Huang Y., Yang B., Blair J.B., Wu L. Synthesis of N-substituted 9-azabicyclo[3.3.1]nonan-3α-yl phenylcarbamate analogs as sigma-2 receptor ligands. *Medicinal Chemistry Research* 2003; 11: 380-398.

Mach R.H., Huang Y., Freeman R.A., Wu L., Vangveravong S., Luedtke R.R. Conformationally-flexible benzamide analogs as dopamine D_3 and σ_2 receptor ligands. *Bioorg Med. Chem. Lett* 2004; 14: 195-202.

Mach R.H., Brown-Proctor C., Vangveravong S., Blair J.B., Buchheimer N., Bottoms J., Wheeler K.T. Receptor-based radiotracers for imaging the proliferative status of breast tumors. *Synthesis and Applications of Isotopically Labelled Compounds, Volume* 8; 2004: 157-160.

Tu Z., Dence C.S., Ponde D.E., Jones L., Wheeler K.T., Welch M.J., Mach R.H. Carbon-11 labeled σ_2 receptor ligands for imaging breast cancer. *Nucl. Med. Biol.*, accepted for publication.

APPENDICES

Med Chem Res 11:7 (2003) 380–398

MEDICINAL CHEMISTRY RESEARCH

SYNTHESIS OF N-SUBSTITUTED 9-AZABICYCLO[3.3.1]NONAN-3α-YL PHENYLCARBAMATE ANALOGS AS SIGMA-2 RECEPTOR LIGANDS

Robert H. Mach,[†,‡*] Suwanna Vangveravong,[†,±] Yunsheng Huang,[†,±]
Biao Yang,[†,±] Joseph B. Blair[†] and Li Wu,[†]

Departments of Radiology[†] and Physiology & Pharmacology,[‡]
Wake Forest University School of Medicine, Winston-Salem, North Carolina 27157

[±] Anasazi Biomedical Research, Inc., Winston-Salem, NC 27101

Abstract. A series of N-substituted-9-azabicyclo[3.3.1]nonan-3α-yl)carbamate analogs was prepared and their affinities for sigma (σ_1 and σ_2) receptors was measured in vitro. The results of this structure-activity relationship study identified a novel compound, *N*-(9-(4-aminophenethyl))-9-azabicyclo[3.3.1]nonan-3α-yl)-*N'*-(2-methoxy-5-methylphenyl)carbamate (**2f**), having a high affinity and excellent selectivity for σ_2 versus σ_1 receptors. This compound should be a useful ligand for characterizing the functional role of σ_2 receptors in vivo.

Sigma (σ) receptors represent a class of proteins that were initially thought to be a subtype of the opiate receptors. Subsequent studies revealed that sigma binding sites are a separate class of receptors located in the central nervous system and in a variety of tissues and organs.[1,2] It is widely accepted that there are two subtypes of the sigma receptor, termed σ_1 and σ_2. Sigma-1 receptors have a molecular weight of ~25 kDa, whereas σ_2 receptors have a molecular weight of ~21.5 kDa.

Address correspondence to: Robert H. Mach, Ph.D. Division of Radiological Sciences, Washington University School of Medicine, 510 S. Kingshighway Blvd., Campus Box 8225, St. Louis, MO 63110

The radioligand [^{3}H](+)-pentazocine has a high affinity (3.2 nM) for the σ_1 receptor and a low (>1,000 nM) affinity for the σ_2 receptor, whereas [^{3}H]DTG is equipotent at both σ_1 and σ_2 receptors.[1] An understanding of the functional significance of sigma binding sites has been limited by the failure to identify an endogenous ligand for these receptors. However, the σ_1 receptor has been cloned and displays a 30% sequence homology with the enzyme yeast sterol isomerase.[3] Progesterone possesses a modest affinity for σ_1 receptors,[4] which suggests that the σ_1 receptor may play a role in steroid biochemistry. The σ_2 receptor has not been cloned, but evidence suggests that it is linked to potassium channels in NCB-20 cells.[1,2] Attempts to clone the σ_2 receptor have been hampered by the shortage of ligands displaying a high affinity and selectivity for this subtype.

A number of structurally-diverse compounds have been shown to possess a high affinity for sigma receptors.[1] Most of these compounds display either a high selectivity for the σ_1 receptor or bind with equal affinity to both σ_1 and σ_2 receptors. Until recently, only a few σ_2 selective ligands have been identified. For example, the phenyl morphan CD-184,[5] the trishomocubane analog ANSTO-20,[6] and the natural product ibogaine[7,8] have been shown to possess a moderate affinity and selectivity for σ_2 versus σ_1 receptors. Other reports have shown that spiro-joined piperidines,[9] and the corresponding 3-(α-aminoalkyl)-1H-indole derivatives of the spiro-joined piperidines and tropanes,[10] exhibit varying degrees of preference for σ_2 versus σ_1 receptors. In addition, the potent 5-HT$_3$ and 5-HT$_4$ ligand, BIMU-1,[11] was also found to have a moderate affinity and high selectivity for σ_2 versus σ_1 receptors.

Using BIMU-1 as a lead compound, we recently reported the synthesis and *in vitro* binding of a number of [3.2.1]azabicyclooctane (i.e., tropane) and [3.3.1]azabicyclononane (i.e., granatane) analogs having a modest affinity and selectivity for σ_2 versus σ_1 receptors.[12] The most active compound in this series was **1a**, which had a σ_2 affinity of 3 nM and a σ_2 versus σ_1 selectivity ratio of 30 (Figure 1). The goal of the current study was to extend the structure-activity relationship study of this class of compounds by: 1) determining the effect of increasing the alkyl spacer group between the benzyl aromatic ring and the bridgehead nitrogen atom; and 2) the nature of the substituent effect in the aromatic ring attached to the bridgehead nitrogen atom. The results of this study led to the identification of **2f** as a highly selective σ_2 ligand.

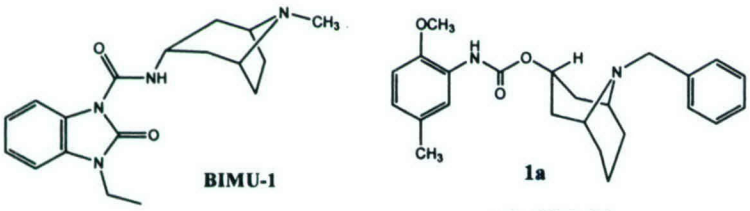

Figure 1. Structures of BIMU-1 and compound **1a**.

Methods

Chemistry. The synthesis of the target compounds is outlined in Schemes I and II. The first step in the synthesis involved the removal of benzyl group from **1a** *via* catalytic hydrogenation (Scheme I). N-alkylation of the secondary amine, **8**, with the corresponding alkyl halide or tosylate gave compounds **1b-j**, **2a-e**, and **3-7** in moderate yield. The synthesis of compound **1k** was achieved using the sequence of reactions outlined in Scheme II.

Pharmacology. σ_1 binding studies were conducted using the σ_1-selective radioligand, [^{3}H](+)-pentazocine in guinea pig brain membranes according to published procedures.[1,2] σ_2 sites were assayed in rat liver membranes with [^{3}H]DTG in the presence of (+)-pentazocine (100 nM) to mask σ_1 sites.[1,2]

Scheme I

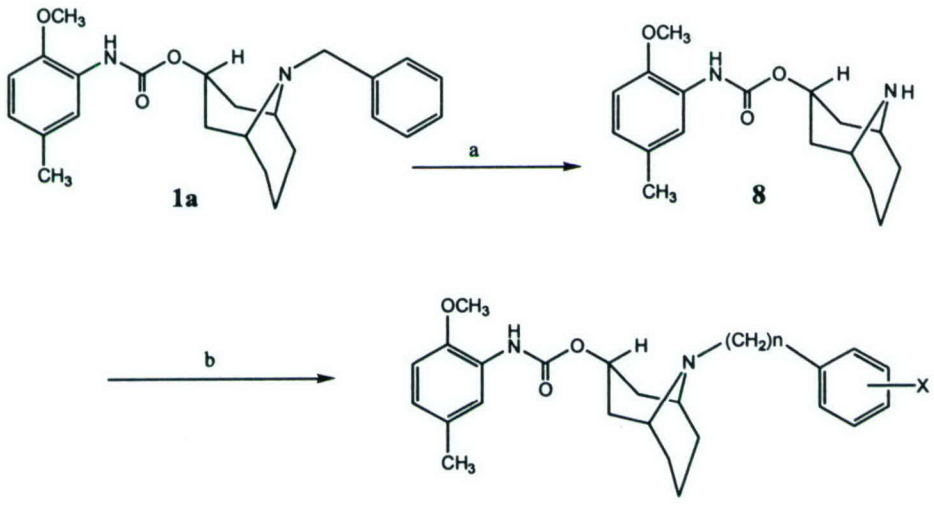

1b-j, 2a-e, 3-7

Reagents: a: H_2/Pd/c/ethanol; Ar-(CH_2)nBr, or Ar-(CH_2)nCl/, or Ar-(CH_2)nOTs/KI/ethanol/reflux.

Scheme II

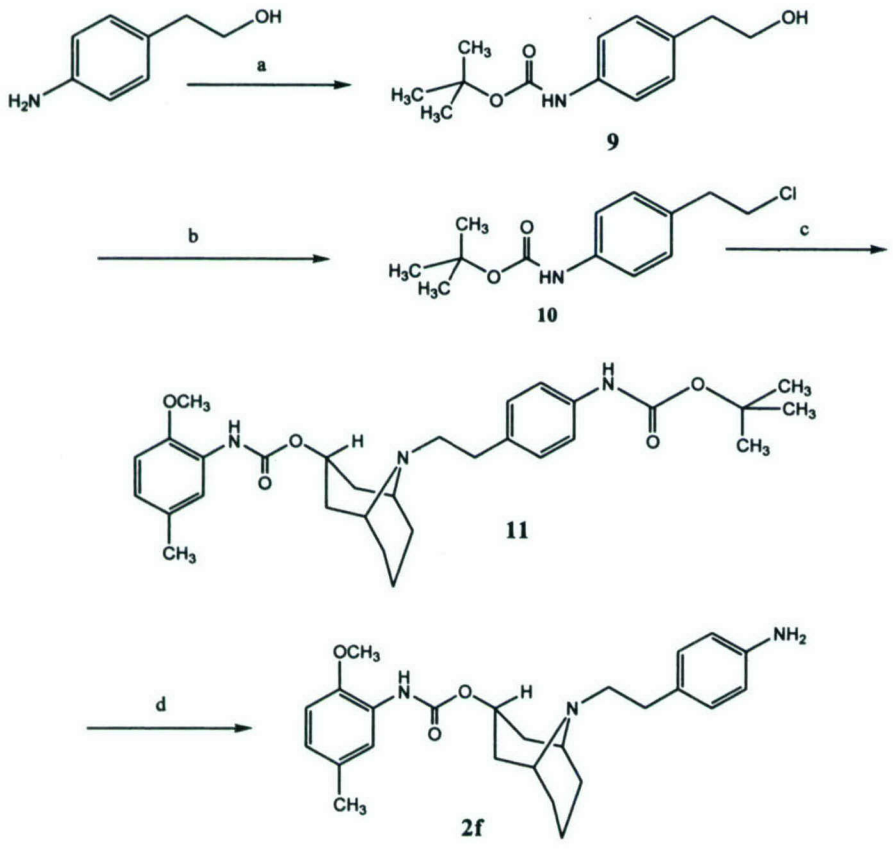

Reagents: a: di-*tert*-butyl dicarbonate/ethyl acetate; b: $(Ph)_3P/CCl_4$/reflux; c: $K_2CO_3/KI/CH_3CN$/reflux; d: CF_3COOH/CH_2Cl_2.

Results

The results of the *in vitro* binding studies are shown in Tables I - III. Sequential extension of the methylene linker group separating the benzene ring and the bridgehead nitrogen atom from n = 1 to n = 7 had little effect on the binding affinity for sigma receptors. All compounds in this series (**1a**, **2a** and **3 – 7**) had a higher affinity for σ_2 versus σ_1 receptors. The σ_1: σ_2 selectivity ratio, which is the ratio of the Ki values for the σ_1 and σ_2 receptors, ranged from 10 to 50 for this class of

compounds. In order to explore the nature of the substituent effect in the aromatic ring of compound **1a**, a number of substituted N-benzyl analogs were prepared and their affinities for σ_1 and σ_2 receptors were measured *in vitro* (Table II). Substitution of either the 2-, 3-, or 4-position of **1a** with any substituent resulted in either a modest or dramatic reduction in affinity for σ_2 receptors. For example, there was a 10-fold reduction in affinity for σ_2 receptors when the 4-position of the benzyl aromatic ring was substituted with a fluorine substituent. However, substitution of either the 2- or 3-position with a fluorine substituent resulted in a 70-100-fold reduction in σ_2 receptor affinity. A similar trend was observed with the iodine-substituted analogs (**1e-g**) and the 2- and 4-nitro analogs, **1i** and **1j**. An interesting observation was the effect of substitution of the benzyl aromatic ring on the σ_1:σ_2 selectivity ratio, which represents the relative selectivity of a compound for σ_2 versus σ_1 receptors. The σ_1: σ_2 selectivity ratio of **1a** was 30, whereas the σ_1:σ_2 selectivity ratio was lower for the substituted benzyl analogs possessing an appreciable affinity for σ_1 and σ_2 receptors (i.e., <1,000 nM). These data suggest that the effect of substitution of the aromatic ring on σ_1 receptor affinity was not as dramatic as that of the σ_2 receptor.

In order to further explore the nature of the substituent effects in this class of compounds, a number of 4-substituted N-phenethyl derivatives were prepared and their affinities for σ_1 and σ_2 receptors were measured (Table III). An unexpected finding was the difference in the substituent effect in the 4-position of the N-phenethyl series versus the N-benzyl series. For example, substitution of the 4-position of the N-benzyl analog with a fluorine atom resulted in a 10-fold reduction in σ_2 receptor affinity, whereas the same substitution resulted in a lower reduction in σ_2 affinity for the N-phenethyl analog, **2b**. In addition, there was no difference in σ_2 receptor affinity for the 4-F and 4-I analogs in the N-benzyl series (compare **1b** and **1e**), but the 4-I analog, **2c**, had a much lower affinity for σ_2 receptors than the corresponding 4-F analog, **2b**. A similar statement can be made for the 4-methyl analogs, **1h** versus **2d**. However, substitution of the 4-position with a nitro substituent resulted in about a 10-fold reduction in σ_2 receptor affinity for both the N-benzyl and N-phenethyl analogs. An unexpected observation was the relatively high σ_2 receptor affinity, and outstanding σ_1: σ_2 selectivity ratio of the 4-amino analog, **2f**. This high σ_1:σ_2 selectivity ratio was caused, in part, by the dramatic reduction in σ_1 receptor affinity on introducing this substituent into the 4-position of the N-phenethyl aromatic ring. It is of interest to note that the N-BOC analog, 11, was devoid of activity at both σ_1 and σ_2 receptors (Table III).

Table I. In vitro binding data for compounds **1** - **7**.

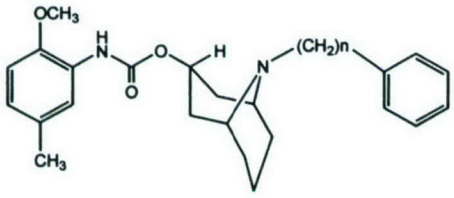

		Ki [nM]		
#	n	σ_1[a]	σ_2[b]	σ_1:σ_2 Ratio[c]
1a	1	92.5 ± 11.0	3.1 ± 0.8	30
2a	2	59.9 ± 4.6	1.2 ± 0.1	50
3	3	73.0 ± 1.6	2.0 ± 0.1	37
4	4	65.5 ± 4.3	2.9 ± 0.2	23
5	5	17.3 ± 1.2	1.8 ± 0.2	9.6
6	6	214 ± 24	7.6 ± 0.4	28
7	7	230 ± 29	7.6 ± 0.2	30

[a]Ki for inhibiting the binding of [^{3}H](+)-pentazocine to guinea pig brain homogenates (mean ± S.E.M.; n = 3); [b]Ki for inhibiting the binding of [^{3}H]DTG to rat liver homogenates (mean ± S.E.M.; n = 3); [c]Ki for σ_1/Ki for σ_2.

Table II. In vitro binding data for the substituted benzyl analogs.

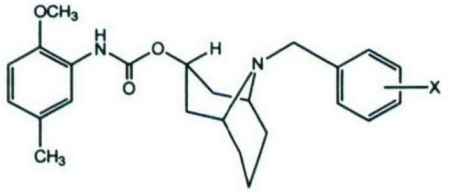

		Ki [nM]		
#	X	σ_1[a]	σ_2[b]	σ_1:σ_2 Ratio[c]
1a	H	92.5 ± 11.0	3.1 ± 0.8	30
1b	4-F	202 ± 22	30.0 ± 2.0	6.7
1c	2-F	>1,000	206 ± 13	>5
1d	3-F	322 ± 37	318 ± 44	1
1e	4-I	454 ± 78	30.6 ± 3.9	14.8
1f	2-I	>1,000	>1,000	-
1g	3-I	1354 ± 213	50.9 ± 3.9	26.6
1h	4-CH_3	273 ± 23	15.5 ± 1.8	17.7
1i	4-NO_2	539 ± 42	25.2 ± 3.8	21.4
1j	2-NO_2	>1,000	>1,000	-

[a,b,c]Refer to Table I.

Table III. In vitro binding data for the 4-substituted phenethyl analogs.

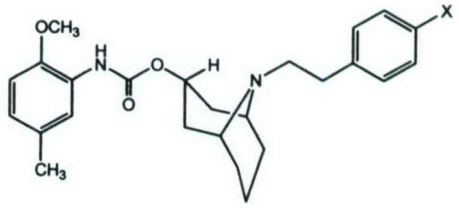

		Ki [nM]		
#	X	σ_1[a]	σ_2[b]	σ_1:σ_2 Ratio[c]
2a	H	59.9 ± 4.6	1.2 ± 0.1	30
2b	F	262 ± 37	5.9 ± 1.5	44
2c	I	175 ± 7	141 ± 9	1.2
2d	CH_3	>1,000	83 ± 6	>12
2e	NO_2	215 ± 39	11.5 ± 2.4	19
2f	NH_2	2,250 ± 73	5.0 ± 0.2	510
11	NHBOC	>1,000	>1,000	-

[a,b,c]Refer to Table I.

Discussion

The goal of the current study was to develop ligand having a high affinity and selectivity for σ_2 versus σ_1 receptors. In an earlier study, we prepared a number of structural analogs of the mixed serotonin 5-HT_3/5-HT_4 ligand, BIMU-1, having a high affinity for σ_2 versus σ_1 receptors and a low (or negligible) affinity at serotonin 5-HT_3 and 5-HT_4 receptors. The structural modification of BIMU-1 in the previous study included: 1) replacing the urea linkage of BIMU-1 with a conformationally-flexible carbamate moiety; 2) replacing the N-methyl group with an N-benzyl group, which had an adverse effect on serotonin receptor affinity while causing little effect on binding to σ_1 and σ_2 receptors; and, 3) comparison of both the tropane and granatane ring systems. The results of this study revealed that the N-benzylgranatane analog, **1a**, as a potential σ_2 selective ligand having no affinity for either 5-HT_3 or 5-HT_4 receptors. The goal of the present study we to explore the N-benzyl region of **1a** in order to determine if it is possible to further improve the affinity and selectivity of this compound for σ_2 versus σ_1 receptors.

The first strategy involved extending the length of the methylene spacer group between the bridgehead nitrogen and the benzene ring of the N-benzyl moiety. The result of this study (Table I)

revealed that this change had little effect on the binding to σ_2 receptors, and a relatively minor effect on binding to the σ_1 receptor. These data suggested that the substituent may not play a key role in binding to the σ_2 receptor. If this was indeed the case, then the addition of a substituent in the aromatic ring of **1a** is expected to have little effect on σ_2 receptor affinity. This turned out to be contrary to what was expected, and substitution of the benzyl aromatic ring of **1a** with any substituent resulted in a reduction in affinity to the σ_2 receptor (Table II). Substitution of the 4-position of the benzyl ring had a lower reduction in σ_2 receptor affinity when compared with the corresponding 2- and 3-substituted analogs. There was no clear trend with respect to the nature of the substituent effect since compounds **1b – 1j** had a lower affinity for σ_2 receptors relative to the unsubstituted analog, **1a**. However, substitution of the benzyl aromatic ring had a lesser effect on σ_1 receptor affinity since the σ_1:σ_2 selectivity ratio of compounds having an appreciable affinity for sigma receptors (<1,000 nM) was less than the ratio of that for **1a**.

As a means of further exploring the nature of the substituent effects for this class of compounds, we prepared a series of 4-substituted N-phenethyl analogs and measured their affinities for sigma receptors *in vitro*. Substitution of the 4-position was chosen since the substitution of this position resulted in a lower reduction in σ_2 receptor affinity in the N-benzyl series of compounds. The results of this study revealed a different structure-activity relationship with respect to σ_2 receptor affinity relative to that of the N-benzyl analogs. In the N-phenethyl series, substitution of the 4-position with a polar substituent such as a fluoro, nitro, or amino group retained a high affinity for σ_2 receptors, whereas the nonpolar substituents, iodo and methyl groups, resulted in a 70 – 100-fold reduction in affinity for the σ_2 receptor. This difference in substituent effect between the N-benzyl and N-phenethyl series is also apparent when one compares the binding properties of the 4-F and 4-I analogs. In the N-benzyl series, the 4-F and 4-I analogs had an identical σ_2 receptor affinity, whereas the 4-F had a 25-fold higher σ_2 receptor affinity versus the 4-I analog. Furthermore, the 4-methyl analog was more potent than the 4-F analog in the N-benzyl series, whereas the reverse is true for the N-phenethyl analogs. An unexpected observation was the outstanding σ_1: σ_2 selectivity ratio of compound **2f**. This high ratio can be attributed to both the retention in σ_2 affinity and the dramatic reduction in σ_1 receptor affinity on introducing an amino group in the 4-position of **2a**. Compound **2f** is one on the most potent and selective σ_2 receptor ligands reported to date.

In conclusion, we have extended our sigma receptor structure activity relationship study of the granatane analog, **1a**, to include an investigation of the N-benzyl region of this molecule. The results of this study revealed a high degree of steric tolerance in this region of the molecule with respect to σ_2 receptor affinity since a methylene spacer group from n = 1 to n = 7 was well tolerated. Substitution of the N-benzyl aromatic ring resulted in a moderate to dramatic reduction in σ_2 receptor affinity, depending on the position of the aromatic ring where the substitution occurred. Substitution of the 4-position of the N-phenethyl analog, **2a**, resulted in compounds having a high σ_2 receptor affinity and good to excellent σ_1: σ_2 selectivity ratio, provided that the substituent was polar (i.e., F, NO_2 or NH_2). Substitution with a nonpolar substituent (i.e., CH_3 or I) resulted in compounds having a low σ_2 receptor affinity. The 4-amino phenethyl analog, **2f**, was found to have a high affinity and an outstanding σ_1:σ_2 selectivity ratio. This compound is likely to be a useful ligand for studying the functional role of σ_2 receptors both in vivo and in vitro.

Experimental

^{1}H NMR spectra were recorded on a Bruker 300 MHz NMR spectrometer. Chemical shifts are reported in δ values (parts per million, ppm) relative to an internal standard of tetramethylsilane (TMS). The following abbreviations are used for multiplicity of NMR signals: br s = broad singlet, d = doublet, dd = doublet of doublets, m = multiplet, q = quintet, s = singlet, t = triplet. Melting points were determined on a Fischer-Johns melting point apparatus and are uncorrected. Elemental analyses were performed by Atlantic Microlab, Inc., Norcross, GA and were within ± 0.4% of the calculated values. Mass spectrometry was provided by the Washington University Mass Spectrometry Resource (St. Louis, MO) with support from the NIH National Center for Research Resources (Grant No. P41RR0954). All reactions were carried out under an inert atmosphere of nitrogen.

General procedure for the synthesis of *N*-substituted-9-azabicyclo[3.3.1]nonan-3α-yl)-*N*-(2-methoxy-5-methylphenyl)carbamates (Scheme I).

A mixture of *N*-(9-azabicyclo[3.3.1]nonan-3α-yl)-*N*-(2-methoxy-5-methylphenyl) carbamate (**8**)[13] (200 mg, 0.66 mmol), appropriate phenalkyl halides (2.64 mmol), potassium iodide (438 mg, 2.64

mmol), and potassium carbonate (729 mg, 5.28 mmol) in acetonitrile (10 mL) was stirred at reflux overnight. The volatile components were evaporated and water (10 mL) was added, and the product extracted into dichloromethane (3 x 10 mL). The organic layers were combined, dried (magnesium sulfate) and concentrated under reduced pressure. The residue was purified by silica gel column chromatography (5% methanol in dichloromethane) to afford the target compounds.

***N*-(9-(4-Fluorobenzyl)-9-azabicyclo[3.3.1]nonan-3α-yl)-*N*-(2-methoxy-5-methylphenyl)-carbamate hydrochloride (1b).** Yield 37% from 4-fluorobenzyl bromide, mp 157-160 °C (HCl salt). ^{1}H NMR (300 MHz, $CDCl_3$) δ 7.96 (s, 1H), 7.29-7.36 (m, 2H), 7.16 (s, 1H), 6.96-7.03 (m, 2H), 6.73-6.80 (m, 2H), 5.24 (q, J = 7.3 Hz, 1 H), 3.84 (s, 3H), 3.76 (s, 2H), 3.02-3.05 (m, 2 H), 2.41-2.51 (m, 2H), 2.30 (s, 3H), 2.10-2.22 (m, 1H), 1.87-1.99 (m, 2H), 1.48-1.54 (m, 3H), 1.16-1.20 (m, 2H). Anal. ($C_{24}H_{29}N_2O_3F$·HCl·0.4H_2O) C, H, N.

***N*-(9-(2-Fluorobenzyl)-9-azabicyclo[3.3.1]nonan-3α-yl)-*N*-(2-methoxy-5-methylphenyl)-carbamate (1c).** Yield 83% from 2-fluorobenzyl bromide. ^{1}H NMR (300 MHz, $CDCl_3$) δ 7.33-7.46 (m, 2H), 6.93-7.20 (m, 5H), 6.71-6.75 (m, 2H), 5.18-5.28 (m, 1H), 3.76 (s, 3H), 3.70 (s, 2H), 2.80-2.99 (m, 2 H), 2.25-2.40 (m, 2H), 2.18 (s, 3H), 1.75-1.98 (m, 3H), 1.25-1.47 (m, 2H), 0.95-1.14 (m, 3H). HRFAB calculated for $C_{24}H_{29}N_2O_3F$ [M+Li] 419.2322, found 419.2330.

***N*-(9-(3-Fluorobenzyl)-9-azabicyclo[3.3.1]nonan-3α-yl)-*N*-(2-methoxy-5-methylphenyl)-carbamate (1d).** Yield 60% from 3-fluorobenzyl bromide. ^{1}H NMR (300 MHz, $CDCl_3$) δ 6.74-7.23 (m, 8H), 6.72-6.75 (m, 1H), 5.14-5.22 (m, 1H), 3.71 (s, 3H), 3.70 (s, 2H), 2.80-2.98 (m, 2 H), 2.25-2.35 (m, 2H), 2.19 (s, 3H), 1.60-1.89 (m, 3H), 1.26-1.35 (m, 2H), 0.86-1.00 (m, 3H). HRFAB calculated for $C_{24}H_{29}N_2O_3F$ [M+Li] 419.2322, found 419.2336.

***N*-(9-(4-Iodobenzyl)-9-azabicyclo[3.3.1]nonan-3α-yl)-*N*-(2-methoxy-5-methylphenyl)-carbamate (1e).** Yield 44% from 4-iodobenzyl bromide, mp 97.5-100 °C. ^{1}H NMR (300 MHz, $CDCl_3$) δ 7.96 (s,1H), 7.68 (d, J = 8.7 Hz, 1H), 7.62 (d, J = 8.7 Hz, 2H), 7.12 (d, J = 8.4 Hz, 2H), 6.73-6.80 (m, 2H), 5.22 (q, J = 7.3 Hz, 1H), 3.84 (s, 3H), 3.74 (s, 2H), 3.01-3.04 (m, 2H), 2.41-2.51 (m, 2H), 2.30 (s, 3H), 2.10-2.21 (m,1H), 1.86-1.97 (m, 2H), 1.48-1.54 (m, 2H), 1.16-1.26 (m, 3H). HRFAB calculated for $C_{24}H_{30}N_2O_3I$ $[M+H]^+$ 521.1301, found 521.1283.

***N*-(9-(2-Iodobenzyl)-9-azabicyclo[3.3.1]nonan-3α-yl)-*N*-(2-methoxy-5-methylphenyl)-carbamate (1f).** Yield 40% from 2-iodobenzyl chloride, mp 53-55 °C (free base). ^{1}H NMR (300 MHz, $CDCl_3$) δ 7.74-7.79 (m, 2H), 7.37-7.49 (m, 2H), 6.88-7.00 (m, 3H), 6.72-6.75 (m, 1H), 5.19-5.30 (m, 1H), 3.76 (s, 3H), 3.69 (s, 2H), 2.86-3.05 (m, 2 H), 2.30-2.40 (m, 2H), 2.17 (s, 3H), 1.75-1.90 (m, 3H), 1.30-1.40 (m, 2H), 0.95-1.10 (m, 3H). HRFAB calculated for $C_{24}H_{29}N_2O_3F$ [M+Li] 527.1383, found 527.1386.

***N*-(9-(3-Iodobenzyl)-9-azabicyclo[3.3.1]nonan-3α-yl)-*N*-(2-methoxy-5-methylphenyl)-carbamate hydrochloride (1g).** Yield 44% from 3-iodobenzyl bromide, mp 167-168 °C (HCl salt). ^{1}H NMR (300 MHz, $CDCl_3$) δ 7.96 (s, 1H), 7.68 (s, 1H), 7.56 (d, J = 7.7 Hz, 1H), 7.35 (d, J = 7.7 Hz, 1H), 7.15 (s, 1H), 7.05 (t, J = 7.7 Hz, 1H), 6.73-6.80 (m, 2H), 5.22 (q, J = 7.1 Hz, 1 H), 3.85 (s, 3H), 3.74 (s, 2H), 3.00-3.04 (m, 2 H), 2.41-2.51 (m, 2H), 2.30 (s, 3H), 2.11-2.21 (m, 1H), 1.87-1.98 (m, 2H), 1.49-1.55 (m, 3H), 1.18-1.22 (m, 2H). Anal. ($C_{24}H_{29}N_2O_3I$·HCl) C, H, N.

***N*-(9-(4-Methylbenzyl)l-9-azabicyclo[3.3.1]nonan-3α-yl)-*N*-(2-methoxy-5-methylphenyl)-carbamate hydrochloride (1h).** Yield 85% from 4-methylbenzyl bromide, mp 146-148 °C (HCl salt). ^{1}H NMR (300 MHz, $CDCl_3$) δ 8.00 (s, 1H), 7.15-7.29 (m, 5H), 6.77-6.82 (m, 2H), 5.26-5.30 (m, 1H), 3.88 (s, 3H), 3.80 (s, 2H), 3.08 (s, 2 H), 2.49 (s, 2H), 2.37 (s, 3H), 2.34 (s, 3H), 2.15-2.20 (m, 1H), 1.92-2.00 (m, 2H), 1.50-1.61 (m, 3H), 1.12-1.20 (m, 2H). Anal. ($C_{25}H_{32}N_2O_3$·HCl·0.5H_2O) C, H, N.

***N*-(9-(4-Nitrobenzyl)-9-azabicyclo[3.3.1]nonan-3α-yl)-*N*-(2-methoxy-5-methylphenyl)-carbamate hydrochloride (1i).** Yield 84% from 4-nitrobenzyl bromide, mp 157-159 °C (HCl salt). ^{1}H NMR (300 MHz, $CDCl_3$) δ 8.17 (d, J = 8.7 Hz, 1H), 7.96 (s, 1H), 7.53 (d, J = 8.7 Hz, 2H), 7.16 (s, 1H), 6.73-6.81 (m, 2H), 5.25 (q, J = 7.4 Hz, 1 H), 3.90 (s, 2H), 3.85 (s, 3H), 3.01-3.04 (m, 2 H), 2.44-2.54 (m, 2H), 2.30 (s, 3H), 2.10-2.24 (m, 1H), 1.88-2.00 (m, 2H), 1.52-1.60 (m, 3H), 1.20-1.25 (m, 2H). Anal. ($C_{24}H_{29}N_3O_5$·HCl) C, H, N.

***N*-(9-(2-Nitrobenzyl)-9-azabicyclo[3.3.1]nonan-3α-yl)-*N*-(2-methoxy-5-methylphenyl)-carbamate (1j).** Yield 45 % from 2-nitrobenzyl bromide, mp 45-47 °C (free base). ^{1}H NMR (300

MHz, $CDCl_3$) δ 7.97 (s, 1H), 7.77-7.80 (m, 1H), 7.50-7.62 (m, 2H), 7.34-7.39 (m, 1H), 7.14 (s, 1H), 6.72-6.80 (m, 2H), 5.16 (q, J = 7.1 Hz, 1 H), 4.06 (s, 2H), 3.84 (s, 3H), 2.95-2.98 (m, 2 H), 2.40-2.50 (m, 2H), 2.30 (s, 3H), 2.09-2.18 (m, 1H), 1.83-1.93 (m, 2H), 1.48-1.56 (m, 3H), 1.18-1.23 (m, 2H). HRFAB calculated for $C_{24}H_{29}N_3O_5$ [M+Li] 446.2267, found 446.2265.

***N*-(9-Phenethyl-9-azabicyclo[3.3.1]nonan-3α-yl)-*N*-(2-methoxy-5-methylphenyl)carbamate (2a).** Yield 45% from phenethyl bromide, mp 183.5-186 °C (free amine). ^{1}H NMR (300 MHz, $CDCl_3$) δ 7.92 (s, 1H), 7.14 (s, 1H), 7.01 (d, J = 8.2 Hz, 2H), 6.74-6.82 (m, 2H), 6.64 (d, J = 8.2 Hz, 2H), 5.10-5.17 (m, 1H), 3.85 (s, 3H), 3.38-3.61 (m, 4H), 3.00-3.13 (m, 2H), 2.50-2.75 (m, 4H), 2.30 (s, 3H), 2.00-2.11 (m, 2H), 1.43-1.77 (m, 6H). Anal. ($C_{25}H_{32}N_2O_3$·HCl·0.25H_2O) C, H, N.

***N*-(9-(4-Fluorophenethyl)-9-azabicyclo[3.3.1]nonan-3α-yl)-*N*-(2-methoxy-5-methylphenyl)-carbamate hydrochloride (2b).** Yield 94% from 4-fluorophenethyl chloride, mp 172-174 °C (HCl salt). ^{1}H NMR (300 MHz, $CDCl_3$) δ 7.96 (s, 1H), 7.15-7.20 (m, 3H), 6.95-7.01 (m, 2H), 6.74-6.81 (m, 2H), 5.13 (q, J = 6.8 Hz, 1H), 3.86 (s, 3H), 3.08-3.15 (m, 2H), 2.80-2.84 (m, 2 H), 2.67-2.72 (m, 2H), 2.42-2.52 (m, 2H), 2.31 (s, 3H), 2.10-2.25 (m, 1H), 1.84-1.94 (m, 2H), 1.51-1.58 (m, 3H), 1.24-1.28 (m, 2H). Anal. ($C_{25}H_{31}N_2O_3F$·HCl) C, H, N.

***N*-(9-(4-Iodophenethyl)-9-azabicyclo[3.3.1]nonan-3α-yl)-*N*-(2-methoxy-5-methylphenyl)-carbamate (2c).** Yield 50% from 4-iodophenethyl chloride, mp 239-242 °C. ^{1}H NMR (300 MHz, $CDCl_3$) δ 7.91 (s, 1H), 7.68 (d, J = 6.0 Hz, 2H), 7.29-7.30 (m, 3H), 6.79-6.87 (m, 2H), 5.17-5.24 (m, 1H), 3.88 (s, 3H), 3.71 (s, 2H), 3.27-3.40 (m, 4H), 2.59-2.62 (m, 2H), 2.33 (s, 3H), 2.07-2.20 (m, 4H), 1.61-1.89 (m, 4H). HRFAB calculated for $C_{25}H_{32}N_2O_3I$ $[M+H]^+$ 535.1458, found 535.1460.

***N*-(9-(4-Nitrophenethyl)-9-azabicyclo[3.3.1]nonan-3α-yl)-*N*-(2-methoxy-5-methylphenyl)-carbamate hydrochloride (2e).** Yield 35% from 4-nitrophenethyl bromide, mp 164-165 °C (HCl salt). ^{1}H NMR (300 MHz, $CDCl_3$) δ 8.15 (d, J = 8.6 Hz, 2H), 7.94 (s, 1H), 7.37 (d, J = 8.6 Hz, 2H), 7.14 (s, 1H), 6.73-6.81 (m, 2H), 5.09 (q, J = 7.0 Hz, 1H), 3.84 (s, 3H), 3.06-3.09 (m, 2H), 2.78-2.88 (m, 4H), 2.39-2.49 (m, 2H), 2.30 (s, 3H), 2.11-2.17 (m, 1H), 1.77-1.89 (m, 2H), 1.43-1.56 (m, 3H), 1.23-1.26 (m, 2H). Anal. ($C_{25}H_{31}N_3O_5$·HCl·0.5H_2O) C, H, N.

***N*-(9-Phenpropyl-9-azabicyclo[3.3.1]nonan-3α-yl)-*N*-(2-methoxy-5-methylphenyl)carbamate hydrochloride (3).** Yield 58% from 1-bromo-3-phenylpropane, mp 174-176.5 °C (HCl salt). ^{1}H NMR (300 MHz, $CDCl_3$) δ 7.95 (s, 1H), 7.14-7.30 (m, 6H), 6.64-6.79 (m, 2H), 5.11-5.17 (m, 1H), 3.84 (s, 3H), 2.85-3.04 (m, 2H), 2.42-2.67 (m, 8H), 2.29 (s, 3H), 1.15-1.88 (m, 8H). Anal. ($C_{26}H_{34}N_2O_3 \cdot HCl \cdot 0.6H_2O$) C, H, N.

***N*-(9-Phenbutyl-9-azabicyclo[3.3.1]nonan-3α-yl)-*N*-(2-methoxy-5-methylphenyl)carbamate hydrochloride (4).** Yield 90% from 1-chloro-4-phenylbutane, mp 179-182 °C (HCl salt). ^{1}H NMR (300 MHz, $CDCl_3$) δ 7.95 (s, 1H), 7.12-7.29 (m, 6H), 6.72-6.76 (m, 2H), 5.08-5.15 (m, 1H), 3.84 (s, 3H), 2.90-3.04 (m, 2H), 2.41-2.62 (m, 6H), 2.29 (s, 3H), 1.18-1.89 (m, 12H). Anal. ($C_{27}H_{36}N_2O_3 \cdot HCl \cdot 0.5H_2O$) C, H, N.

***N*-(9-Phenpentyl-9-azabicyclo[3.3.1]nonan-3α-yl)-*N*-(2-methoxy-5-methylphenyl)carbamate hydrochloride (5).** Yield 63% from 1-chloro-5-phenylpentane, mp 192-195 °C (HCl salt). ^{1}H NMR (300 MHz, $CDCl_3$) δ 7.95 (s, 1H), 7.25-7.30 (m, 6H), 6.72-6.79 (m, 2H), 5.10-5.15 (m, 1H), 3.84 (s, 3H), 3.03 (s, 2H), 2.40-2.64 (m, 6H), 2.28 (s, 3H), 1.17-2.20 (m, 14H). Anal. ($C_{28}H_{38}N_2O_3 \cdot HCl \cdot 0.5H_2O$) C, H, N.

***N*-(9-Phenhexyl-9-azabicyclo[3.3.1]nonan-3α-yl)-*N*-(2-methoxy-5-methylphenyl)carbamate hydrochloride (6).** Yield 37% from 1-chloro-6-phenylhexane, mp 180.5-185 °C (HCl salt). ^{1}H NMR (300 MHz, $CDCl_3$) δ 7.95 (s, 1H), 7.13-7.34 (m, 6H), 6.72-6.79 (m, 2H), 5.19-5.15 (m, 1H), 3.84 (s, 3H), 3.03 (s, 2H), 2.41-2.63 (m, 6H), 2.29 (s, 3H), 1.18-1.88 (m, 16H). Anal. ($C_{29}H_{40}N_2O_3 \cdot HCl$) C, H, N.

***N*-(9-Phenheptyl-9-azabicyclo[3.3.1]nonan-3α-yl)-*N*-(2-methoxy-5-methylphenyl)carbamate hydrochloride (7).** Yield 83% from 1-chloro-7-phenylheptane, mp 142-143.5 °C (HCl salt). ^{1}H NMR (300 MHz, $CDCl_3$) δ 7.95 (s, 1H), 7.13-7.27 (m, 6H), 6.72-6.76 (m, 2H), 5.11-5.15 (m, 1H), 3.84 (s, 3H), 3.03 (s, 2H), 2.38-2.60 (m, 8H), 2.29 (s, 3H), 1.83-1.90 (m, 2H), 1.19-1.59 (m, 14H). Anal. ($C_{30}H_{42}N_2O_3 \cdot HCl \cdot 0.75H_2O$) C, H, N.

***N*-(9-(4-Methylphenethyl)-9-azabicyclo[3.3.1]nonan-3α-yl)-*N*-(2-methoxy-5-methylphenyl)-carbamate (2d).** A mixture of 4-methylphenethyl alcohol (1.00 g, 7.34 mmol) and p-toluenesulfonyl chloride (1.78 g, 9.34 mmol) in triethylamine (20 mL) was stirred at room temperature overnight. The resulting solid was filtered, dissolved in dichloromethane, washed with water, dried (magnesium sulfate) and concentrated *in vacuo* to give 4-methylphenethyl tosylate as a solid (52%), which was used crude for the next reaction. ^{1}H NMR (300 MHz, $CDCl_3$) δ 7.68-7.78 (m, 2H), 7.19-7.29 (m, 2H), 6.98-7.04 (m, 4H), 4.16-4.20 (m, 2H), 2.89-2.93 (m, 2H), 2.43 (s, 3H), 2.31 (s, 3H).

A mixture of *N*-(9-azabicyclo[3.3.1]nonan-3α-yl)-*N*-(2-methoxy-5-methylphenyl) carbamate (**8**) (400 mg, 1.31 mmol), 4-methylphenethyl tosylate (400 mg, 1.38 mmol) and 1,8-diazabicyclo[5.4.0]undec-7-ene (400 mg, 2.62 mmol) in dry toluene (8 mL) was refluxed overnight. The resulting residue after concentrating in vacuo was purified by silica gel column chromatography (5% methanol in dichloromethane) to give **2d** as a white solid (40%), mp 148-150 °C. ^{1}H NMR (300 MHz, $CDCl_3$) δ 8.01 (s, 1H), 7.14 (s, 1H), 7.07-7.13 (m, 5H), 6.73-6.77 (m, 2H), 5.14 (d, J = 6.7 Hz, 1H), 4.43-4.48 (m, 2H), 3.85 (s, 3H), 3.08-3.13 (m, 2H), 2.65-2.82 (m, 4H), 2.37-2.48 (m, 4H), 2.32 (s, 3H), 2.29 (s, 3H), 1.68-1.93 (m, 4H). HRFAB calculated for $C_{26}H_{35}N_2O_3$ $[M+H]^+$ 423.2648, found 423.2624.

***N*-(9-(4-Aminophenethyl))-9-azabicyclo[3.3.1]nonan-3α-yl)-*N*-(2-methoxy-5-methylphenyl)-carbamate (2f). Scheme II**

4-(*tert*-Butoxyformamido)phenethyl alcohol (9). To a solution of 4-aminophenethyl alcohol (5.00 g, 36.4 mmol) in ethyl acetate (50 mL) was added di-*tert*-butyl dicarbonate (7.95 g, 36.4 mmol). The reaction mixture was stirred at room temperature for 48 h. Volatile components were removed *in vacuo* to give a pale brown solid (99%), which was used crude for the next reaction. ^{1}H NMR (300 MHz, $CDCl_3$) δ 7.29 (d, J = 8.4 Hz, 2H), 7.14 (d, J = 8.4 Hz, 2H), 6.48 (br s, 1H), 3.82 (t, J = 6.5 Hz, 2H), 2.82 (t, J = 6.5 Hz, 2H), 1.51 (s, 9H).

4-(*tert*-Butoxyformamido)phenethyl chloride (10). To a solution of **9** (2.40 g, 10.0 mmol) in carbon tetrachloride (40 mL) was added triphenyl phosphine (2.65 g, 10.0 mmol). The reaction

mixture was reflux for 24 h. Volatile components were removed *in vacuo* to give an oil that was purified by silica gel column chromatography to afford **10** as a white solid (95 %): mp 79-81^{0}C. ^{1}H NMR (300 MHz, $CDCl_3$) δ 7.30 (d, J = 8.4 Hz, 2H), 7.14 (d, J = 8.4 Hz, 2H), 6.45 (br s, 1H), 3.67 (t, J = 7.5 Hz, 2H), 3.01 (t, J = 7.5 Hz, 2H), 1.51 (s, 9H).

***N*-(9-(4-*tert*-Butoxyformamido)phenethyl)-9-azabicyclo[3.3.1]nonan-3 α-yl-*N'*-(2-methoxy-5-methylphenyl)]carbamate (11).** Solid Potassium carbonate (1.35 g, 9.7 mmol), potassium iodide (325 mg, 1.9 mmol) and compound **10** (545 mg, 2.13 mmol) were added to a solution of *N*-(9-azabicyclo[3,3,1]nonan-3 α-yl)-*N'*(2-methoxy-5-methylphenyl)carbamate (**8**) (620 mg, 2.03 mmol) in acetonitrile (10 mL). The reaction mixture was refluxed for 48 h. Volatile components were removed *in vacuo* to give an oil that was purified by silica gel column chromatography to afford **11** as a yellow oil (38 %). ^{1}H NMR (300 MHz, $CDCl_3$) δ 7.95 (s, 1H), 7.25-7.33 (m, 2H), 7.12-7.14 (m, 3H), 6.73-6.80 (m, 2H), 6.42 (s, 1H), 5.08-5.17 (m, 1H), 3.84 (s, 3H), 3.09-3.12 (m, 2H), 2.77-2.81 (m, 2H), 2.63-2.68 (m, 2H), 2.40-2.51 (m, 2H), 2.30 (s, 3H), 2.09-2.24 (m, 1H), 1.84-1.93 (m, 2H), 1.61-1.72 (m, 2H), 1.51 (s, 9H), 1.21-1.30 (m, 3H); HRFAB calculated for $C_{30}H_{42}N_3O_5$ $[M+H]^+$ 524.3124, found 524.3108.

***N*-(9-(4-Aminophenethyl))-9-azabicyclo[3.3.1]nonan-3 α-yl)-*N*-(2-methoxy-5-methylphenyl)-carbamate (2f).** Trifluoroacetic acid (2 mL) was added to a solution of compound **11** (300 mg, 0.57 mmol) in dichloromethane (1 mL), and the reaction mixture was stirred at room temperature for 3 h. Volatile components were removed *in vacuo*. The resulting residue was dissolved in saturated aqueous bicarbonate (10 mL), and adjusted to pH 10 with an aqueous solution of 10 % sodium hydroxide. The mixture was extracted with dichloromethane (4 x 5 mL). The combined organic extracts were dried (magnesium sulfate), filtered, and concentrated to give **2f** as a yellow oil (97%). ^{1}H NMR (300 MHz, $CDCl_3$) δ 7.92 (s, 1H), 7.14 (s, 1H), 7.01 (d, J = 8.2 Hz, 2H), 6.74-6.82 (m, 2H), 6.64 (d, J = 8.2 Hz, 2H), 5.10-5.17 (m, 1H), 3.85 (s, 3H), 3.38-3.61 (m, 4H), 3.00-3.13 (m, 2H), 2.50-2.75 (m, 4H), 2.30 (s, 3H), 2.00-2.11 (m, 2H), 1.43-1.77 (m, 6H); HRFAB calculated for $C_{25}H_{34}N_3O_3$ $[M+H]^+$ 424.2600, found 424.2589.

Receptor Binding Studies

σ receptor assays. σ_1 binding sites were labeled with the σ_1-selective radioligand, [^{3}H](+)-pentazocine (DuPont-NEN, Billerica, MA) in guinea pig brain membranes (Rockland Biological, Gilbertsville, PA) according to published procedures.[1,2] σ_2 sites were assayed in rat liver membranes with [^{3}H]DTG (DuPont-NEN, Boston, MA) in the presence of (+)-pentazocine (100 nM) to mask σ_1 sites.[1,2]

Membrane Preparation. Crude synaptosomal (P_2) membrane homogenates were prepared from frozen guinea pig brains without cerebellum.[1,2] Brains were allowed to thaw slowly on ice before homogenization. Crude P_2 membranes were also prepared from the livers of male Sprague-Dawley rats (300-350 g). Animals were sacrificed by decapitation and the livers were removed and minced before homogenization. Tissue homogenization was carried out at 4 °C in 10 ml/g tissue weight of 10 mM Tris-HCl/0.32 M sucrose, pH 7.4 using a Potter-Elvehjem tissue grinder. The crude homogenate was centrifuged for 10 min at 1000 g and the supernatant saved on ice. The pellet was resuspended in 2 ml/g tissue weight of ice-cold 10 mM Tris-HCl/0.32 M sucrose, pH 7.4 by vortexing. After centrifuging at 1000 g for 10 min, the pellet was discarded and the supernatants were combined and centrifuged at 31,000 g for 15 min. The pellet was resuspended in 3 ml/g 10 mM Tris-HCl, pH 7.4 by vortexing, and the suspension was allowed to incubate at 25 °C for 15 min. Following centrifugation at 31,000 g for 15 min, the aliquots were stored at -80 °C until used. The protein concentration of the suspension was determined by the method of Bradford[14] and generally ranged from 6-11 mg protein/ml.

σ_1 Binding Assay. Guinea pig brain membrane homogenates (100 μg protein) were incubated with 3 nM [^{3}H](+)-pentazocine (31.6 Ci/mmol) in 50 mM Tris-HCl (pH 8.0) at 25 °C for either 120 or 240 min. Test compounds were dissolved in ethanol then diluted in buffer for a total incubation volume of 0.5 ml. Test compounds were added in concentrations ranging from 0.005 to 1000 nM. Assays were terminated by the addition of ice-cold 10 mM Tris-HCl (pH 8.0) followed by rapid filtration through Whatman GF/B glass fiber filters (presoaked in 0.5 % polyethylenimine) using a Brandel cell harvester (Gaithersburg, MD). Filters were washed twice with 5 ml of ice cold buffer. Nonspecific binding was determined in the presence of 10 μM (+)-pentazocine. Liquid scintillation

counting was carried out in EcoLite(+) (ICN Radiochemicals; Costa Mesa, CA) using a Beckman LS 6000IC spectrometer with a counting efficiency of 50%.

σ_2 Binding Assay. Rat liver membrane homogenates (35 μg of protein) were incubated with 3 nM [^{3}H]DTG (38.3 Ci/mmol) in the presence of 100 nM (+)-pentazocine to block σ_1 sites. Incubations were carried out in 50 mM Tris-HCl (pH 8.0) for 120 min at 25 °C in a total incubation volume of 0.5 ml. Test compounds were added in concentrations ranging from 0.005 to 1000 nM. Assays were terminated by the addition of ice-cold 10 mM Tris-HCl (pH 8.0) followed by rapid filtration through Whatman GF/B glass fiber filters (presoaked in 0.5% polyethylenimine) using a Brandel cell harvester (Gaithersburg, MD). Filters were washed twice with 5 ml of ice cold buffer. Nonspecific binding was determined in the presence of 5 μM DTG. Liquid scintillation counting was carried out in EcoLite(+) (ICN Radiochemicals; Costa Mesa, CA) using a Beckman LS 6000IC spectrometer with a counting efficiency of 50%.

Data Analysis.

The IC_{50} values at sigma sites were generally determined in triplicate from non-linear regression of binding data as analyzed by JMP (SAS Institute; Cary, NC), using 8 concentrations of each compound. K_i values were calculated using the method of Cheng-Prusoff[15] and represent mean values ± SEM. All curves were best fit to a one site fit and gave Hill coefficients of 0.8 – 1.0. The K_d value used for [^{3}H]DTG in rat liver was 17.9 nM and was 4.8 nM for [^{3}H](+)-pentazocine in guinea pig brain.[1,2]

Acknowledgments

This research was funded by grants CA 80452 awarded by the National Cancer Institute, DE-FG02-00ER82945 awarded by the Department of Energy, and DAMD17-01-1-0446 awarded by the Department of Defense Breast Cancer Research Program of the US Army Medical Research and Materiel Command Office.

References

1. Walker J.M., Bowen W.D., Walker F.O., Matsumoto R.E., De Costa B. and Rice K.R. *Pharmacol. Rev.* **1990**, *42*, 355-402.

2. Hellewell S.B., Bruce A., Feinstein G., Orringer J., Williams W. and Bowen, W.D. *Eur. J. Pharmacol. Mol. Pharmacol. Sec.* **1994**, *268*, 9-18.

3. Hanner M., Moebius F.F., Flandorfer A., Knaus H.-G., Striessnig J., Kempner E. and Glossmann H. *Proc. Natl. Acad. Sci. USA* **1996**, *93*, 8072-8077.

4. Su T.-P., London E. and Jaffe J. *Science* **1988**, *240*, 219-221.

5. Bowen W.D., Bertha C.M., Vilner B.J. and Rice K. *Eur. J. Pharmacol.* **1995**, *278*, 257-260.

6. Nguyen V.H., Kassiou M., Johnston G.A.R. and Christie M.J. *Eur. J. Pharmacol.* **1996**, *311*, 233-240.

7. Bowen W.D., Vilner B.J., Bertha C.M., Kuehne M.E. and Jocabson A.E. *Eur. J. Pharmacol.* **1995**, *279*, R1-3.

8. Mach R.H., Smith C.R. and Childers S.R. *Life Sci.* **1995**, *57*, PL 57-62.

9. Perredgaard J., Moltzen E.K., Meier E. and Sanchez C. *J. Med. Chem.* **1995**, *38*, 1998-2008.

10. Moltzen, E.K., Perregaard J. and Meier E. *J. Med. Chem.* **1995**, *38*, 2009-2017.

11. Bonhaus D.W., Loury D.N., Jakeman L.B., To Z., DeSouza A., Eglen R.M. and Wong E.H.F. *J. Pharmacol. Exp. Ther.* **1993**, *267*, 961-970.

12. Mach R.H., Yang B., Kuhner R.J., Whirrett B.R. and West T. *Med. Chem. Res.* **2001**, *10*, 339-355.

13. Mach R.H., Wheeler K.T., Blair S., Yang B., Day C.S., Blair J.B., Choi S.-R. and Kung H.F. *J. Labelled Cmpds. Radiopharm.* **2001**, *44*, 899-908.

14. Bradford M.M. *Anal. Biochem.* **1976**, *72*, 248-254.

15. Cheng Y.C. and Prusoff W.H. *Biochem. Pharmacol.* **1973**, *22*, 3099-4022.

Received: 12-27-02 Accepted: 3-21-03

Available online at www.sciencedirect.com
SCIENCE DIRECT®
Bioorganic & Medicinal Chemistry Letters
ELSEVIER
Bioorganic & Medicinal Chemistry Letters 14 (2004) 195–202

Conformationally-flexible benzamide analogues as dopamine D_3 and σ_2 receptor ligands

Robert H. Mach,[a,b,*] Yunsheng Huang,[a] Rebekah A. Freeman,[c] Li Wu,[a] Suwanna Vangveravong[a] and Robert R. Luedtke[c]

[a]*Department of Radiology, PET Center, Wake Forest University School of Medicine, Winston-Salem, NC 27157, USA*
[b]*Department of Physiology & Pharmacology, Wake Forest University School of Medicine, Winston-Salem, NC 27157, USA*
[c]*Department of Pharmacology and Neuroscience, University of North Texas Health Science Center, Fort Worth, TX 76107, USA*

Received 14 July 2003; accepted 25 September 2003

Abstract—A series of conformationally-flexible analogues was prepared and their affinities for D2-like dopamine (D_2, D_3 and D_4) were determined using in vitro radioligand binding assays. The results of this structure–activity relationship study identified one compound, **15**, that bound with high affinity (K_i value = 2 nM) and moderate selectivity (30-fold) for D_3 compared to D_2 receptors. In addition, this series of compounds were also tested for affinity at σ_1 and σ_2 receptors. We evaluated the affinity of these dopaminergic compounds at sigma receptors because (a) several antipsychotic drugs, which are high affinity antagonists at dopamine $D_{2\text{-like}}$ receptors, also bind to sigma receptors and (b) sigma receptors are expressed ubiquitously and at high levels (picomoles per mg proteins). It was observed that a number of analogues displayed high affinity and excellent selectivity for σ_2 versus σ_1 receptors. Consequently, these novel compounds may be useful for characterizing the functional role of σ_2 receptors and for imaging the σ_2 receptor status of tumors in vivo with PET.

The dopamine receptor subtypes are members of the G protein coupled receptor protein superfamily. Based upon genetic and cDNA cloning studies it is currently thought that there are five functionally active dopamine receptor subtypes expressed in mammalian brain. These five subtypes have been classified into two major classes, the $D_{1\text{-like}}$ and $D_{2\text{-like}}$ receptors. Stimulation of the $D_{1\text{-like}}$ receptor subtypes, which include the D_1 (D_{1a}) and the D_5 (D_{1b}) receptors, results in an activation of adenylyl cyclase and an increase in the production of cAMP. Agonist stimulation of the $D_{2\text{-like}}$ receptors, which consist of the D_2, D_3 and D_4 receptors, results in an inhibition of adenylyl cyclase activity, an increase in the release of arachadonic acid, and an increase in phosphatidylinositol hydrolysis.

Over the past 5 years, there has been interest in developing agents that are antagonists of the dopamine D_3 receptor.[1,2] This interest was largely generated by the hypothesis that dopamine D_3 receptors may play a pivotal role in the development of a number of neurological and neuropsychiatric disorders. Receptor autoradiography studies have shown that both D_2 and D_3 receptors are widely distributed in striatal regions of human[3] and monkey[4] brain. However, the higher ratio of D_3 versus D_2 receptors in limbic structures indicates that the D_3 receptor may play an integral role in the pathological abnormalities that occur in neuropsyciatric disorders. Autoradiography studies have also revealed a decrease of D_3 receptors in the frontal cortex and an increase in expression in the ventral striatum of schizophrenics compared to normal individuals.[5,6] Dopamine D_3 receptors are also believed to play a role in the dyskinesias associated with l-dopa treatment of patients with Parkinson's Disease. For example, chronic treatment of squirrel monkeys with the neurotoxin, 1-methyl-4-phenyl-1,2,3,4-tetrahydropyridine (MPTP), which causes a selective destruction of the nigrostriatal dopaminergic system, results in a decline of D_3 receptors in the caudate (motor region) but not the putamen of globus pallidus (limbic regions). However, treatment

Keywords: dopamine D_3 receptors; atypical antipsychotics; σ_2 receptors.
* Corresponding author at present address: Division of Radiological Sciences, Washington University School of Medicine, Campus Box 8225, 510 S. Kingshighway Blvd., St. Louis, MO 63110, USA. Fax: +1-314-362-0039; e-mail: rhmach@mir.wustl.edu

0960-894X/$ - see front matter © 2003 Elsevier Ltd. All rights reserved.
doi:10.1016/j.bmcl.2003.09.083

with the drug levodopa led to a restoration of D_3 receptor levels and a reversal of Parkinsonian symptoms in MPTP-treated animals. Finally, the activation of dopamine D_3 receptors in the nucleus accumbens is believed to be involved in the sensitization/rewarding properties of psychostimulants, such as cocaine. Therefore, agents that can block the interaction of psychostimulant-induced increases in synaptic dopamine levels with the D_3 receptor have potential for the pharmacological treatment of cocaine abuse.[1]

A number of conformationally-flexible benzamide analogues displaying a high affinity and selectivity for D_3 versus D_2 receptors have been reported in recent years. Examples of this include NGB 2849, NGB 2904, and the structural congeners **1**–**3** (Fig. 1). A common structural feature in the conformationally-flexible benzamide analogues is the *N*-2,3-dichlorophenylpiperazine ring and the four carbon spacer group separating the benzamide and the basic amino moieties.[7–10]

We have recently reported two different classes of compounds, naphthamide analogues and pyrrole derivatives, displaying a modest affinity and selectivity for D_3 versus D_2 receptors.[11,12] For example, the naphthamide analogues **4** and **5** have a moderate selectivity for D_3 versus D_2 receptors. Unfortunately, these compounds were found to have a relatively high affinity for sigma receptors (Fig. 2). Because sigma receptors are expressed ubiquitously and at high levels (picomoles per mg proteins), the high affinity of these compounds for sigma receptors limits their utility for in vitro and in vivo studies of dopamine D_3 receptors.[11] The pyrrole analogues **6** and **7** have a high affinity and 10-fold selectivity for D_3 versus D_2 receptors. However, unlike the naphthamide analogues, the pyrrole analogues bound with low affinity at sigma receptors.[12] As part of a continuing effort to develop potent and selective D_3 receptor ligands as potential radiotracers for studies of the dopaminergic system with the noninvasive imaging procedure, Positron Emission Tomography (PET), we explored the possibility of preparing hybrid ligand structures of the conformationally-flexible benzamide analogues (Fig. 1) and the naphtamide and pyrrole analogues (Fig. 2). The results of this study led to the identification of a number of compounds possessing a high affinity and moderate selectivity for dopamine D_3 versus D_2 receptors.

In addition, the results of this structure–activity relationship study led to the identification of a number of conformationally-flexible benzamide analogues that had a high affinity and excellent selectivity for σ_2 versus σ_1 receptors. Sigma-2 receptors have been shown to be a potential biomarker for determining the proliferative status of breast tumors.[13–15] Therefore, the results of this study have led to the identification of lead compounds for radiotracer development with two completely different functions: (1) D_3 receptor imaging agents for studying the change in dopamine receptor function in a variety of neurological and neuropsychiatric disorders and, (2) σ_2 selective imaging agents for measuring the proliferative status of breast tumors in vivo with PET.

The strategy chosen for the current study involved the combination of the following structural moieties of the lead compounds: (a) the 2,3-dichlorophenylpiperazine

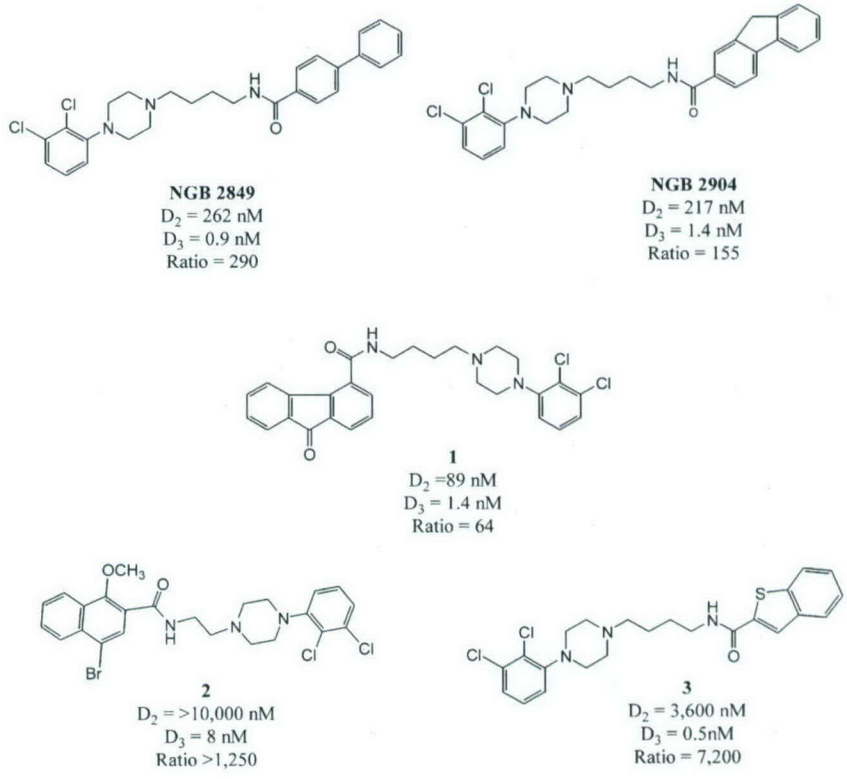

Figure 1.

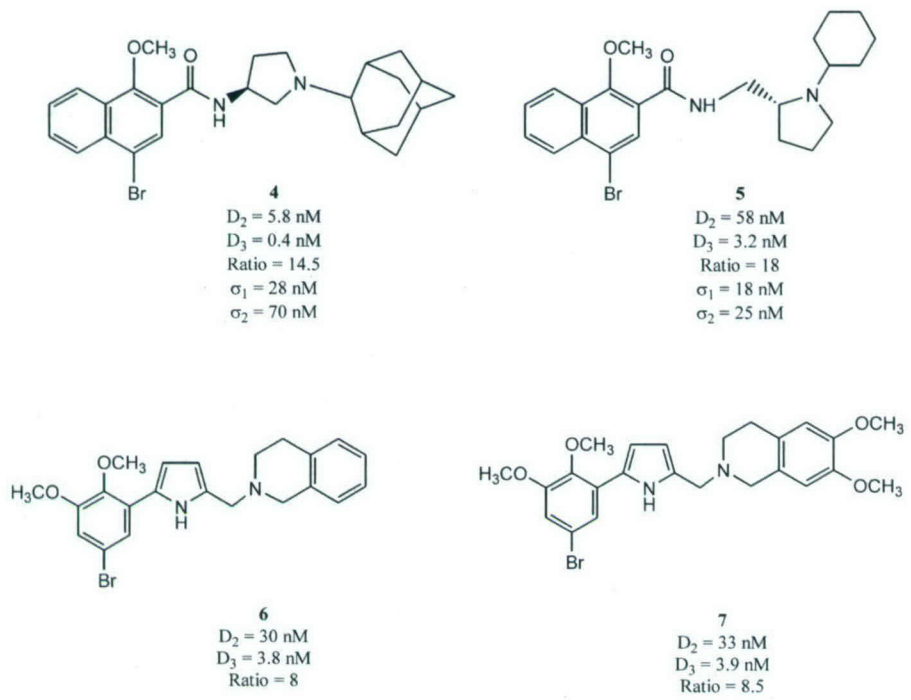

Figure 2.

and the two- and four-carbon spacer groups of the conformationally-flexible benzamide analogues shown in Figure 1; (b) the naphthyl group of naphthamide compounds shown in Figure 2; and, (c) the 2,3-dimethoxyphenyl and tetrahydroisoquinoline moieties of the pyrrole analogues shown in Figure 2.

The synthesis of the target tetrahydroisoquinoline analogues is shown in Scheme 1.[16] Reaction of the secondary amine of **8a** and **8b** with either bromoacetonitrile or bromobutyronitrile gave *N*-alkylated products, **9a–d**, in 75–85% yield. Reduction with either lithium aluminum hydride in THF or hydrogenation over palladium on charcoal gave the corresponding amines, **10a–d**, in quantitative yields. Condensation of amines **10a–d** with either 2-methoxy-5-bromonaphthoyl chloride[12] or 5-bromo-2,3-dimethoxybenzoic acid[13] gave the corresponding amide analogues, **11–14**, in excess of 90% yield. Synthesis of the 2,3-dichlorophenylpiperazine benzamide and naphthamide analogues, **15** and **16**, was accomplished using a similar reaction sequence as outlined in Scheme 2.[16]

Table 1. Binding affinities for dopamine D_2/D_3 and sigma σ_1/σ_2 receptors

Compd	K_i (nM)[a]			
	D_2[b]	D_3[c]	σ_1[d]	σ_2[e]
11a	131.6±24.6	81.6±21.28	15.1±1.7	47.7±2.5
11b	240.5±19.4	126.5±42.4	189.1±2.6	21.2±0.1
12	741.0±287.3	106.5±24.3	1,159±7	17.6±0.7
13a	429.7±76.1	17.8±0.5	276.5±35.7	716.5±9.8
13b	714.0±133.7	21.4±2.3	2932±28	16.4±2.0
14	2200±390	627±244	12,900±111	8.2±1.4
15	58.8±13.7	2.1±0.4	809±66	75.0±4.1
16	107.0±19.0	10.2±5.3	751±6	26.4±1.4

[a] Mean ± SEM, K_i values were determined by at least three experiments.
[b] K_i values for D_2 receptors were measured on rat $D_{2(long)}$ expressed in Sf9 cells using [^{125}I]IABN as the radioligand.[18]
[c] K_i values for D_3 receptors were measured on rat D_3 expressed in Sf9 cells using [^{125}I]IABN as the radioligand.[18]
[d] K_i values for σ_1 receptors were measured on quinea pig brain membranes using [^{3}H](+)-pentazocine as the radioligand.[17]
[e] K_i values for σ_2 receptors were measured on rat liver membranes using [^{3}H]-DTG as the radioligand in the presence of (+)-pentazocine.[17]

The naphthamide analogue **11a**, which contains a two-carbon spacer group between the amide nitrogen and the basic amino group had a relatively low affinity for dopamine D_3 and D_2 receptors (Table 1). Compound **11a** also had an appreciable affinity for both σ_1 and σ_2 receptors. Introduction of a methoxy groups into the 4- and 5-positions of the tetrahydro-isoquinoline ring resulted in a reduction in affinity for D_2, D_3 and σ_1 receptors, and an increase in affinity for σ_2 receptors. Increasing the length of the spacer group from two carbon units in **11b** to four carbon units (i.e., **12**) resulted in no change in affinity for D_3 and σ_2 receptors, but a dramatic reduction in affinity for D_2 and σ_1 receptors. Replacement of the naphthamide group of **11a** with a 5-bromo-2,3-dimethoxy benzamide group (i.e., **13a**) resulted in an increase in affinity for dopamine D_3 receptors, and a decrease in affinity for D_2, σ_1 and σ_2 receptors. Introduction of the methoxy groups into the 4- and 5-positions of the tetrahydroisoquinoline ring of **13a** to give **13b** resulted in no change in affinity for D_3 receptors and a reduction in affinity for D_2 receptors. However, this change in substitution pattern resulted in

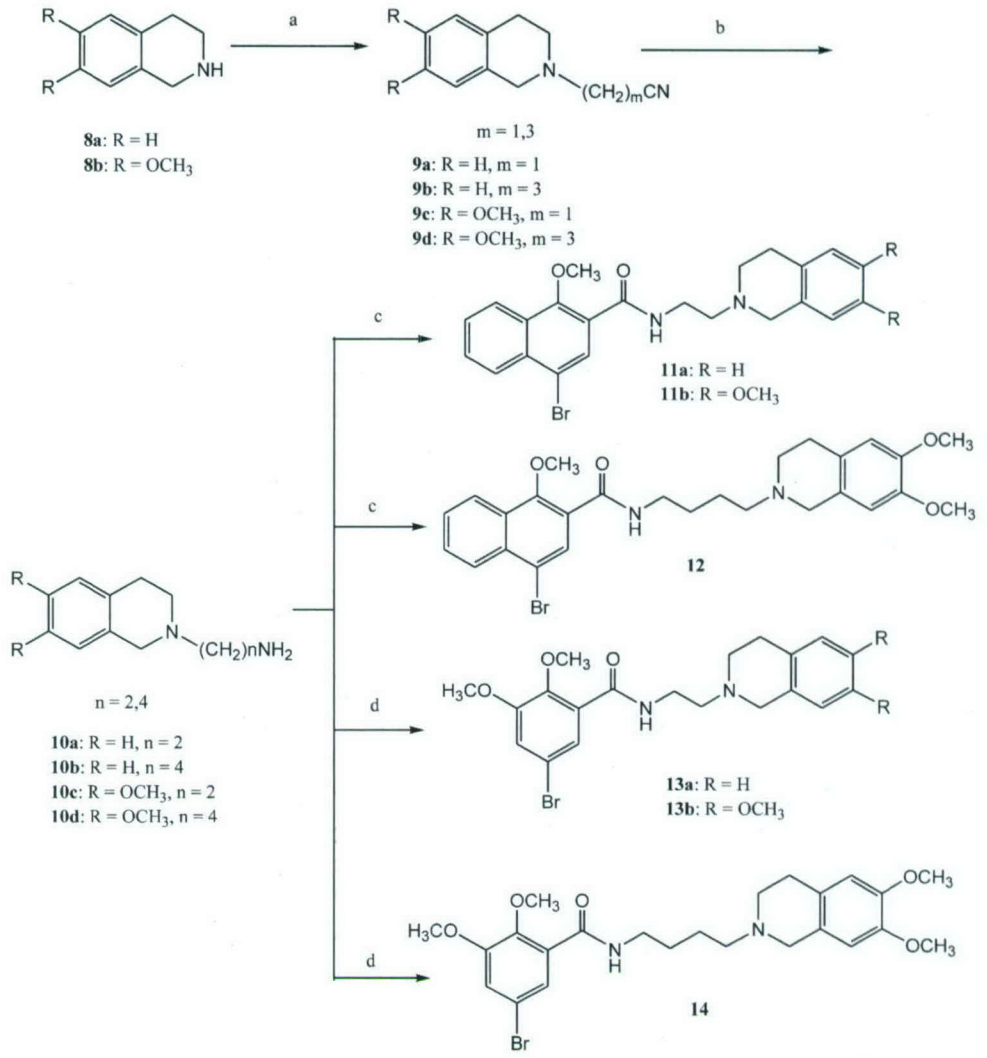

Scheme 1. (a) $BrCH_2CN$ or $BrCH_2CH_2CH_2CN$, Et_3N, CH_2Cl_2, rt; (b) $LiAlH_4$, THF or H_2, Pd(c), ethanol; (c) ref 10; (d) ref 12.

a dramatic decrease in affinity for σ_1 receptors and a large increase in affinity for σ_2 receptors. Increasing the length of the spacer group from two carbons in **13b** to four carbons in **14** resulted in large decrease in affinity for D_2, D_3, and σ_1 receptors and an increase in σ_2 receptor affinity. Compound **14** is unique in that is has over a 1500-fold higher affinity for σ_2 versus σ_1 receptors. Although many different classes of compounds have been shown to bind with high affinity to sigma receptors, most compounds studied to date have either (a) a higher affinity for σ_1 versus σ_2 receptors, or (b) equipotency with respect to binding to σ_1 and σ_2 receptors. Compound **14** is one of the most potent and selective σ_2 receptor ligands reported to date.

Compound **15** was prepared to determine the effect of introducing the 5-bromo-2,3-dimethoxy benzamide moiety into NGB 2904 and its structural congeners (Fig. 1) on D_2 and D_3 receptor affinity. In addition, compound **16** was prepared to assess the effect that increasing the two-carbon spacer group of **2** (Fig. 1) to four carbons would have on dopamine receptor affinity. Compounds **15** and **16** had the highest affinity for D_3 receptors of the analogues prepared in this study, which further emphasizes the importance in the 2,3-dichlorophenyl-piperazine group for binding to dopamine D_3 receptors.

Compounds **17–20** were prepared with the goal of increasing the σ_2 receptor affinity and reducing the dopamine D_2 and D_3 receptor affinity of this class of compounds (Scheme 3). The results of our previous structure–activity relationship studies indicated that both the 5-bromo and 3-methoxy groups were important for the binding the binding of pyrrole analogues shown in Figure 2 to dopamine D_2 and D_3 receptors. Therefore, removal of the 3-methoxy group, or replacement of the 5-bromo moiety with a methyl group, was expected to result in a reduction in affinity for D_2 and D_3 receptors. The results of the structure–activity relationship study are shown in Table 2. Compound **14** is included in Table 2 for comparison. Removal of the 3-methoxy group of **13a** to give **17** resulted in a large reduction in affinity for D_2 and D_3 receptors and an increase in affinity for σ_1 and σ_2 receptors. The same change in the structure of **13b** to give compound **18** resulted in a similar effect on dopamine receptor binding. However, there was a marked decrease in affinity of **18** for σ_1 receptors relative to that **13b**. Compound **18** also had a

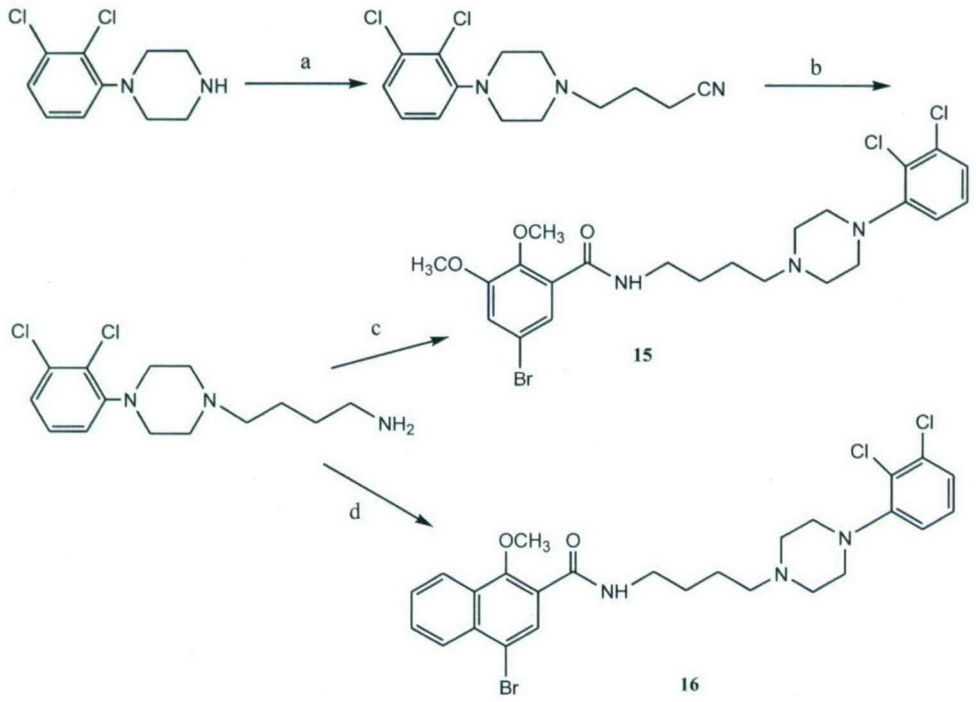

Scheme 2. (a) $BrCH_2CH_2CH_2CN$, Et_3N, CH_2Cl_2; (b) H_2, Pd(c), ethanol; (c) ref 12; (d) ref 10.

Table 2. Binding affinities of **17–20** for dopamine D_2/D_3 and sigma σ_1/σ_2 receptors

Compd	K_i (nM)[a]				
	D_2[b]	D_3[c]	σ_1[d]	σ_2[e]	σ_1/σ_2 ratio
14	2200±390	627±244	12,900±111	8.2±1.4	1573
17	2190±351	310.7±54.4	21.8±5.6	89.4±13.9	0.24
18	3570±796	488.0±70.7	5484±266	12.4±1.8	442
19	2850±316	3760±618	10,412±462	13.3±0.1	783
20	642.0±141.0	313.0±141.0	3078±87	10.3±1.5	300

[a] Mean±SEM, K_i values were determined by at least three experiments.
[b] K_i values for D_2 receptors were measured on rat $D_{2(long)}$ expressed in Sf9 cells using [^{125}I]IABN as the radioligand.
[c] K_i values for D_3 receptors were measured on rat D_3 expressed in Sf9 cells using [^{125}I]IABN as the radioligand.
[d] K_i values for σ_1 receptors were measured on guinea pig brain membranes using [^{3}H](+)-pentazocine as the radioligand.
[e] K_i values for σ_2 receptors were measured on rat liver membranes using [^{3}H]-DTG as the radioligand in the presence of (+)-pentazocine.

higher affinity for σ_2 receptors than that of **13b**. Replacement of the 5-bromo moiety of **18** with a methyl group (i.e., **19**) resulted in a further reduction in affinity for D_3 and σ_1 receptors, and no change in affinity for D_2 and σ_2 receptors. Increasing the length of the spacer group of **19** from two carbons to four carbons (i.e., **20**) resulted in an increase in affinity for D_2, D_3 and σ_1 receptors, and no change in affinity for σ_2 receptors. The high σ_1/σ_2 selectivity ratio of compounds **14**, **18**, **19**, and **20** indicate that they have the potential to be useful lead compounds for the development of imaging agents for determining the σ_2 receptor status of breast tumors with PET.

Binding assays were also conducted on compounds **13a**, **13b**, **15** and **16** to determine their affinity for dopamine $D_{4.4}$ receptors. The results of this study are shown in Table 3. All four compounds had a lower affinity for $D_{4.4}$ receptors relative to their binding potencies at dopamine D_3 receptors. Compound **15** had the highest D_3 receptor affinity and highest D_2/D_3 and D_4/D_3 selectivity ratios of the four compounds listed in Table 3. The presence of the methoxy groups indicates that a carbon-11 labeled version of **15** can be prepared by

Table 3. In vitro binding data for dopamine D_4 receptors

Compd	K_i (nM)[a]				
	D_2[b]	D_3[c]	D_4[d]	D_2/D_3 ratio[e]	D_4/D_3 ratio[f]
13a	429.7±76.1	17.8±0.5	47.9±11.6	24	2.7
13b	714.0±133.7	21.4±2.3	265.0±60.0	33	12.4
15	58.8±13.7	2.1±0.4	800.0±330.0	28	381
16	107.0±19.0	10.2±5.3	1345±448	10.5	132

[a] Same as Table 1.
[b] Same as Table 1.
[c] Same as Table 1.
[d] K_i for inhibiting the binding of [^{125}I]IABN to human $D_{4.4}$ receptors.
[e] K_i for D_2/K_i for D_3.
[f] K_i for D_4/K_i for D_3.

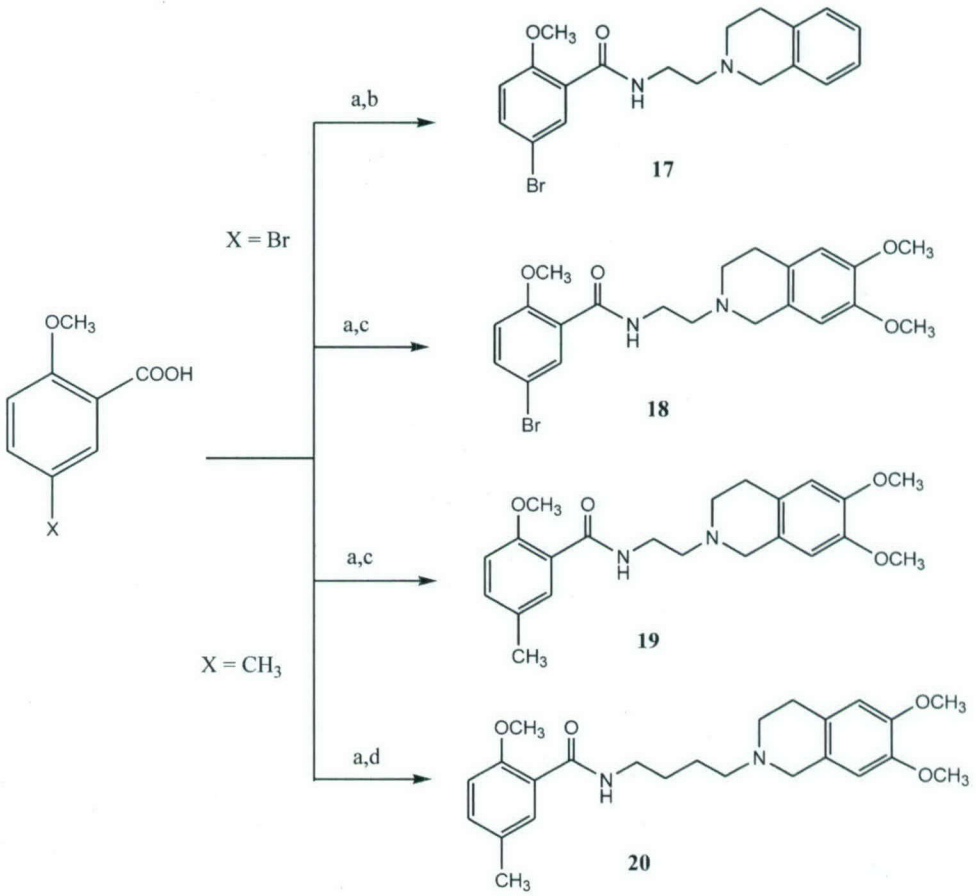

Scheme 3. (a) $SOCl_2$, benzene, reflux; (b) **10a**, Et_3N, CH_2Cl_2, rt; (c) **10c**, Et_3N, CH_2Cl_2, rt; (d) **10d**, CH_2Cl_2, Et_3N, rt.

alkylation of the des-methyl precursor with ^{11}C-methyl iodide. We are currently exploring [^{11}C]**15** as a potential radiotracer for imaging dopamine D_3 receptors with PET and the relatively low affinity of **15** for σ_1 and σ_2 receptors indicates that there will be minimal in vivo binding to sigma receptors.

In conclusion, we have completed a structure–activity relationship study on a series of benzamides with the goal of identifying a potential radiotracer for imaging dopamine D_3 receptors with PET. The results of this study revealed compound **15** as a candidate for labeling D_3 dopamine receptors in vivo. The low affinity binding of **15** at sigma receptors subtypes servers to minimize sigma receptor interactions as a potential source of nonspecific/background binding. In addition, this study has lead to the identification of a number of novel, σ_2-receptor selective ligands. Based upon those findings we are also exploring the potential of ^{11}C-labeled versions of **14**, **18**, **19** and **20**, and ^{76}Br-labeled versions of **14** and **18**, as potential radiotracers for imaging the σ_2 receptor status of breast tumors.

Acknowledgements

This research was funded by grants DA 12647 awarded by the National Institute on Drug Abuse and DAMD17-01-1-0446 awarded by the Department of Defense Breast Cancer Research Program of the US Army Medical Research and Materiel Command Office.

References and notes

1. Luedtke, R. R.; Mach, R. H. *Curr. Pharm. Des.* **2003**, *9*, 643.
2. Hackling, A. E.; Stark, H. *ChemBioChem.* **2002**, *3*, 946.
3. Morissette, M.; Goulet, M.; Grodin, R.; Blancet, P.; Bedard, P. J.; Di Paolo, T.; Levesque, D. *Eur. J. Neurosci.* **1998**, *10*, 1565.
4. Ryoo, H. L.; Pierrotti, D.; Joyce, J. N. *Movement Disorders* **1998**, *13*, 788.
5. Gurevich, E. V.; Bordelon, Y.; Shapiro, R. M.; Arnold, S. E.; Gur, R. E.; Joyce, J. N. *Arch. Gen. Psych.* **1997**, *54*, 225.
6. Gurevich, E. V.; Joyce, J. N. *Neuropsychopharmacology* **1999**, *20*, 60.
7. Glase, S. A.; Akunne, H. C.; Hefner, T. G.; Johnson, S. J.; Kesten, S. R.; MacKenzie, R. G.; Manley, P. J.; Pugsley, T. A.; Wright, J. L.; Wise, L. D. *Bioorg. Med. Chem. Lett.* **1996**, *6*, 1361.
8. Yuan, J.; Chen, X.; Brodbeck, R.; Primus, R.; Braun, J.; Wasley, J. W. F.; Thurkauf, A. *Bioorg. Med. Chem. Lett.* **1998**, *8*, 2715.
9. Robarge, M. J.; Husbands, S. M.; Kielytka, A.; Brodbeck, R.; Thurkauf, A.; Newman, A. H. *J. Med. Chem.* **2001**, *44*, 3175.
10. Bettinetti, L.; Schlotter, K.; Hubner, H.; Gmeiner, P. *J. Med. Chem.* **2002**, *45*, 4597.

11. Huang, Y.; Luedtke, R. R.; Freeman, R. A.; Wu, L.; Mach, R. H. *J. Med. Chem.* **2001**, *44*, 1815.
12. Mach, R. H.; Huang, Y.; Freeman, R. A.; Wu, L.; Blair, S.; Luedtke, R. R. *Bioorg. Med. Chem.* **2003**, *11*, 225.
13. Mach, R. H.; Smith, C. R.; Al-Nabulsi, I.; Whirrett, B. R.; Childers, S. R.; Wheeler, K. T. *Cancer Res.* **1997**, *57*, 156.
14. Al-Nabulsi, I.; Mach, R. H.; Sten, K.; Childers, S. R.; Wheeler, K. T. *Br. J. Cancer* **1999**, *81*, 925.
15. Wheeler, K. T.; Wang, L.-M.; Wallen, C. A.; Childers, S. R.; Cline, J. M.; Keng, P. C.; Mach, R. H. *Br. J. Cancer* **2000**, *82*, 1223.
16. Data for **11a**. Mp 180–182 °C (oxalate salt); ^{1}H NMR (DMSO-d_6) δ 3.02 (s, 2H), 3.19 (9s, 2H), 3.72–3.74 (m, 3H), 3.94 (s, 3H), 4.21 (s, 3H), 7.16–7.25 (m, 4H), 7.75 (t, J = 8.1 Hz, 1H), 7.81 (t, J = 8.1 Hz, 1H), 8.05 (s, 1H), 8.15 (d, J = 8.3 Hz, 1H), 8.24 (d, J = 8.3 Hz, 1H), 8.77 (t, J = 5.4 Hz, 1H). Calcd: C: 56.72; H: 4.76; N: 5.29. Obsvd: C: 56.50; H: 4.91; N: 5.14.
Data for **11b**. Mp 187–189 °C (oxalate salt); ^{1}H NMR (DMSO-d_6) δ 2.94 (s, 3H), 3.19 (s, 4H), 3.71 (s, 3H), 3.73 (s, 3H), 3.94 (s, 3H), 4.12 (s, 3H), 6.74 (s, 1H), 6.79 (s, 1H), 7.75 (t, J = 7.6 Hz, 1H), 7.82 (t, J = 7.6 Hz, 1H), 8.05 (s, 1H), 8.15 (d, J = 8.3 Hz, 1H), 8.25 (d, J = 8.3 Hz, 1H), 8.76 (s, 1H). Calcd: C: 55.02; H: 4.96; N: 4.75. Obsvd: C: 54.76; H: 5.04; N: 4.65.
Data for **12**. Mp 165–167 °C (oxalate salt); ^{1}H NMR (DMSO-d_6) δ 1.61–1.80 (m, 4H), 2.96 (s, 2H), 3.36–3.39 (m, 5H), 3.71 (s, 3H), 3.73 (s, 3H), 3.95 (s, 3H), 4.19 (s, 3H), 6.77 (s, 1H), 6.80 (s, 1H), 7.75 (t, J = 7.4 Hz, 1H), 7.81 (t, J = 7.4 Hz, 1H), 7.95 (s, 1H), 8.15 (d, J = 8.3 Hz, 1H), 8.25 (d, J = 8.3 Hz, 1H), 8.60 (t, J = 5.6 Hz, 1H). Calcd: C: 56.41; H: 5.39; N: 4.54. Obsvd: C: 56.32; H: 5.45; N: 4.45.
Data for **13a**. Mp 142–144 °C (oxalate salt); ^{1}H NMR (DMSO-d_6) δ 2.99 (s, 2H), 3.10 (s, 2H), 3.61–3.63 (m, 3H), 3.73 (s, 3H), 3.85 (s, 3H), 4.15 (s, 3H), 7.13–7.23 (m, 4H), 7.34 (s, 1H), 7.36 (s, 1H), 8.59 (t, J = 5.0 Hz, 1H). Calcd: C: 51.88; H: 4.95; N: 5.50. Obsvd: C: 51.73; H: 4.95; N: 5.51.
Data for **13b**. Mp 91–93 °C (oxalate salt); ^{1}H NMR (DMSO-d_6) δ 2.92 (s, 2H), 3.13 (s, 2H), 3.59–3.63 (m, 3H), 3.71 (s, 3H), 3.73 (s, 3H), 3.74 (s, 3H), 3.85 (s, 3H), 4.10 (s, 3H), 6.72 (s, 1H), 6.78 (s, 1H), 7.34 (s, 1H), 7.37 (s, 1H), 8.60 (s, 1H). Calcd: C: 50.63; H: 5.13; N: 4.92. Obsvd: C: 50.49; H: 5.30; N: 4.60.
Data for **14**. ^{1}H NMR ($CDCl_3$) δ 1.70–1.79 (m, 4H), 2.59 (s, 2H), 2.73–2.76 (m, 2H), 2.81–2.84 (m, 2H), 3.51–3.52 (m, 2H), 3.58 (s, 2H), 3.85 (s, 3H), 3.86 (s, 3H), 3.88 (s, 3H), 3.90 (s, 3H), 6.52 (s, 1H), 6.60 (s, 1H), 7.12 (d, J = 2.7 Hz, 1H), 7.78 (d, J = 2.7 Hz, 1H), 8.05 (s, 1H). Calcd: C: 52.27; H: 5.57; N: 4.69. Obsvd: C: 52.07; H: 5.40; N: 4.64.
Data for **15**. ^{1}H NMR ($CDCl_3$) δ 1.66 (s, 4H), 2.44–2.66 (m, 6H), 3.06 (s, 2H), 3.17–3.21 (m, 2H), 3.48–3.50 (m, 2H), 3.88 (s, 6H), 6.76–6.96 (m, 2H), 7.12–7.16 (m, 2H), 7.77–7.79 (m, 1H), 7.99 (s, 1H).
Data for **16**. ^{1}H NMR ($CDCl_3$) δ 1.72 (s, 4H), 2.47–2.67 (m, 6H), 3.03 (s, 2H), 3.15–3.20 (m, 2H), 3.54–3.63 (m, 2H), 3.99 (s, 3H), 6.73–6.93 (m, 2H), 7.11–7.17 (m, 1H), 7.60–7.72 (m, 2H), 8.01–8.26 (m, 3H), 8.38 (s, 1H).
Data for **17**. Mp 166–168 °C (oxalate salt); ^{1}H NMR (DMSO-d_6) δ 3.02 (s, 3H), 3.14 (s, 2H), 3.66 (s, 2H), 3.83 (s, 3H), 4.19 (s, 3H), 7.12–7.25 (m, 5H), 7.65–7.67 (m, 1H), 7.86 (s, 1H), 8.56 (t, J = 5.4 Hz, 1H). Calcd: C: 52.62; H: 4.84; N: 5.84. Obsvd: C: 52.38; H: 4.75; N: 5.69.
Data for **18**. Mp 158–160 °C (oxalate salt); ^{1}H NMR (DMSO-d_6) δ 2.93 (s, 2H), 3.16 (s, 2H), 3.60–3.66 (m, 3H), 3.71 (s, 3H), 3.73 (s, 3H), 3.84 (s, 3H), 4.14 (s, 3H), 6.73 (s, 1H), 6.78 (s, 1H), 7.13 (d, J = 8.9 Hz, 1H), 7.66 (d, J = 8.7 Hz, 1H), 7.86 (s, 1H), 8.57 (t, J = 5.4 Hz, 1H). Calcd: C: 51.22; H: 5.05; N: 5.19. Obsvd: C: 51.23; H: 5.07; N: 5.04.
Data for **19**. Mp 160–162 °C (oxalate salt); ^{1}H NMR (DMSO-d_6) δ 2.27 (s, 3H), 2.94 (s, 2H), 3.16 (s, 2H), 3.65–3.66 (m, 3H), 3.72 (s, 3H), 3.73 (s, 3H), 3.82 (s, 3H), 4.14 (s, 3H), 6.73 (s, 1H), 6.79 (s, 1H), 7.03 (d, J = 8.4 Hz, 1H), 7.29 (d, J = 8.4 Hz, 1H), 7.63 (s, 1H), 8.51 (s, 1H). Calcd: C: 60.18; H: 6.42; N: 5.85. Obsvd: C: 60.32; H: 6.39; N: 5.56.
Data for **20**. ^{1}H NMR ($CDCl_3$) δ 1.70–1.79 (m, 4H), 2.32 (s, 3H), 2.59 (s, 2H), 2.73–2.76 (m, 2H), 2.81–2.84 (m, 2H), 3.51–3.52 (m, 2H), 3.58 (s, 2H), 3.81 (s, 3H), 3.83 (s, 3H), 3.89 (s, 3H), 6.50 (s, 1H), 6.58 (s, 1H), 6.86–6.96 (m, 2H), 7.11 (s, 1H), 8.00 (s, 1H). Calcd: C: 62.14; H: 6.82; N: 5.57. Obsvd: C: 62.33; H: 6.60; N: 5.06.
17. **σ Receptor binding assays.** The σ_1 receptor binding assay was conducted using guinea pig brain membrane homogenates (100 μg protein). Membrane homogenates were incubated with 3 nM [^{3}H](+)-pentazocine (31.6 Ci/mmol) in 50 mM Tris–HCl (pH 8.0) at 25 °C for either 120 or 240 min. Test compounds were dissolved in ethanol then diluted in buffer for a total incubation volume of 0.5 mL. Test compounds were added in concentrations ranging from 0.005 to 1000 nM. Assays were terminated by the addition of ice-cold 10 mM Tris–HCl (pH 8.0) followed by rapid filtration through Whatman GF/B glass fiber filters (presoaked in 0.5% polyethylenimine) using a Brandel cell harvester (Gaithersburg, MD, USA). Filters were washed twice with 5 mL of ice cold buffer. Nonspecific binding was determined in the presence of 10 μM (+)-pentazocine. Liquid scintillation counting was carried out in EcoLite(+) (ICN Radiochemicals; Costa Mesa, CA, USA) using a Beckman LS 6000IC spectrometer with a counting efficiency of 50%.
The σ_2 receptor binding assay was conducted using rat liver membrane homogenates (35 μg of protein). Membrane homogenates were incubated with 3 nM [^{3}H]DTG (38.3 Ci/mmol) in the presence of 100 nM (+)-pentazocine to block σ_1 sites. Incubations were carried out in 50 mM Tris–HCl (pH 8.0) for 120 min at 25 °C in a total incubation volume of 0.5 mL. Test compounds were added in concentrations ranging from 0.005 to 1000 nM. Assays were terminated by the addition of ice-cold 10 mM Tris–HCl (pH 8.0) followed by rapid filtration through Whatman GF/B glass fiber filters (presoaked in 0.5% polyethylenimine) using a Brandel cell harvester (Gaithersburg, MD, USA). Filters were washed twice with 5 mL of ice cold buffer. Nonspecific binding was determined in the presence of 5 μM DTG. Liquid scintillation counting was carried out in EcoLite(+) (ICN Radiochemicals; Costa Mesa, CA, USA) using a Beckman LS 6000IC spectrometer with a counting efficiency of 50%.
The IC_{50} values at sigma sites were generally determined in triplicate from non-linear regression of binding data as analyzed by JMP (SAS Institute; Cary, NC, USA), using eight concentrations of each compound. K_i values were calculated using the method of Cheng–Prusoff[19] and represent mean values ± SEM. All curves were best fit to a one site fit and gave Hill coefficients of 0.8–1.0. The K_d value used for [^{3}H]DTG in rat liver was 17.9 nM and was 4.8 nM for [^{3}H](+)-pentazocine in guinea pig brain.[11,12]
18. **Dopamine receptor binding assays.** A filtration binding assay was used to characterize the binding properties of membrane-associated receptors. For rat $D2_{Long}$, rat D3 receptors expressed in Sf9 cells and human D4 dopamine receptors expressed in HEK 293 cells, tissue homogenates (50 μL) were suspended in 50 mM Tris–HCl/150 mM NaCl/10 mM EDTA buffer, pH 7.5 and incubated with

50 μL of ^{125}I-IABN at 37 °C for 60 min. Nonspecific binding was be defined using 25 μM (+)-butaclamol. For competition experiments the radioligand concentration is generally equal to 0.5 times the K_d value and the concentration of the competitive inhibitor ranges over five orders of magnitude. Binding will be terminated by the addition of cold wash buffer (10 mM Tris–HCl/150 mM NaCl, pH 7.5) and filtration over a glass-fiber filter (Schleicher and Schuell No. 32). Filters will be washed with 10 mL of cold buffer and the radioactivity will be measured using a Packard Cobra gamma counter. Estimates of the equilibrium dissociation constant and maximum number of binding sites are obtained using unweighted nonlinear regression analysis of data modeled according to the equation describing mass action binding.[20] Data from competitive inhibition experiments are modeled using nonlinear regression analysis to determine the concentration of inhibitor that inhibits 50% of the specific binding of the radioligand. Competition curves will be modeled for a single site and the IC_{50} values will be converted to equilibrium dissociation constants (K_i values) using the Cheng–Prusoff[19] correction. Mean K_i values ± SEM are reported for at least three independent experiments.

19. Cheng, Y. C.; Prusoff, W. H. *Biochem. Pharmacol.* **1973**, *22*, 3099.
20. McGonigle, P.; Molinoff, P. B. In *Basic Neurochemistry*, 4th ed.; Siegle Agranoff, Albers, Molinoff, Eds., Raven: 1989; Chapter 9.

RECEPTOR-BASED RADIOTRACERS FOR IMAGING THE PROLIFERATIVE STATUS OF BREAST TUMORS

Robert H. Mach,[1] Clive Brown-Proctor,[2] Suwanna Vangveravong,[2,3] Joseph B. Blair,[2] Nancy Buchheimer,[2] Joey Bottoms,[2] and Kenneth T. Wheeler[2]

[1]Division of Radiological Sciences, Washington University School of Medicine, St. Louis, MO
[2]Wake Forest University School of Medicine, Winston-Salem, NC
[3]Anasazi BioMedical Research, Inc., Winston-Salem, NC

INTRODUCTION

A number of studies have reported an overexpression of sigma receptors in a variety of human and murine tumors (1,2). The observation that the density of σ_2 receptors is greater than that of σ_1 receptors in a wide panel of tumor cells grown under cell culture conditions (3) suggests that the σ_2 receptor is a suitable target for developing receptor-based radiotracers for noninvasive imaging procedures such as Positron Emission Tomography (PET) and Single Photon Emission Computed Tomography (SPECT). In addition, the observation that the density of σ_2 receptors is 10-fold higher in proliferating versus quiescent mouse mammary adenocarcinoma cells both in vitro (4,5) and in vivo (6) suggests that radioligands possessing a high affinity and selectivity for σ_2 receptors have the potential to measure the proliferative status of breast tumors using noninvasive imaging procedures such as PET and SPECT.

A number of structurally-diverse compounds have been shown to bind with high affinity to sigma receptors. However, most compounds display either a high selectivity for the σ_1 receptor or bind with equal affinity to both σ_1 and σ_2 receptors. We previously reported that *N*-(9-(4-fluorobenzyl))-9-azabicyclo[3.3.1]nonan-3α-yl-*N'*-(2-methoxy-4-methylphenyl)carbamate, **1** (Figure 1), has a modest affinity and moderate selectivity for σ_2 versus σ_1 receptors (7). The higher affinity of **1** for σ_2 versus σ_1 receptors, and the observation that the fluorine-18 labeled analog of **1** could be prepared via alkylation of the des-benzyl precursor with [^{18}F]4-fluorobenzyl iodide, led us to explore the use of [^{18}F]**1** as a potential PET radiotracer for imaging the σ_2 receptor status of breast tumors. The goal of the current study was to synthesize [^{18}F]**1** and conduct preliminary in vivo studies of this radiotracer in a murine model of breast cancer.

Radiochemistry

The synthesis of [^{18}F]**1** was accomplished via N-alkylation of the des-benzyl precursor, **2**, with [^{18}F]4-fluorobenzyl iodide (Scheme 1). The product was obtained in an overall yield of ~10% from solublized [^{18}F]CsF in a specific activity of 2320 ± 1384 mCi/μmol (85.1 ± 51.2

Synthesis and Applications of Isotopically Labelled Compounds, Volume 8.
Edited by D. C. Dean, C. N. Filer and K. E. McCarthy.
 ISBN 0 470 86365 X

GBq/μmol). The radiotracer was of sufficient radiochemical purity (>95%) for the in vivo tumor uptake studies.

Biodistribution Studies

Preliminary in vivo biodistribution studies were conducted in nude mice containing xenografts of the mouse mammary adenocarcinoma tumor cell line, 66. The results of this study are shown in Table I. There was a gradual increase in the uptake of [^{18}F]**1** in the tumor xenografts between 30-min and 60-min post-i.v. injection of the radiotracer. There was a slow rate of washout of radiotracer from the tumor and a progressive increase in the tumor:blood and tumor:muscle ratios over time (Table I). Blocking studies with haloperidol (50 μg), a known sigma ligand, resulted in a reduction in tumor uptake and tumor:background ratios. These data are consistent with the labeling of σ_2 receptors in vivo (Figure 2).

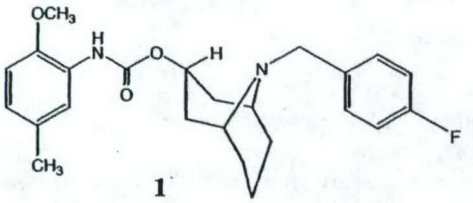

1

σ_1 = 202 nM
σ_2 = 30 nM
Ratio = 6.7

Figure **1**. Structure and in vitro binding affinity of **1** for sigma receptors.

Scheme I

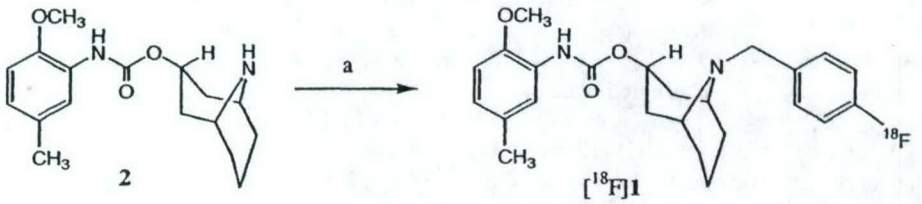

2 [^{18}F]**1**

Reagents: [^{18}F]4-fluorobenzyl iodide/triethylamine/DMF/90°C.

Discussion. Previous studies have shown that the □$_2$ receptor is a useful target for developing radiotracers for imaging breast tumors. Sigma-2 receptors are expressed in high density in breast tumor cells both in vitro and in vivo, whereas surrounding normal tissue is devoid of □$_2$ receptors (7). Also, the density of □$_2$ receptors is 10-fold higher in proliferating versus nonproliferating (i.e., quiescent) mouse mammary adenocarcinoma cells growing both in vitro and in vivo (3-5).

Therefore, a σ_2-selective imaging agent is predicted to not only image breast tumors, but has the added feature of potentially providing information regarding the proliferative status of the tumor. Most sigma receptor-based radiotracers for imaging tumors reported to date have a higher affinity for σ_1 versus σ_2 receptors, or bind with equal affinity to both σ_1 and σ_2 receptors (8,9). Although the σ_2 receptor affinity of **1** is somewhat lower than traditionally used for receptor-imaging studies, the relatively high selectivity of this compound for σ_2 versus σ_1 receptors, and the fact that the corresponding ^{18}F-labeled derivative was readily accessible via alkylation of **2** with [^{18}F]4-fluorobenzyl iodide indicated that this was a radiotracer worth evaluating in vivo. This agent demonstrated a high tumor uptake and reasonable tumor:blood and tumor:muscle ratios, which further suggests that [^{18}F]**1** may be a useful agent for imaging breast tumors with PET.

Table I. Results of biodistribution studies of [^{18}F]**1** in tumor-bearing mice.

%I.D./c.c. Tissue

Tissue	*30 min*	*60 min*	*120 min*	*240 min*
Brain	1.18 ± 0.19	1.92 ± 0.24	1.18 ± 0.19	0.13 ± 0.01
Blood	1.47 ± 0.10	3.07 ± 0.45	1.90 ± 0.18	0.37 ± 0.06
Lung	6.81 ± 0.85	5.11 ± 1.36	3.77 ± 0.39	0.65 ± 0.11
Heart	2.10 ± 0.18	3.30 ± 0.54	1.80 ± 0.21	0.31 ± 0.05
Liver	7.92 ± 1.18	10.93 ± 1.00	7.36 ± 0.89	1.14 ± 0.18
Kidney	6.40 ± 0.25	14.71 ± 4.57	5.50 ± 0.76	1.08 ± 0.11
Intestine	6.49 ± 0.69	17.92 ± 3.19	9.40 ± 0.87	2.23 ± 0.21
Muscle	1.25 ± 0.23	3.43 ± 0.58	1.84 ± 0.24	0.23 ± 0.02
Spleen	4.55 ± 0.33	5.87 ± 0.71	3.45 ± 0.39	0.55 ± 0.11
Tumor	1.34 ± 0.21	5.02 ± 0.85	3.18 ± 0.12	0.89 ± 0.03
Tumor:Blood[a]	0.80 ± 0.08	1.66 ± 0.23	1.72 ± 0.17	2.48 ± 0.22
Tumor:Muscle[b]	1.13 ± 0.27	1.78 ± 0.48	1.78 ± 0.18	3.98 ± 0.30

[a]%I.D. tumor/%I.D. blood; [b]%I.D. tumor/%I.D. muscle.

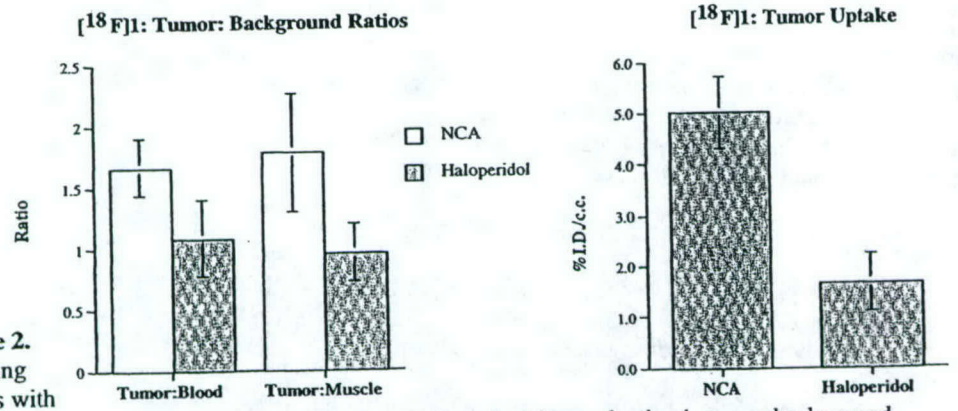

Figure 2. Blocking studies with haloperidol. Co-injection of 50 μg of haloperidol resulted in a reduction in tumor:background ratios and uptake of [^{18}F]**1** at 60 min post-i.v. injection of the radiotracer.

The results of the biodistribution study indicate that there is a high uptake of the radiotracer in mouse mammary adenocarcinoma xenografts (Table 1). The highest tumor:blood and tumor:muscle ratios was observed at 4 hr post-i.v. injection. In vivo blocking studies conducted with haloperidol, a known sigma receptor ligand, resulted in a dramatic reduction in the tumor uptake of [^{18}F]**1** at 60 min post-i.v. injection, which corresponds to the time of peak radiotracer accumulation in the no-carrier-added (N.C.A.) studies. Haloperidol also reduced the tumor:blood and tumor:muscle ratios to ~1.0 at this time point (Figure 2). These data are consistent with the labeling of σ_2 receptors in vivo.

Conclusion

In conclusion, we report in this communication the synthesis and preliminary in vivo evaluation of an ^{18}F-labeled σ_2-receptor radiotracer possessing a modest affinity and selectivity for σ_2 versus σ_1 receptors. The in vivo studies indicate that there is a high uptake of this radiotracer in mouse mammary adenocarcinoma xenografts, and that co-injecting with a known sigma ligand reduces the uptake of the radiotracer. Additional studies are currently being conducted in order to determine if this radiotracer is suitable for PET studies aimed at determining the σ_2 receptor status of solid tumors.

Acknowledgements. This research was funded by grants CA 80452 awarded by the National Cancer Institute, DE-FG02-00ER82945 awarded by the Department of Energy, and DAMD17-01-1-0446 awarded by the Department of Defense Breast Cancer Research Program of the US Army Medical Research and Materiel Command Office.

References

1. Bem W.T., Thomas G.E., Mammone J.Y., Homan S.M., Levy B.K., Johnson, F.E., Coscia C.J. Cancer Research **1991**; *51*: 6558-6562.
2. Vilner B.J., John C.S., Bowen W.D. Cancer Research **1995**; *55*: 408-413.
3. Mach R.H., Smith C.R., Al-Nabulsi I., Whirrett B.R., Childers S.R., Wheeler KT. *Cancer Research* **1997**; *57*: 156-161.
4. Al-Nabulsi I., Mach R.H., Sten K., Childers S.R., Wheeler KT. Brit. J. Cancer **1999**; *81*: 925-933.
5. Wheeler K.T., Wang L.-M., Wallen C.A., Childers S.R., Cline J.M., Keng P.C., Mach R.H. British J. Cancer **2000**; *82*: 1223-1232.
6. Mach R.H., Vangveravong S., Huang H., Yang B., Blair J.B., Wu L. Med. Chem. Res. **2003**; 11: 380-398.
7. John C.S., Vilner B.J., Schwartz A.M., Bowen W.D. J. Nucl. Med. **1996**; *37*: 267P.
8. John C.S., Vilner B.J., Gulden M.E., Efange S.M.N., Langason R.B., Moody T.W., Bowen W.D. Cancer Research **1995**; *55*: 3022-3027.
9. Caveliers V., Everaert H., John C.S., Lahoutte T. J. Nucl. Med. **1995**; *43*: 1647-1649.

Carbon-11 Labeled σ_2 Receptor Ligands for Imaging Breast Cancer

Zhude Tu[a], Carmen S. Dence,[a] Datta E. Ponde[a], Lynne Jones,[a] Kenneth T. Wheeler,[b] Michael J. Welch,[a] and Robert H. Mach[a*]

[a] Mallinckrodt Institute of Radiology, Washington University School of Medicine, St. Louis, MO 63110, and [b] Wake Forest University School of Medicine, Winston-Salem, NC 27157

Abbreviated title: C-11 labeled σ_2 receptor radiotracers

Keywords: Sigma-2 receptors, PET, Tumor imaging agents

Total pages: 25

Figures: 3

Tables: 3

Schemes: 2

Address correspondence to:

Robert H. Mach, Ph.D.
Division of Radiological Sciences
Washington University School of Medicine
Campus Box#: 8225
510 South Kingshighway
St. Louis, MO 63110
phone: (314) 362-8538
fax: (314) 362-0039
email: rhmach@mir.wustl.edu

Abstract

Four conformationally-flexible benzamide analogs having a high affinity and outstanding selectivity for σ_2 versus σ_1 receptors were synthesized and radiolabeled with carbon-11 by reaction with [^{11}C]methyl iodide. The four ^{11}C-labeled radiotracers were evaluated for their potential to image the proliferative status of breast tumors with Positron Emission Tomography (PET). In vivo studies in female Balb/C mice bearing EMT-6 breast tumors showed one radiotracer, (2-methoxy-^{11}C)-N-(4-(3,4-dihydro-6,7-dimethoxy-isoquinolin-2(1H)-*yl*)butyl)-5-methylbenzamide ([^{11}C]**2**) had a high tumor uptake and suitable tumor:background ratio for imaging purposes. Blocking studies were consistent with the labeling of σ_2 receptors in vivo. A study comparing the in vivo properties of [^{11}C]**2** and ^{18}F-3'-fluoro-3'-deoxy-L-thymidine ([^{18}F]FLT) indicated that [^{11}C]**2** had either similar (lung, fat) or better (blood, muscle) tumor:organ ratios than [^{18}F]FLT in the tissues that are important for breast tumor imaging. Consequently, [^{11}C]**2** is a potential radiotracer for imaging the proliferative status of breast tumors in vivo with PET.

1. Introduction

Sigma (σ) receptors are a distinct class of receptors that are expressed in many normal tissues, including liver, kidneys, endocrine glands and brain [1]. It has been well established that there are at least two types of σ receptors, σ_1 and σ_2. The σ_1 receptor has been cloned and displays a 30% sequence homology with the enzyme, yeast sterol isomerase [2]. The σ_2 receptor has not been cloned, but evidence suggests that this receptor is linked to potassium channels and intracellular calcium release in NCB-20 cells [1,3,4].

Previous studies have reported an overexpression of sigma receptors in a variety of human and murine tumors [4-6]. The observation that the density of σ_2 receptors is greater than that of σ_1 receptors in a wide panel of tumor cells grown under cell culture conditions [4] suggests that the σ_2 receptor is a suitable target for developing receptor-based radiotracers for noninvasive imaging procedures such as Positron Emission Tomography (PET) and Single Photon Emission Computed Tomography (SPECT). In addition, the recent observation that the density of σ_2 receptors is 10-fold higher in proliferating versus quiescent mouse mammary adenocarcinoma cells both in vitro [7,8] and in vivo [9] suggests that radioligands possessing a high affinity and selectivity for σ_2 receptors have the potential to measure the proliferative status of breast tumors using noninvasive imaging procedures such as PET and SPECT.

A number of structurally-diverse compounds have been shown to bind with high affinity to sigma receptors. However, most compounds display either a high selectivity for the σ_1 receptor or bind with equal affinity to both σ_1 and σ_2 receptors [1]. We recently

reported the synthesis and in vitro binding of a number of conformationally-flexible benzamide analogs having a high affinity and outstanding selectivity for σ_2 versus σ_1 receptors [10]. The presence of an ortho methoxy group in each compound (Table I) indicated that it is possible to prepare the corresponding ^{11}C-labeled radiotracer via O-alkylation of the corresponding phenol precursor with [^{11}C]methyl iodide. The goals of the current study were to: a) evaluate the use of [^{11}C]**1** - **4** as PET imaging agents in a rodent model of breast cancer, and 2) compare the in vivo properties of our ^{11}C-labeled σ_2 receptor ligands with those of the radiolabeled nucleoside, [^{18}F]FLT [11].

2. Methods and Materials

2.1. General. All chemicals were obtained from Aldrich Chemical Co. (Sigma-Aldrich, St. Louis, MO) and used without further purification unless otherwise stated. ^{1}H NMR spectra were recorded at 300 MHz on a Varian Mercury-VX spectrometer. All chemical shift values are reported in ppm (δ). Elemental analyses (C, H, N) were determined by Atlantic Microlab, Inc. and the analytical results were within $\pm$0.4% of the theoretical values for the formula given unless otherwise listed. The radiolabeled nucleoside, [^{18}F]FLT, was prepared using the procedure described by Shields et al. [11].

2.2.2. General Procedure for the preparation of N-substituted 6,7-Dimethoxy-1,2,3,4-tetrahydroisoquinoline benzamides.

Method A: A solution of substituted 2-methoxy benzoic acid (300 mmol), 1.0 equivalent of *N*-(6,7-dimethoxy-1,2,3,4-tetrahydro-1H-isoquinolin)-4-aminobutane or *N*-(6,7-dimethoxy-1,2,3,4-tetrahydro-1H-isoquinolin)-2-aminoethane in methylene chloride (30

mL) was stirred at 0°C. Then, 1.0 equivalent of benzotriazol-1-yl-oxytris(dimethylamino)phosphonium hexafluorophosphate (BOP) or 1,3-dicyclohexylcarbodiimide (DCC) and 2.5 equivalents of triethylamine were added, and the solution was allowed to warm up to ambient temperature. The reaction mixture was stirred at ambient temperature for 18 hrs. The mixture was then washed with saturated aqueous sodium bicarbonate, and the organic layer was separated and dried over anhydrous sodium sulfate. The solvent was removed under reduced pressure to provide the crude product, which was purified on a silica gel column using hexane/ethyl ether/triethylamine (50:50:1) as the eluent.

N-[4-(6,7-Dimethoxy-3,4-dihydro-1H-isoquinolin-2-yl)-butyl]-2-methoxy-5-methyl-benzamide(**2**). 59.2% yield. ^{1}H-NMR (300 MHz, $CDCl_3$): 1.21-1.72 (t, 4H), 2.31 (s,3H), 2.52-2.58 (t, 2H), 2.68-2.7 3 (t, 2H), 2.79-2.84 (t, 2H), 3.46-3.49 (t, 2H), 3.55(s, 2H), 3.82 (s, 3H), 3.83 (s, 3H), 3.89(s. 3H), 6.50 (s, 1H), 6.58 (s, 1H), 6.83-6.86 (d, 1H), 7.19-7.23 (d, 1H), 7.93 (s, 1H), 7.90 (s, 1H).

5-Bromo-N-[2-(6,7-dimethoxy-3,4-dihydro-1H-isoquinolin-2-yl)-ethyl]-2-methoxy-benzamide (**3**). 72.0% yield. ^{1}H-NMR (300 MHz, $CDCl_3$): 2.73-2.84 (m, 4H), 3.61 (s, 3H), 3.62-3.67 (m, 4H), 3.83 (s, 3), 3.85 (s, 3H), 6.54 (s, 1H), 6.74-6.78 (d, 1H), 7.25-7.49 (d, 1H), 8.29 (s, 1H), 8.53 (s, 1H).

5-Bromo-N-[4-(6,7-dimethoxy-3,4-dihydro-1H-isoquinolin-2-yl)-butyl]-2,3-dimethoxy-benzamide (**4**). 52.0% yield. ^{1}H-NMR (300 MHz, $CDCl_3$): 1.67-1.72 (m, 4H), 2.51-2.56 (t 2), 2.65-2.69 (t, 2H), 2.77-2.81 (t, 2H), 3.30-3.50 (t, 2H), 3.53 (s, 2H), 3.83 (s, 3H), 3.84 (s, 3), 3.85 (s, 3H), 3.87 (s, 3H), 6.50 (s, 1H), 6.57 (s, 1H), 7.76 (d, 1H), 8.05 (s, 1H).

Method B: A solution of 5-bromosalicylic acid (217 mg, 1.0 mmol) and *N*-(6,7-dimethoxy-1,2,3,4-tetrahydro-1*H*-isoquinolin)-4-aminoethane (306 mg, 1.3 mmol) in methylene chloride (30 mL) was cooled to 0°C (ice bath) and 1,3-dicyclohexyl-carbodiimide (278 mg, 1.35 mmol) was added. The solution was removed from the ice bath and the reaction mixture was stirred at ambient temperature for 18 hrs. The mixture was washed with saturated aqueous sodium bicarbonate, and the organic layer was dried over anhydrous sodium sulfate. The solution was filtered, and the volatiles were removed in vacuo. The residue was purified using a silica gel column (1.0 x 20 inches) and methanol : ether (1:4) as the eluent; 74 mg of final product, **9**, was obtained. The yield was 17%. ^{1}H-NMR (300MHz, $CDCl_3$): 2.70-2.90 (m, 6H), 3.55–3.63 (m, 2H), 3.65-3.70 (s, 2H), 3.84 (s, 3H), 3.86 (s, 3H), 6.54 (s, 1H), 6.62 (s, 1H), 6.84 (d, 1H), 7.18 (s, 1H), 7.43 (d, 1H), 7.45 (s, 1H).

N-[2-(6,7-Dimethoxy-3,4-dihydro-1H-isoquinolin-2-yl)-ethyl]-2-hydroxy-5-methyl-benzamide (**8**) 15% yield. ^{1}H-NMR (300 MHz, $CDCl_3$): 2.24 (s, 3H), 2.70-2.90 (m, 6H), 3.60 – 3.63 (m, 2H), 3.65 (s, 2H), 3.85 (s, 3H), 3.87 (s, 3H), 6.55 (s, 1H), 6.63 (s, 1H), 6.87 (d, 1H), 7.10 (s, 1H), 7.16 (d, 1H), 7.16 (t, 1H).

N-[2-(6,7-dimethoxy-3,4-dihydro-1H-isoquinolin-2-yl)-butyl]-2-hydroxy-5-methyl-benzamide(**10**). 60% yield. ^{1}H-NMR (300 MHz, $CDCl_3$): 1.73-1.78 (t, 4H), 2.09 (s, 3H), 2.68 - 2.64 (t, 2H), 2.77 - 2.84 (t, 4H), 3.46-3.49 (t, 2H), 3.61(s, 2H), 3.82 (s, 3H), 3.84 (s, 3H), 6.49 (s, 1H), 6.59 (s, 1H), 6.84-6.87 (d, 1H), 7.05 (s, 1H), 7.10 - 7.16 (d, 1H), 7.26 (s, 1H).

5-Bromo-N-[4-(6,7-dimethoxy-3,4-dihydro-1H-isoquinolin-2-yl)-butyl]-2-hydroxy-3-methoxy-benzamide (**11**). 29% yield. ^{1}H-NMR (300 MHz, $CDCl_3$): 1.16 - 1.25 (m, 2H), 1.60 - 1.80 (m, 2H), 2.54 - 2.66 (m, 4H), 2.66 - 2.90 (t, 2H), 3.43 - 3.46 (m, 2H), 3.46-3.58 (s, 2H), 3.81 (s, 3H), 3.82 (s, 3H), 3.84 (s, 3H), 5.29 (s, 1H), 6.48 (s, 1H), 6.55 (s, 1H), 6.97 (d, 1H), 7.13 (d, 1H), 7.26 (s, 1H).

2.2.3. Radiolabeling

Synthesis of [^{11}C]**1**. A stream of [^{11}C]methyliodide in helium was bubbled for 5 min. period into a solution of **8** (1.5 - 2.0 mg) in DMF (0.18 mL) and 5N NaOH (2 μl) at 0^{o}C (ice-water bath). The sealed reaction vessel was heated at 85^{0}C (oil bath) for 5 min. The reaction was quenched by the addition of HPLC solvent (1.8 mL) and the residue was purified by C-18 reversed-phase semi-preparative HPLC using 17.5 % THF/82.5 % of 0.1M ammonium formate (with 0.1% formic acid) buffer at pH = 4.0 as the mobile phase (flow rate = 4.0 mL/min). Under these conditions the retention time of the [^{11}C]**1** was 14.50 min. The product was collected into a 50 ml round bottom flask, and the volatile

components were removed in vacuo. The residue was diluted with saline (5 mL) and an aliquot (50 ul) was taken for HPLC analysis using the same HPLC conditions described above.

The other three radiotracers ([^{11}C]**2,** [^{11}C]**3,** and [^{11}C]**4**) were synthesized with the same procedure. The radiochemical purities were greater than 95% for all four ^{11}C-labeled radiotracers. The HPLC solvent, retention time, labelling yield and specific activity of each radiotracer is shown in Table II. The total radiosynthesis time, including production of [^{11}C]methyliodide, ranged from 50 – 60 min.

2.3. Mouse tumor model

All animal experiments were conducted under IACUC approved protocols in compliance with the Guidelines for the Care and Use of Research Animals established by the Washington University Medical School Animal Studies Committee. The mouse mammary carcinoma cell line EMT6 (12,13) was obtained from the laboratory of Dr. Ronald S. Pardini at the University of Nevada and maintained by serial passage in RPMI1640 containing 10% FCS in a 37°C humidified 95% air, 5% CO_2 incubator. Cells were harvested during exponential growth and viability of the cell suspension was greater than 90%. Female BALB/c mice, 5–6 weeks of age, were purchased from NIH-Frederick. Tumors were implanted subcutaneously in the nape of the neck using 5 x 10^5 cells per 100 μL and grown for 8-12 days prior to use. At the time of the study, mouse weight averaged 18 - 22 grams and average tumor size was between 100 - 250 mg.

2.4. Biodistribution and tumor uptake studies

A solution of [^{11}C]**1**, [^{11}C]**2**, [^{11}C]**3**, [^{11}C]**4** (100-150 μCi) diluted in saline (100-150 μL) was injected via the tail vein into EMT6 tumor-bearing female BALB/C mice. Groups of at least four mice were used for each time point. At 5, 30 and 60 minutes after injection, the mice were euthanized. Samples of target and non-target tissue including blood, lung, liver, kidney, muscle, fat, heart, brain and tumor were removed by dissection. Activity in each sample quantified using a Beckman Gamma 8000 well counter. A dilution of the injectate was also counted with the samples from each animal. Tissues were weighed and the percentage injected dose (%I.D.) per gram tissue was calculated. The tumor:organ ratios were calculated by dividing the %I.D./gram for tumor by the %I.D./g for the tissue.

Blocking studies were conducted with [^{11}C]**2** by co-injecting the unlabeled nonselective σ_1/σ_2 ligand, N-(4'-fluorobenzyl)piperidinyl-4-(3-bromophenyl)acetamide (2 mg/kg, i.v.). The mice were sacrificed 30 minutes after. injection of the radiotracer and biodistribution studies were conducted as described above.

3. Results

The results of the radiolabeling studies are shown in Table II. The labeling yield represents the %yield of the O-alkylation step and is based on the starting activity of [^{11}C]methyl iodide. The % yield of [^{11}C]**1** and [^{11}C]**2** was quite high whereas the labeling yield of [^{11}C]**3** and [^{11}C]**4** were somewhat lower for reasons that were not clear. No attempt was made to optimize the labeling yield of [^{11}C]**3** and [^{11}C]**4**. The radiochemical purity of all tracers was over 99% and all four ^{11}C-labeled radiotracers were obtained in a specific activity suitable for in vivo studies.

The tissue distribution of the radioactivity after injection of each of the four tracers into mice is summarized in Table III. Of the four ^{11}C-labeled radiotracers, [^{11}C]**2** had the highest tumor uptake at all times, with percent injected dose/g tumor (% I.D./g) values of 4.22 at 5 min, 2.35 at 30min, 1.32 at 60min, respectively. A plot of the % I.D./g tumor at 60 min versus log P for each radiotracer indicates that lipophilicity of the radiotracer may be an important property in determining tumor uptake (Figure 1). A similar relationship was demonstrated for the earlier time points (data not shown). Among the peripheral tissues, the kidney and liver showed a very high initial uptake of all four ^{11}C-labeled tracers, but the levels decreased rapidly. There was a rapid clearance of the radioactivity from blood, muscle, and fat. As shown in Table IV, [^{11}C]**2** had the highest tumor:blood and tumor:lung ratios at the 1 hr. post-i.v. injection time point. The higher tumor:organ ratios of [^{11}C]**2** indicate that this radiotracer is the best candidate for imaging breast tumors.

In order to determine that the in vivo binding of [^{11}C]**2** was specific for sigma receptors, [^{11}C]**2** was co-injected with N-(4'-fluorobenzyl)piperidinyl-4-(3-bromophenyl)acetamide (a.k.a., YUN 143), which is a sigma ligand displaying a high affinity for both σ_1 and σ_2 receptors [14]. Co-injection of [^{11}C]**2** with YUN 143 (2 mg/kg, i.v.) resulted in a decrease in the tumor:blood (-32%), tumor:lung (-18%), tumor:muscle (-46%) and tumor:fat (-46%) ratios at 30 min. post-i.v.-injection of the radiotracer (Figure 2). These data are consistent with the labeling of σ_2 receptors in vivo.

A study was also conducted comparing the tumor uptake and tumor:organ ratios of [^{11}C]**2** with that of [^{18}F]FLT, a radiolabeled nucleoside analog that is believed to measure tumor proliferation [11]. The results of this study, which are shown in Figure 3, indicate

that [^{18}F]FLT has a higher tumor uptake than [^{11}C]**2**. However, [^{11}C]**2** had either similar (lung, fat) or better (blood, muscle) tumor:organ ratios than [^{18}F]FLT in the tissues that are important for breast tumor imaging. Consequently, [^{11}C]**2** is a potential radiotracer for imaging the proliferative status of breast tumors in vivo with PET.

4. Discussion

Previous studies have shown that many tumors of human origin possess a high density of σ_2 receptors relative to that of surrounding normal tissue [4]. Although several types of human tumors possess σ_1 and σ_2 receptors, the density of σ_1 receptors in tumor cells is generally less than that present in normal tissues [4]. Therefore, a σ_2 selective imaging agent is predicted to be a better tumor imaging agent since it should have higher tumor:normal tissue ratios relative to σ_1 selective or σ_1/σ_2 nonselective imaging agents. This prediction was confirmed in our earlier studies with [^{18}F]YUN 143, which had much higher tumor:organ ratios when only σ_2 receptors were labeled than when both σ_1 and σ_2 receptors were labeled [14]. However, the absence of ligands displaying a higher affinity for σ_2 versus σ_1 receptors has limited the likelihood of developing σ_2-selective imaging agents for PET and SPECT.

We recently reported a series of conformationally-flexible benzamide analogs having a high affinity and selectivity for σ_2 versus σ_1 receptors [10]. The presence of an ortho methoxy group in these compounds (Table I) indicated that it is possible to prepare the corresponding ^{11}C-labeled radiotracer using standard radiochemistry techniques. Therefore, the goal of the current study was to evaluate the four ^{11}C-labeled benzamide analogs shown in Table I and determine whether they would be useful imaging agents for

assessing the anatomic and/or proliferative status of breast tumors. A second goal of this study was to compare the best of the ^{11}C-labeled radiotracers with [^{18}F]FLT, a nucleoside-based radiotracer that is currently being used to measure the tumor proliferation with PET [11].

Although the σ_2 receptor affinities of [^{11}C]**1**, [^{11}C]**2**, [^{11}C]**3**, [^{11}C]**4** are similar, the vivo biodistribution indicated that [^{11}C]**2** has the highest tumor uptake at all time points (Table III). One possible explanation for this is that [^{11}C]**2** may have the optimal lipophilicity since a parabolic relationship was observed between the % I.D./g tumor and the calculated log P of the radiotracer (Figure 1). These data indicate that both receptor affinity and lipophilicity are important properties that must be considered in the design of receptor-based tumor imaging agents.

In vivo blocking studies were conducted by co-injecting the nonselective sigma ligand, YUN 143 (2 mg/kg), with [^{11}C]**2**. This compound was chosen because our previous studies with the ^{18}F-labeled version of this ligand, showed that [^{18}F]YUN 143 had a high tumor uptake and efficiently labeled σ_2 receptors in vivo [14]. In the σ_2 blocking study, the tumor:organ ratios were reduced by 18 – 46%. Thus, these data are consistent with the labeling of σ_2 receptors in the tumor xenograft by [^{11}C]**2**.

In the previous study described above, we reported that the tumor:organ ratios of [^{18}F]YUN 143 under conditions favoring the labeling of σ_2 receptors was higher than the tumor:organ ratios of the radiolabeled nucleoside, [^{125}I]IUdR [14]. Therefore, one of the goals of the current study was to compare our best ^{11}C-labeled σ_2 receptor ligand with the ^{18}F-labeled DNA precursor, [^{18}F]FLT. This radiolabeled analogue of thymidine has a greater metabolic stability than [$^{123/124}$I]IUdR and [^{11}C]thymidine, and was introduced

recently as a radiotracer for measuring the proliferative status of solid tumors in vivo with PET [11]. The biodistribution data for [^{18}F]FLT and [^{11}C]**2** in female Balb/C mice bearing EMT-6 tumors is shown in Figure 3. The top graph demonstrates that [^{18}F]FLT has a higher uptake in the tumor xenograft relative to [^{11}C]**2** at 60 min post-i.v. injection.. However, the uptake of [^{18}F]FLT was also higher than [^{11}C]**2** in all organs. This resulted in similar tumor:lung and tumor:fat ratios for both [^{11}C]**2** and [^{18}F]FLT. However, [^{11}C]**2** had a higher tumor:blood and tumor:muscle ratio than [^{18}F]FLT. We are currently conducting studies comparing [^{11}C]**2** and [^{18}F]FLT with "gold standard" measures of proliferation.

5. Conclusion

In present study, we have successfully synthesized four ^{11}C-labeled conformationally-flexible benzamide analogues having a high affinity and selectivity for σ_2 versus σ_1 receptors. The four analogs, [^{11}C]**1,** [^{11}C]**2,** [^{11}C]**3,** [^{11}C]**4** were evaluated as potential radiotracers for imaging σ_2 receptors in Balb/C mice bearing EMT-6 breast tumors. Of the four ^{11}C-labeled analogues, [^{11}C]**2** showed the best tumor uptake and tumor:organ ratios. Our data also indicates that [^{11}C]**2** displays either similar or better tumor:organ ratio as that of the radiolabeled nucleoside, [^{18}F]FLT. Additional studies are clearly needed to compare [^{11}C]**2** and [^{18}F]FLT with "gold standard" measures of proliferation in order to determine if the σ_2 receptor approach is appropriate for measuring the proliferative status of breast tumors with PET.

Acknowledgments. This work was supported by grants CA102869 awarded by the National Institutes of Health and grant DAMD17-01-1-0446 awarded by the Department of Defence Breast Cancer Research Program of the US Army Medical Research and Materiel Command Office. The authors gratefully thank Susan Adams and Pat Margenau for their excellent technical assistance.

References

[1] Walker JM, Bowen WD, Walker FO, Matsumoto RE, De Costa B, Rice KR. Sigma receptors: biology and function. Pharmacol. Rev. 1990; 42: 355-402.

[2] Hanner M, Moebius FF, Flandorfer A, Knaus H-G, Striessnig J, Kempner E, Glossmann H. Purification, molecular cloning, and expression of the mammalian $sigma_1$-binding site. Proc. Natl. Acad. Sci. USA 93 1996; 93: 8072-8077.

[3] Hellewell SB, Bruce A, Feinstein G, Orringer J, Williams W, Bowen, WD. Rat liver and kidney contain high densities of σ_1 and σ_2 receptors: characterization by ligand binding and photoaffinity labeling. Eur. J. Pharmacol. Mol. Pharmacol. Sec. 1994; 268: 9-18.

[4] Vilner BJ, John CS, Bowen WD. Sigma-1 and sigma-2 receptors are expressed in a wide variety of human and rodent tumor cell lines. Cancer Res. 1995; 55: 408-413.

[5] Bem WT, Thomas GE, Mammone JY, Homan SM, Levy BK, Johnson FE, Coscia CJ. Overexpression of σ receptors in nonneural human tumors. Cancer Res. 1991; 51: 6558–6562.

[6] Vilner BJ and Bowen WD. Characterization of sigma-like binding properties of NB41A3, S-20Y, and N1E-115 neuroblastomas, C6 gliomas, and NG108–15 neuroblastoma-glioma hybrid cells: further evidence for sigma-2 receptors. In: J.M. Kamenka and E.F. Domino (eds.), Multiple sigma and PCP receptor ligands: mechanisms for neuromodulation and neuroprotection? pp. 341–353. Ann Arbor, MI: NPP Books (1992).

[7] Mach RH, Smith CR, Al Nabulsi I, Whirrett BR, Childers SR, Wheeler KT. Sigma-2 receptors as potential biomarkers of proliferation in breast cancer. Cancer Res. 1997: 57: 156–161.

[8] Al-Nabulsi I, Mach RH, Wang L-M, Wallen CA, Keng PC, Sten K, Childers SR, Wheeler KT. Effect of ploidy, recruitment, environmental factors, and tamoxifen treatment on the expression of sigma-2 receptors in proliferating and quiescent tumor cells. Br J Cancer 1999; 81: 925-933.

[9] Wheeler KT, Wang L-M, Wallen CA, Childers SR, Cline JM, Keng PC, Mach RH. Sigma-2 receptors as a biomarker of proliferation in solid tumors, Br. J. Cancer 2000; 82: 1223–1232.

[10] Mach RH, Huang Y, Freeman RA, Wu L, Vangveravong S, Luedtke RR. Conformationally-flexible benzamide analogues as dopamine D_3 and σ_2 receptor ligands. Bioorg. Med. Chem. Lett. 2004; 14: 195-202.

[11] Shields AF, Grierson JR, Dohmen BM, Machulla HJ, Stayanoff JC, Lawhoirn-Crews JM, Obradovich JE, Muzik O, Manger TJ. Imaging proliferation in vivo with [^{18}F]FLT and positron emission tomography. Nature Medicine 1998; 4: 1334–1336.

[12] Rockwell SC, Kallman RF, Fajardo LF. Characteristics of a serially transplanted mouse mammary tumor and its tissue-culture-adapted derivative. J. Natl. Cancer Inst. 1972; 49: 735–747.

[13] Rockwell SC. In vivo-in vitro tumor systems: New models for studying the response of tumors to therapy. Lab. Anim. Sci. 1977; 27: 831–851.

[14] Mach RH, Huang Y, Buchheimer N, Kuhner R, Wu L, Morton TE, Wang L-M, Ehrenkaufer RL, Wallen CA, Wheeler KT. [^{18}F]N-4′-Fluorobenzyl-4-(3-bromophenyl) acetamide for imaging the sigma receptor status of tumors: comparison with [^{18}F]FDG and [^{125}I]IUDR. Nucl Med Biology 2001; 28: 451-458.

Figure Legends

Figure 1. Relationship between tumor uptake and lipophilicity of the σ_2 receptor ligands.

Figure 2. Comparison of the tumor:blood, tumor:lung, tumor:muscle, and tumor:fat ratios of the [^{11}C]**2** under no-carrier-added conditions and under conditions of σ_1 and σ_2 blockade with YUN-143 (2 mg/kg i.v.). The animals were sacrificed at 30 min post-i.v. injection.

Figure 3. Comparison of [^{18}F]FLT versus [^{11}C]**2** at 30 and 60 min. post-i.v. injection of the radiotracer.

Table I. Structures and in vitro binding of the benzamide analogs.

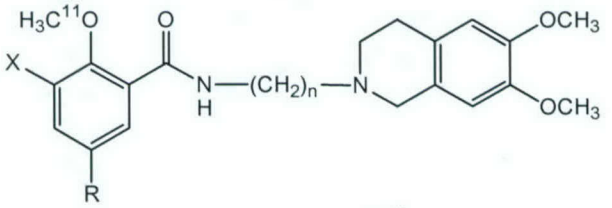

				Ki[a]			
#	X	R	n	σ_1[b]	σ_2[c]	σ_1: σ_2 Ratio[d]	Log P[e]
1	H	CH_3	2	10,412	13.3	783	2.31
2	H	CH_3	4	3,078	10.3	300	2.84
3	H	Br	2	5,484	12.2	442	3.17
4	OCH_3	Br	4	12,900	8.2	1,573	3.33

[a] Mean $\pm$ SEM, K_i values were determined by at least three experiments [10].

[b] K_i values for σ_1 receptors were measured on guinea pig brain membranes using [^{3}H](+)-pentazocine as the radioligand.

[c] K_i values for σ_2 receptors were measured on rat liver membranes using [^{3}H]-DTG as the radioligand in the presence of (+)-pentazocine.

[d] K_i for σ_1/K_i for σ_2.

[e] calculated value using the program Clog P.

Table II. The HPLC solvent, retention time, labeling yield and specific activity

#	HPLC solvent	Retention time	%Yield	Specific Activity (EOB)[a]
1	17.5%THF : 82.5% 0.1M buffer	14.5 min	60-75	~5000 mCi/umol
2	15%THF : 85% 0.1M buffer	12.5 min	60-75	~4000 mCi/umol
3	15%THF : 85% 0.1M buffer	17.5 min	10-15	~1000 mCi/umol
4	18.5%THF : 81.5% 0.1M buffer	15.5 min	30-40	~4000 mCi/umol

[a]Decay corrected to end-of-bombardment (EOB)

Table III. [^{11}C]**1 - 4** Biodistribution in female Balb/C mice bearing EMT-6 Tumors

%I.D./g Tissue

	5 min.	30 min.	1 hour
[^{11}C]**1**			
blood	5.89 ± 0.29	2.62 ± 0.22	1.98 ± 0.35
lung	5.69 ± 0.70	1.42 ± 0.15	1.39 ± 0.67
liver	18.49 ± 2.87	3.87 ± 0.67	1.70 ± 0.23
kidney	44.07 ± 1.67	2.77 ± 0.42	1.01 ± 0.12
muscle	1.75 ± 0.21	0.56 ± 0.19	0.41 ± 0.22
fat	3.07 ± 0.40	0.38 ± 0.12	0.26 ± 0.09
heart	2.89 ± 0.36	0.76 ± 0.06	0.76 ± 0.46
brain	1.63 ± 0.30	0.11 ± 0.01	0.10 ± 0.04
tumor	3.10 ± 0.25	1.08 ± 0.08	0.85 ± 0.14
[^{11}C]**2**			
blood	3.09 ± 0.33	1.31 ± 0.11	0.73 ± 0.05
lung	14.02 ± 1.40	2.27 ± 0.42	1.09 ± 0.26
liver	12.32 ± 1.73	9.65 ± 2.00	3.00 ± 0.21
kidney	20.50 ± 1.86	4.12 ± 0.51	2.26 ± 0.36
muscle	4.49 ± 0.45	0.75 ± 0.13	0.49 ± 0.11
fat	1.88 ± 0.50	0.68 ± 0.19	0.33 ± 0.24
heart	5.86 ± 0.47	0.95 ± 0.17	0.50 ± 0.11
brain	2.29 ± 0.28	0.28 ± 0.03	0.15 ± 0.01
tumor	4.22 ± 1.01	2.35 ± 0.27	1.32 ± 0.17
[^{11}C]**3**			
blood	5.25 ± 0.39	2.35 ± 0.16	1.88 ± 0.16
lung	5.72 ± 0.40	1.83 ± 0.13	1.32 ± 0.11
liver	19.88 ± 3.10	5.89 ± 0.82	2.65 ± 0.29
kidney	51.03 ± 7.14	34.19 ± 1.74	19.78 ± 1.99
muscle	1.73 ± 0.11	0.52 ± 0.23	0.36 ± 0.08
fat	2.05 ± 0.49	0.63 ± 0.19	0.37 ± 0.13
heart	3.18 ± 0.26	0.77 ± 0.08	0.56 ± 0.05
brain	2.52 ± 0.15	0.26 ± 0.10	0.14 ± 0.02
tumor	1.82 ± 0.39	1.06 ± 0.09	0.87 ± 0.09
[^{11}C]**4**			
blood	7.12 ± 1.01	0.99 ± 0.15	0.45 ± 0.04
lung	6.01 ± 0.77	1.34 ± 0.23	0.70 ± 0.26
liver	25.02 ± 3.70	2.48 ± 0.52	1.19 ± 0.17
kidney	19.48 ± 1.46	2.57 ± 0.78	1.34 ± 0.19
muscle	1.94 ± 0.13	2.11 ± 0.77	0.46 ± 0.40
fat	1.48 ± 0.55	0.63 ± 0.33	0.20 ± 0.08
heart	3.54 ± 0.31	0.68 ± 0.12	0.29 ± 0.10
brain	0.33 ± 0.09	0.08 ± 0.03	0.03 ± 0.00
tumor	2.82 ± 0.36	0.92 ± 0.10	0.50 ± 0.09

Table IV. Tumor:background ratios at 1 hr. post-i.v. injection of the radiotracer

Ratio	[^{11}C]**1**	[^{11}C]**2**	[^{11}C]**3**	[^{11}C]**4**
tumor : blood	0.44 ± 0.06	1.81 ± 0.11	0.46 ± 0.02	1.10 ± 0.11
tumor : lung	0.68 ± 0.19	1.28 ± 0.41	0.66 ± 0.03	0.79 ± 0.30
tumor : muscle	2.40 ± 0.84	2.78 ± 0.62	2.52 ± 0.66	1.52 ± 0.67
tumor : fat	3.46 ± 0.91	5.36 ± 2.38	2.64 ± 1.12	2.77 ± 0.82

Scheme I

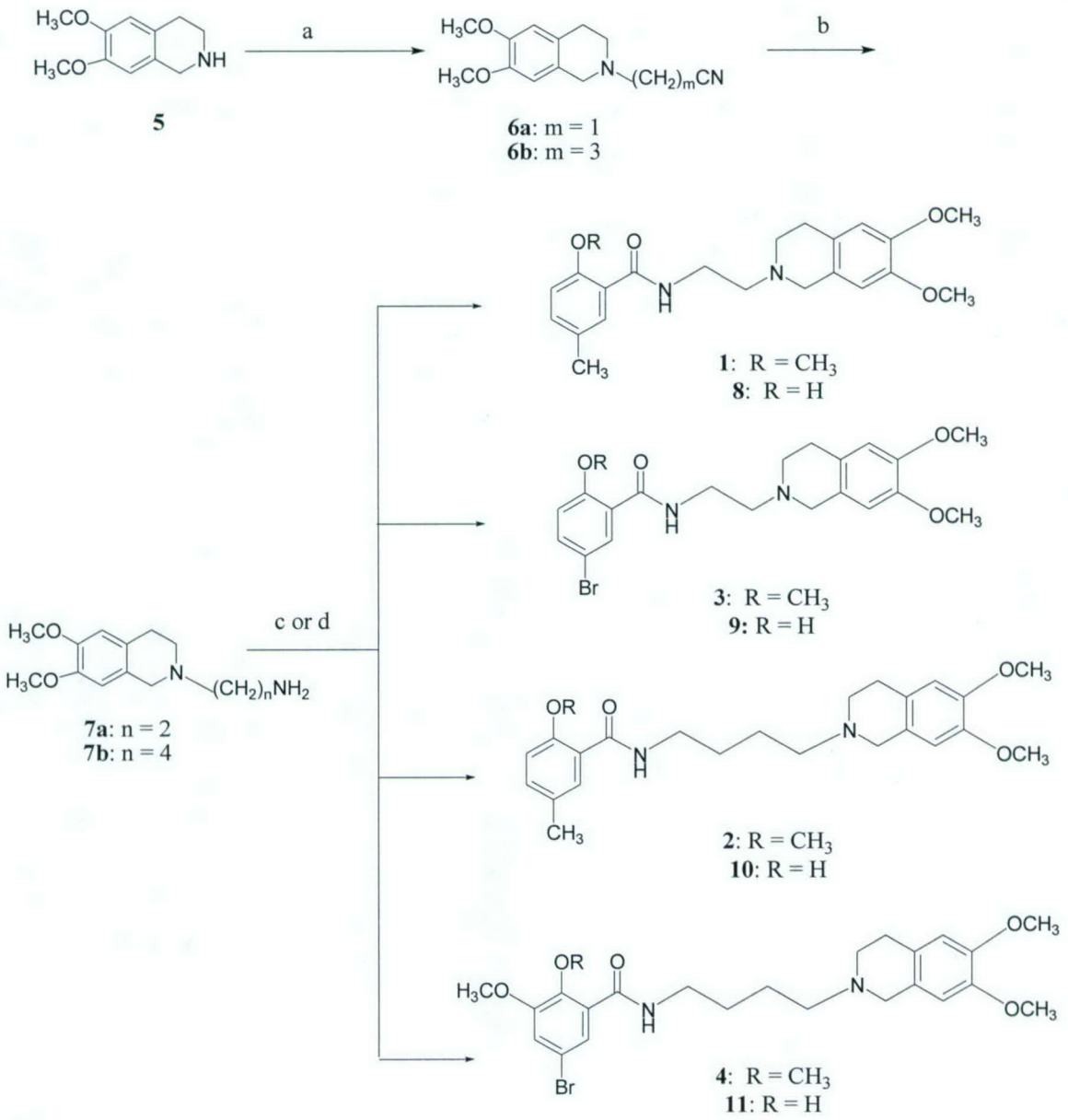

Reagents: (a) $BrCH_2CN$ or $BrCH_2CH_2CH_2CN$, Et_3N, CH_2Cl_2;
(b) $LiAlH_4$, THF or H_2, Pd/charcoal, ethanol; (c) $BoP/C_2H_2Cl_2$ or DCC / $C_2H_2Cl_2$.

Scheme II

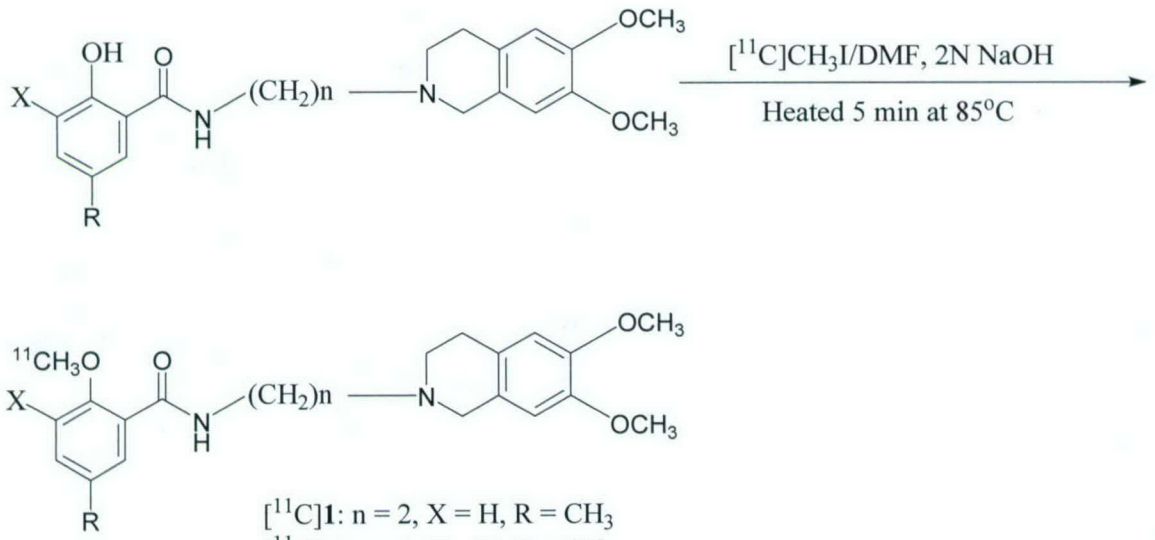

[^{11}C]**1**: n = 2, X = H, R = CH_3
[^{11}C]**2**: n = 4, X = H, R = CH_3
[^{11}C]**3**: n = 2, X = H, R = Br
[^{11}C]**4**: n = 4, X = OCH_3, R = Br

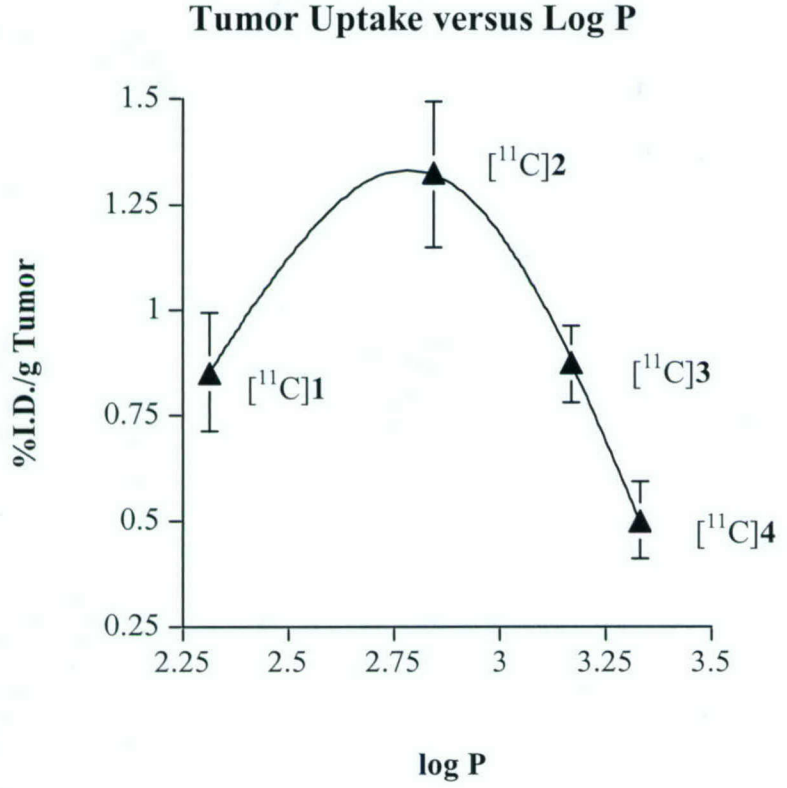
Tumor Uptake versus Log P
%I.D./g Tumor
1.5
1.25
1
0.75
0.5
0.25
2.25
2.5
2.75
3
3.25
3.5
log P
[11C]1
[11C]2
[11C]3
[11C]4

Figure 1

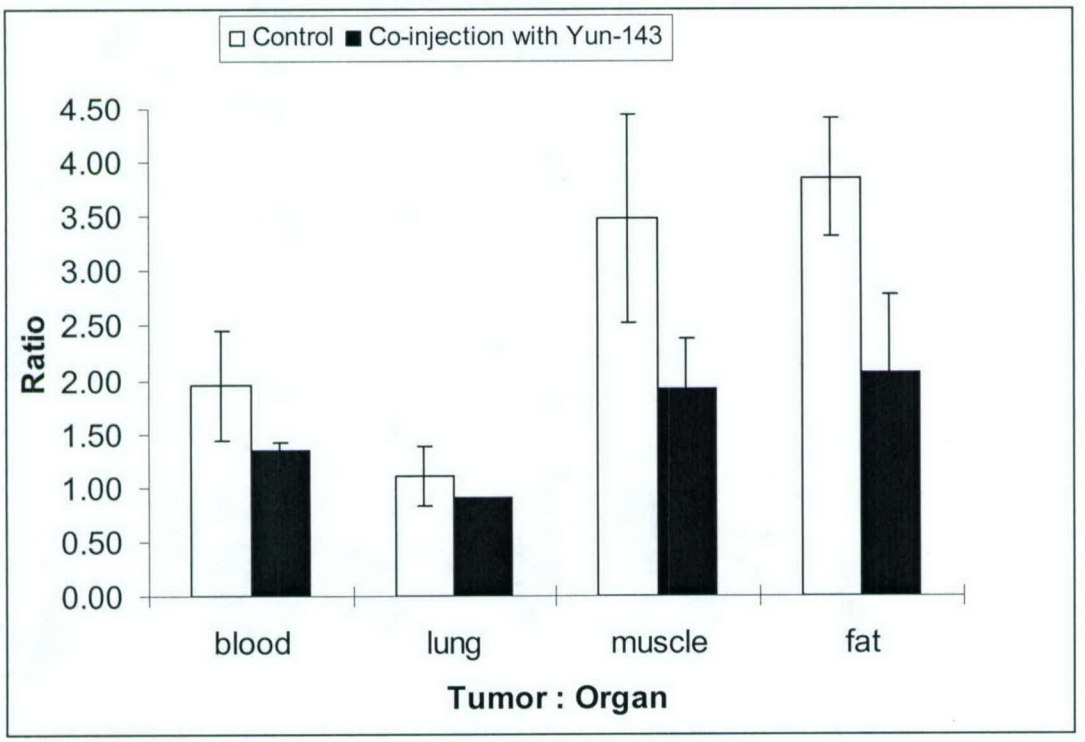
□ Control ■ Co-injection with Yun-143
4.50
4.00
3.50
3.00
2.50
2.00
1.50
1.00
0.50
0.00
Ratio
blood
lung
muscle
fat
Tumor : Organ

Figure 2.

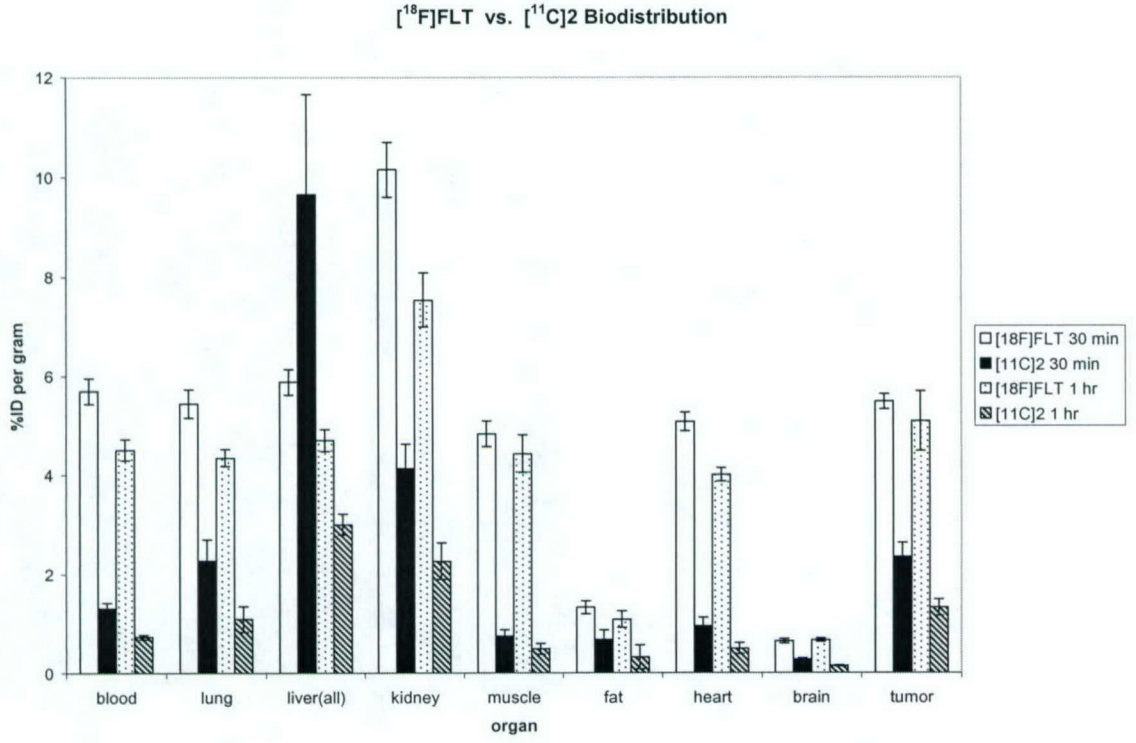
[18F]FLT vs. [11C]2 Biodistribution
%ID per gram
12
10
8
6
4
2
0
blood
lung
liver(all)
kidney
muscle
fat
heart
brain
tumor
organ
[18F]FLT 30 min
[11C]2 30 min
[18F]FLT 1 hr
[11C]2 1 hr

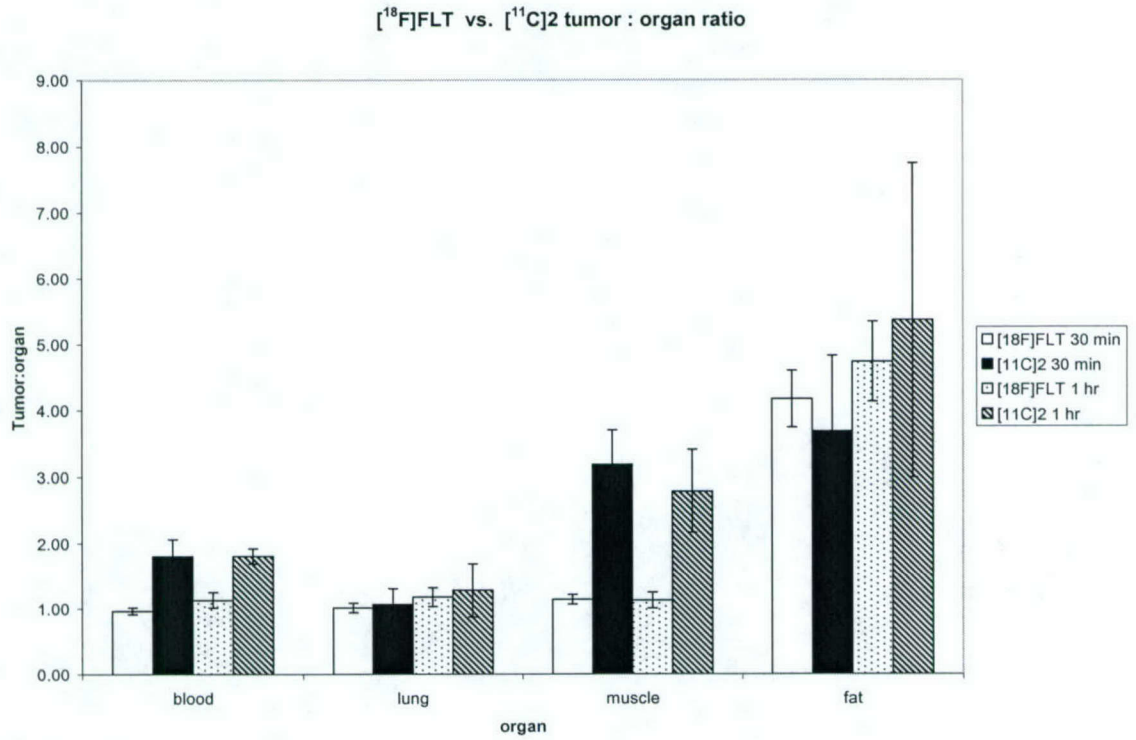
[18F]FLT vs. [11C]2 tumor : organ ratio
Tumor:organ
9.00
8.00
7.00
6.00
5.00
4.00
3.00
2.00
1.00
0.00
blood
lung
muscle
fat
organ
[18F]FLT 30 min
[11C]2 30 min
[18F]FLT 1 hr
[11C]2 1 hr

Figure 3